

HETEROGENEOUS THALAMIC RETICULAR NUCLEUS NEURONS AND THEIR FUNCTIONAL ROLE IN
THALAMOCORTICAL PROCESSING

By

Laura Harding-Jackson

A DISSERTATION

Submitted to
Michigan State University
in partial fulfillment of the requirements
for the degree of

Genetics and Genome Science— Doctor of Philosophy

2021

ABSTRACT

HETEROGENEOUS THALAMIC RETICULAR NUCLEUS NEURONS AND THEIR FUNCTIONAL ROLE IN THALAMOCORTICAL PROCESSING

By

Laura Harding-Jackson

The thalamic reticular nucleus (TRN) is an integral regulator of information flow between the thalamus and cortex. The TRN receives synaptic inputs from both cortical and thalamic regions and based upon this information it selectively inhibits thalamic activity. TRN neurons produce action potentials in two distinct modes: a fast, transient burst discharge from a hyperpolarized state, and a prolonged, tonic discharge from a relatively depolarized state. While previous studies have characterized burst discharge as a transient high frequency discharge (> 250 Hz), these electrophysiological studies reveal a highly variable range of burst frequencies (4-342 Hz). In these studies, I aim to discover the mechanisms underlying these highly variable burst frequencies, as well as their functional role in thalamocortical processing.

In Chapter 2, I found that bursts from TRN neurons with relatively higher frequency discharge (> 100 Hz) contain more action potentials per burst. These neurons also have higher input resistances, broader action potentials, higher action potential thresholds, and larger somas. The amplitude of the T-type calcium channel-mediated low-threshold spike, which underlies the burst discharge, is positively correlated with both the burst discharge frequency and the number of action potentials per burst. I next investigated whether small conductance calcium-activated potassium channels (SK channels) could mediate the differences in burst firing rate and action potential number. Blocking SK channels increased the frequency and duration of the burst but did not increase the amplitude of the underlying T-type calcium current.

Prior studies suggest that T-type calcium channels are distributed along the dendrites in TRN neurons with high frequency burst discharge. In Chapter 3, I examine the distribution of dendritic calcium activity within the lower frequency bursting neurons. While the calcium signal was lower in these neurons all along the dendrites, the calcium signal was evenly distributed across proximal, intermediate, and distal dendritic regions. Investigation of SK channel activity revealed significant location-specific effects. In lower frequency bursting neurons, SK channels had the greatest influence at proximal and distal locations. In higher frequency bursting neurons, SK channels had the greatest influence at proximal and intermediate dendritic locations. Heterogeneous TRN burst discharge frequencies may represent a diverse cell population with unique dendritic ion channel composition and distribution. These results may improve our understanding of the mechanisms of TRN neuron afferent synaptic integration as well as modulation of thalamocortical inhibition.

In Chapter 4 I investigate whether intrinsic properties of TRN neurons are altered in the *Fmr1*-KO mouse model of Fragile X Syndrome (FXS). Individuals with FXS experience a variety of comorbidities that could involve TRN function, such as altered sensory perceptions, sleep disorders, and epilepsy. Analysis of intrinsic cellular properties revealed no differences in TRN neuron properties. Further investigation of synaptic plasticity, which is an abnormal finding in several other brain regions in FXS, also revealed no pathology. These findings suggest that TRN dysfunction does not contribute to FXS pathology.

Copyright by
LAURA HARDING-JACKSON
2021

Dedicated to Scott and Ruby for their unwavering love and support.

ACKNOWLEDGEMENTS

The works within this dissertation were made possible by the collective support and encouragement from countless individuals in both my academic and personal life. I am grateful to have had the privilege to complete these studies within an environment where I was surrounded by brilliant, kind, and curious minds, intent on facilitating new knowledge of the biomedical world. I am excited to now share these findings widely on a public forum, however I would first like to thank a number of individuals for their considerable contribution.

First and foremost, I thank the individuals who were present for these studies on a daily basis: the members of the Cox Lab. Dr. Charles “Lee” Cox has truly been an invaluable advisor and mentor. His encouragement of scientific curiosity inspired my excitement in these studies and made me eager to discover more each day. His guidance challenged me to always work towards improvement and allowed me to gain independence and confidence as a research scientist. I would also like to thank Dr. Joseph Beatty for his contribution to the success of this work. Dr. Beatty has been an invaluable scientific advisor and dependable friend and mentor throughout these studies. Thank you also to Bronson Gregory for his unwavering support and dependability. I am grateful for his friendship and cannot imagine a better lab mate to have had present throughout these studies. I am also appreciative of the support and generosity from the past members of the Cox Lab: Dawn Autio, Dr. Kathleen Louis-Gray, and Dr. Jacqueline Fenn. While I have had the pleasure to work with many undergraduate researchers, I would especially like to thank Mia Railing, Madison Haynes, Jon Skjaerlund, Allison Nieto, Kermanjot Sidhu, and Harmant Grewal for their contributions through technical assistance, encouragement, and exuberance. I wish them all the utmost success in their post graduate careers.

I also extend my sincerest thanks to my dissertation advisory committee, Dr. Shane Crandall, Dr. Gina Leinninger, Dr. Daniel Vogt, and Dr. Hongbing Wang. Their shared guidance, motivation, and constructive criticisms have improved not only this work, but my competence as a research scientist.

The support of my graduate programs has also been paramount to the success of these studies. I would like to thank the individuals who have served as directors and administrators of the DO-PhD program at Michigan State University: Dr. Justin McCormick, Dr. Brian Schutte, Bethany Heinlen, and Michelle Volker. Thank you also to the Genetics and Genome Science Graduate Program director and administrator, Dr. Catherine Ernst and Alaina Burghardt. The dependability and unyielding commitment to student success from all of these individuals has made these works possible.

Thank you to my father, James Harding, for sharing your excitement and respect for science, nature, and technology. Thank you also to my mother, Dr. Shirley Harding, for sharing her passion, strength, and integrity in serving her community while paving the way for women in science and medicine. I am also grateful for my sister, Alissa Berry, for her enthusiastic and faithful support of every endeavor that I undertake both professionally and personally. Together they have all been an infallible force of love and support.

I would like to thank the friends who I have made throughout this journey: Aaron Chow, Quynh Duong, Yajing Ji, Yan Levitsky, Sarah McNitt, Sean Misek, Briana To, and Elise Yoon. Thank you all for the laughter, adventures, and dependable advice.

Finally, I cannot express well enough how thankful I am for my husband, Scott Jackson, for his unwavering love, kindness, patience, and encouragement. He has supported this work, and all my aspirations, in a thousand different ways and I could not imagine a better life partner.

TABLE OF CONTENTS

LIST OF TABLES	xii
LIST OF FIGURES.....	xiii
KEY TO ABBREVIATIONS.....	xv
CHAPTER 1: INTRODUCTION	1
Overview of the Thalamic Reticular Nucleus	1
<i>Physical properties of the thalamic reticular nucleus</i>	<i>1</i>
<i>Topographic organization and subnetworks of the TRN</i>	<i>3</i>
<i>TRN function and pathophysiology.....</i>	<i>6</i>
Intrinsic Properties of TRN Neurons	9
<i>Morphological Properties of TRN Neurons</i>	<i>9</i>
<i>Action potential discharge of TRN neurons</i>	<i>10</i>
<i>T-type calcium channels in the TRN</i>	<i>13</i>
<i>Ion channels in the TRN</i>	<i>14</i>
<i>TRN neuron subtypes</i>	<i>15</i>
Synapses Within The TRN.....	18
<i>Afferent and efferent chemical synapses</i>	<i>18</i>
<i>Electrical synapses</i>	<i>20</i>
<i>Synaptic plasticity in the TRN</i>	<i>20</i>
Concluding Remarks.....	22
REFERENCES.....	23
CHAPTER 2: HETEROGENEITY OF BURST DISCHARGE IN THE THALAMIC RETICULAR NUCLEUS	38
Abstract	38
Introduction.....	39
Materials and Methods.....	42
<i>Slice preparation.....</i>	<i>42</i>
<i>Electrophysiology.....</i>	<i>43</i>
<i>Pharmacology.....</i>	<i>43</i>
<i>Morphology</i>	<i>44</i>
<i>Data Analysis</i>	<i>44</i>
Results	45
<i>Heterogeneous burst frequencies in the TRN</i>	<i>45</i>
<i>Synaptically evoked bursts.....</i>	<i>47</i>
<i>Intrinsic properties of high and low frequency bursting TRN neurons.....</i>	<i>50</i>
<i>Morphologic study of TRN neurons</i>	<i>52</i>
<i>Low threshold spike properties in high and low frequency bursting neurons.....</i>	<i>54</i>
<i>T-type calcium current in high and low frequency bursting neurons.....</i>	<i>56</i>

<i>Impact of SK channels on burst discharge of TRN neurons</i>	60
<i>Lower frequency bursting TRN neurons cannot be identified by SOM-Cre fluorescent labeling within the SOM⁺/Ai32 transgenic animal</i>	65
<i>Phenylephrine increases the burst frequency of TRN neurons</i>	66
Discussion	68
REFERENCES	74

CHAPTER 3: DENDRITIC CALCIUM CHANNEL ACTIVITY AND DISTRIBUTION IN HETEROGENEOUS TRN NEURONS..... **80**

Abstract	80
Introduction	81
Materials and Methods	84
<i>Slice preparation</i>	84
<i>Electrophysiology</i>	85
<i>Pharmacology</i>	85
<i>Calcium imaging</i>	86
<i>Data Analysis</i>	86
Results	88
<i>Dendritic calcium response to somatically evoked burst discharge in high-frequency bursting neurons</i>	88
<i>Dendritic burst mode-evoked calcium activity is reduced in lower frequency bursting neurons</i>	91
<i>Activation of SK channels reduces the duration of the dendritic calcium responses</i>	93
Discussion	98
REFERENCES	106

CHAPTER 4: ALTERED PROPERTIES OF TRN NEURONS IN FRAGILE X SYNDROME..... **110**

Abstract	110
Introduction	111
Materials and Methods	116
<i>Slice Preparation</i>	116
<i>Electrophysiology</i>	116
<i>Optogenetic Targeting</i>	117
<i>Plasticity Induction</i>	118
<i>Analysis</i>	118
Results	119
<i>Intrinsic properties of TRN neurons in WT and Fmr1-KO mice</i>	119
<i>Burst evoked synaptic plasticity of electrically stimulated TRN afferent and efferent fibers in WT and Fmr1-KO mice</i>	120
<i>DHPG induced synaptic plasticity of TRN synapses in WT and Fmr1-KO mice</i>	122
<i>Burst-evoked synaptic plasticity of corticothalamic TRN synapses in WT and Fmr1-KO mice</i>	123
<i>DHPG induced synaptic plasticity of corticothalamic TRN synapses in WT and Fmr1-KO mice</i>	124

Discussion	126
REFERENCES.....	129
CHAPTER 5: CONCLUSION	136
Summary and Future Directions.....	136
REFERENCES.....	143

LIST OF TABLES

Table 2.0: Intrinsic properties of higher and lower frequency bursting TRN neurons.....	51
Table 4.0: Comparison of TRN neuron intrinsic properties within WT and <i>Fmr1</i> -KO mice.....	120

LIST OF FIGURES

Figure 1.0: Schema of the thalamocortical sensory circuit.	2
Figure 2.0: Burst characteristics of TRN neurons	46
Figure 2.1: Comparison of synaptic vs. somatic activation of a burst in TRN neurons.....	49
Figure 2.2: Morphologic comparison of higher and lower frequency bursting TRN neurons	53
Figure 2.3: LTS amplitude is correlated with burst frequency.....	55
Figure 2.4: Calcium mediated low-threshold current underlies the low-threshold depolarization in all TRN neurons	58
Figure 2.5: Nickel decreases the inward current amplitude in all TRN neurons	59
Figure 2.6: Apamin prolongs burst discharge in TRN neurons	62
Figure 2.7: Burst discharge frequencies of fluorescently labeled SOM+ neurons.....	66
Figure 2.8: Phenylephrine does not affect TRN neuron burst frequency or action potential number	68
Figure 3.0: Dendritic calcium imaging of TRN neurons	87
Figure 3.1: Dendritic calcium activity in higher frequency bursting TRN neurons	90
Figure 3.2: Dendritic calcium activity is reduced in lower frequency bursting TRN neurons	92
Figure 3.3: Comparison of dendritic calcium activity in higher and lower frequency bursting neurons.....	93
Figure 3.4: Apamin increases the duration of the calcium transient in both higher and lower frequency bursting neurons at different locations.....	96
Figure 3.5: (Supplemental) Rebound bursts activate an additional longer lasting calcium transient	104
Figure 4.0: Electrical stimulation of afferent and efferent fibers can induce potentiation or depression of synapses onto TRN neurons	121
Figure 4.1: Effect of DHPG on synaptic strength within the TRN	123
Figure 4.2: Synaptic plasticity induction via burst-paired optical stimulation of corticothalamic synapses	124

Figure 4.3: Effect of DHPG on corticothalamic synaptic strength in the TRN.....125

Figure 4.4. Summary of plasticity changes seen via DHPG or burst-paired induction in WT and Fmr1-KO mice128

KEY TO ABBREVIATIONS

ACSF	Artificial cerebrospinal fluid
ADHD	Attention deficit hyperactivity disorder
AHP	After hyperpolarization
AP	Action potential
ASD	Autism Spectrum Disorder
CCK	Cholecystokinin
EEG	Electroencephalogram
EPSC	Excitatory postsynaptic current
EPSP	Excitatory postsynaptic potential
FMRP	Fragile X Mental Retardation Protein
<i>Fmr1</i>	Gene encoding Fragile X Mental Retardation Protein
GABA	γ -Aminobutyric acid
GABA _A	γ -Aminobutyric acid type A (receptor)
GABA _B	γ -Aminobutyric acid type B (receptor)
GABAergic	Release γ -Aminobutyric acid
I _{SK}	Small conductance calcium-activated potassium channel current
I _T	T-type calcium channel current
KO	Knock-out (referring to gene)
LTD	Long-term depression
LTP	Long-term potentiation
LTS	Low-threshold spike

mGluR	Metabotropic glutamate receptor
PND	Postnatal day
SERCA	Selective sarcoplasmic reticulum calcium ATPase
SOM	Somatostatin
SK	Small conductance calcium-activated potassium channel
TRN	Thalamic reticular nucleus
TTX	Tetrodotoxin
WT	Wild-type

CHAPTER 1: INTRODUCTION

Overview of the Thalamic Reticular Nucleus

Physical properties of the thalamic reticular nucleus

The thalamic reticular nucleus (TRN) of the mammalian brain is a thin complex of inhibitory GABAergic neurons that surrounds the dorsolateral thalamus (Houser et al., 1980; Pinault and Deschênes, 1998). While the thalamus is associated with many functions including consciousness, limbic function, motor function, sleep, and epilepsy, the circuits evaluated within this dissertation focus on the primary sensory pathways. Synaptic inputs to the TRN predominantly originate from collateral projections of corticothalamic and thalamocortical axon fibers (Bourassa and Deschênes, 1995; Jones, 1975; Scheibel and Scheibel, 1966). Thalamocortical fibers relay primary sensory information from the thalamus to the neocortex, while corticothalamic fibers, from layer VI of the neocortex, relay neocortical feedback to the thalamus. The consequential placement of the TRN between these pathways ensures that the TRN is continually informed of ongoing thalamocortical network activity (Guillery and Harting, 2003; Jones, 1975). While TRN neurons receive synaptic inputs from both thalamocortical and corticothalamic pathways, they only project to the thalamus (Figure 1.0). With the exception of olfaction, all sensory information is transmitted via the thalamocortical network and thus TRN is a prominent inhibitory modulator of these sensory processing circuits. (Coleman and Mitrofanis, 1996; Cox et al., 1997, 1996; Lee et al., 1994).

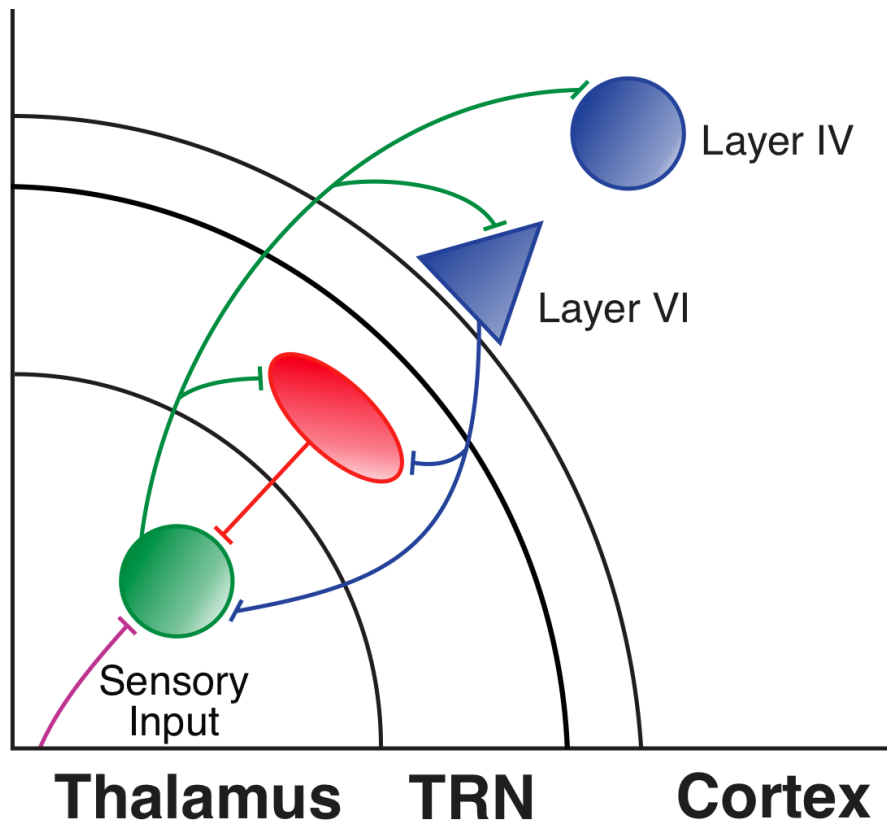


Figure 1.0: Schema of the thalamocortical sensory circuit. This simplified diagram depicts the interplay of thalamus, TRN, and cortex within the corticothalamic (blue) and thalamocortical (green) circuits. The red TRN neuron is excited by both corticothalamic and thalamocortical collateral inputs and sends an inhibitory axonal projection back to the thalamus.

Topographic organization and subnetworks of the TRN

The TRN influences thalamocortical network activity in a complex yet elegant manner. First, TRN neurons are not randomly distributed with the nucleus, but rather arranged in topographically organized sectors based on the sensory modality (visual, auditory, gustatory, and somatosensory), with additional sectors for motor and limbic functions (Cicirata et al., 1990; Cox et al., 1996; Crabtree, 1996, 1992; Guillery and Harting, 2003; Hayama et al., 1994; Lam and Sherman, 2011; Lozsádi, 1994; Pinault and Deschênes, 1998; Shosaku et al., 1984; Sokhadze et al., 2019). Neurons of a specific sector tend to receive similar inputs and project to similar target nuclei. Visual sector inputs originate from the dorsolateral geniculate nucleus, auditory inputs from the ventral medial geniculate nucleus, gustatory from the ventral posteromedial nucleus, and somatosensory inputs from the ventrobasal nucleus. In general, visual and auditory sectors are dorsocaudal and ventrocaudal sectors, respectively, somatosensory is more central, and the most rostral regions of the nucleus receive motor input (Crabtree, 2018; Sokhadze et al., 2019; Zikopoulos and Barbas, 2007).

Second, while most TRN neurons form closed loop reciprocal thalamic circuits, meaning they project to and receive inputs from a single thalamic nucleus, others project to and/or receive inputs from different or multiple thalamic nuclei creating an open circuit. While a TRN neuron may reside within a given sector, these neurons can have large, planar dendritic arbors allowing them to receive afferent inputs from multiple sectors (Guillery and Harting, 2003; Ohara and Havton, 1996). This architecture permits direct feedback in some instances, as well as crosstalk among regions that relay functionally related information. This level of crosstalk may allow TRN neurons to effectively integrate multiple sensory modalities (Crabtree, 1996; Cruikshank et al.,

2010; Fitzgibbon et al., 1995; Warren et al., 1994). Additionally, this anatomical arrangement may allow feedback from one circuit to result in lateral inhibition of the same or different nearby circuits, perhaps further focusing the receptive fields and allowing focus on selected stimuli. Cumulatively, these organizational systems allow the TRN to act as a complex hub of multisensory integration as it produces both feedback inhibition to thalamic nuclei due to thalamocortical influence, and feedforward inhibition as a result of corticothalamic influence.

Third, TRN neurons have been shown to form inhibitory synapses with neighboring neurons within the nucleus to create a lateral inhibitory network (Ahlsén and Lindström, 1982; Cox et al., 1996; Huntsman et al., 1999; Sohal and Huguenard, 2003). Lateral inhibition is thought to occur when excited TRN neurons release GABA onto neighboring neurons within the nucleus, causing them to disinhibit the downstream thalamic targets of similar or neighboring circuits. While the prevalence and magnitude of such inhibition is unclear (Hou et al., 2016), the result of this activity would decrease the gain of the central circuit while increasing that of laterally inhibited thalamocortical neurons, allowing focus to shift to specific novel or important sensory inputs (Zhang and Jones, 2004). Neighboring TRN neurons have also been shown to have electrical synapses, or gap junctions, can also act to synchronize inhibitory actions of TRN. The electrical synapses would have the opposite effect of the intra-TRN chemical synapses and lateral inhibition. Electrical synapses would act to couple neighboring neurons and, depending on their coupling coefficient, could result in strengthened clusters of downstream inhibition at target thalamic nuclei and could also impact synchronized rhythmic oscillations (Landisman et al., 2002; Long et al., 2004).

When viewing the TRN as a major contributor of thalamic inhibition, it is important to note that TRN is responsible for this to a greater extent in the rodent than in other mammals. This is due to the limited number of thalamic inhibitory interneurons in multiple thalamic nuclei within the rodent (Arcelli et al., 1997). Many brain regions contain GABAergic interneurons that act to inhibit local circuit activity, however a unique feature of the mouse thalamus is the severe decrease of interneurons in every thalamic nucleus except for the visual dorsolateral geniculate nucleus (Seabrook et al., 2013). In the human as well as many other non-rodent mammals, interneurons can comprise up to 25% of the total neuron population within certain thalamic nuclei, and as thalamic interneurons rise, the relative size and cell-density of the TRN decreases (Arcelli et al., 1997; Letinic and Rakic, 2001). A possible consequence of these findings is that the TRN may play a larger role in inhibiting thalamic activity in the mouse than in the human, and studies that utilize mouse TRN must be viewed within this context.

While initially regarded as a homogeneous nucleus, numerous studies have clearly revealed that the TRN is a complex nucleus of heterogeneous neurons. These neurons participate in a variety of functions such as the modulation of sensory information processing, maintaining intercranial rhythms in sleep, and attentional gating. Whether or not certain populations of these neurons differently participate in these activities is not clear. What is known, however, is that the TRN has an important role in the integration and processing sensory inputs, and the subsequent inhibitory circuit modulation is critical to appropriately facilitating many complex neurological processes.

TRN function and pathophysiology

In 1984, Francis Crick proposed that the TRN may function as an “attentional searchlight” within the brain (Crick, 1984). As such, it would selectively inhibit and disinhibit circuits to allow the brain to focus on selective stimuli while dampening other noisy or irrelevant stimuli. In the thirty-seven years since this hypothesis was published, our knowledge base has grown to better understand the structure and function of the TRN. The idea that the TRN modulates the flow of information between the cortex and thalamus has been strongly supported, while the ways in which it modulates this information has grown far more elaborate. Many other complexities and additional functions have been discovered and while the TRN clearly plays a critical role in many neural circuits, there is still much to be learned about the region.

Each day, an individual’s brain is inundated with sensory stimuli that must be effectively processed and relayed to appropriate brain regions. Glutamatergic sensory inputs from both the neocortex and the thalamus excite TRN neurons, and in response to this activity, the TRN releases GABA neurotransmitter that inhibits downstream thalamic neurons. This ultimately decreases the activity of the downstream circuit while allowing neighboring circuits, potentially of different sensory modalities, to proceed disinhibited (Cox et al., 1997; Crabtree, 2018. Pinault, 2004). Through these activities, the TRN actively regulates the gain of various sensory circuits in relation to the synaptic afferent input. In modulating circuit activity levels, the GABAergic TRN output then also acts to shape the receptive field of the thalamocortical neurons, further facilitating precise modulation of sensory inputs. Experiments in which the TRN was lesioned *in vivo* found that the number of whiskers that a certain ventroposterior nucleus neuron would respond to the movement of significantly increased following the lesioning (Lee et. al. 1994).

In addition to this role in processing sensory stimuli, the TRN also participates in sleep rhythmogenesis. TRN neurons facilitate rhythmic patterns of action potential bursts between the thalamus and cortex during slow-wave sleep and may also initiate sleep spindles (Steriade et al. 1986; Pellegrini et al., 2016). The TRN may also play a role in selective attention, or the ability to focus on specific relevant stimuli among many. Neurons within the TRN were found to be most active during inhibition of redundant or irrelevant stimuli which could allow for more targeted perception (McAlonan et al., 2006). TRN-facilitated interplay between all of these associated processes is likely important to appropriate behavioral processes (Chen et al., 2016; Halassa et al., 2014). Given these many functional roles, TRN pathophysiology can have detrimental effects and altered TRN function is implicated in many disorders such as: attention deficit hyperactivity disorder (ADHD), schizophrenia, sleep disorders, epilepsy, and sensory processing disorders (Friedberg and Ross, 1993; Pratt and Morris, 2015; Steriade, 2005; Steullet et al., 2017; Wells et al., 2016).

The TRN is also a target of study in several neurodevelopmental disorders. *CHD2* and *PTCHD1* are two separate genes involved in genetic models of autism spectrum disorder with speculation of TRN-related pathology. *CHD2* is involved in chromatin remodeling protein while *PTCHD1* is a transmembrane protein with relation to neurodevelopment. Both are highly expressed within the TRN (Lossifov et al., 2012; Krol et al., 2018; Lamar and Carvill, 2018; Noor et al., 2010). In the *PTCHD1* deletion autism model mouse specifically, a calcium-dependent potassium ion channel (SK) deficit in the TRN was linked to behavioral attentional deficits (Kleiman-Weiner et al., 2009; Wells et al., 2016). The implication of TRN dysfunction on

these measurable disease phenotypes exemplifies the potential of TRN pathology to affect behavioral outcomes.

In addition to altered neurodevelopment, TRN pathophysiology may also manifest in seizure disorders. Seizures are essentially strong, lasting bursts of action potentials that can overcome circuits and block transmission within the brain. TRN pathology is especially implicated in absence epilepsy, which is a generalized epilepsy characterized by highly synchronized rhythmic discharges. Absence epilepsy typically arises in childhood and is characterized by short-lasting non-responsive staring spells without loss of consciousness. Absence seizure discharges originate between the TRN and thalamocortical cells and manifest with characteristic 3 Hz spike-wave rhythms recorded in an electroencephalogram (EEG) (Avanzini et al., 1992; Bovenkamp-Janssen et al., 2004; Broicher et al., 2008; Chen et al., 2014; Jahnsen and Llinás, 1984a; Liu et al., 1992; Sun et al., 2002; Tsakiridou et al., 1995, Williams, 1953). These seizure discharges strongly activate the TRN and the resultant reciprocal TRN and thalamocortical burst rhythms may decrease the relay of ascending sensory afferent input (Steriade, 2005). Lesioning of the TRN was found to abolish seizure discharges, further implicating TRN pathophysiology in the seizure activity (Avanzini et al., 1993).

Due to a significant correlation between the function of the TRN and symptoms of schizophrenia, TRN has also been a focus of this body of research. Studies of schizophrenia have revealed deficits in sleep spindles and attentional and auditory gating, and TRN highly expresses several genes shown to be affected in the disorder (Ferrarelli and Tononi, 2011; Krol et al., 2018; Pratt and Morris, 2015; Steullet et al., 2017). The extent to which TRN pathology may be a direct

cause of these conditions is not yet resolved, however it is evident that perturbations to TRN function result in measurable behavioral defects.

Intrinsic Properties of TRN Neurons

Morphological Properties of TRN Neurons

The morphological properties of TRN neurons have been evaluated by several studies with varied findings, likely due to differences in animal models and methodology. Some studies have found clear neuronal subtypes differentiated by soma morphology and dendritic arborization (Lübke, 1993; Spreafico et al., 1991, 1988), however to date distinct electrophysiological properties have not been tied to specific TRN neuron subtypes. Other researchers have reported that TRN neurons have more uniform somata with a large and roughly discoid dendritic structure (Mulle et al., 1986; Ohara and Havton, 1996).

A recent study reported that neurons near the anatomical borders of the TRN were more likely to display weaker bursting properties (Martinez-Garcia et al., 2020). This study additionally found that cells within the medial and lateral edges of the TRN were associated with slightly smaller somas when compared to cells in the central regions of the nucleus, however the intrinsic properties of individual neurons were not correlated with this distinctive morphology. In addition to studies of soma and dendritic morphologies, reports that neurons may vary in their axonal arborization may also be considered. Several distinct axonal morphologies have been identified from TRN neurons (Cox et al., 1996; Kolmac and Mitrofanis, 1997; Pinault and Deschênes, 1998; Yen and Jones, 1983). The potential functional consequences of distinct axonal morphologies could lend insight into how the downstream targets of TRN neurons correlate with

the intrinsic properties and afferent inputs. While axonal arborization was not investigated in our studies, the correlation of this property with electrophysiological findings warrants further investigation.

Action potential discharge of TRN neurons

Many neurons in the brain discharge tonic action potentials through mechanisms where the action potential frequency is linearly related to the magnitude of membrane depolarization. The thalamus is one region known for being able to produce discrete, robust bursts of action fast action potentials (Jahnsen and Llinás, 1984b; Pinault and Deschênes, 1992; Steriade et al. 1993; Sherman, 2001). Burst discharge is a critical mechanism by which the TRN engages in intracranial rhythms and modulates thalamocortical circuit inhibition (David et al., 2013; Fernandez et al., 2018). TRN neurons produce action potentials in two different modes determined by membrane voltage: burst and tonic discharge. When TRN neurons are relatively hyperpolarized, a depolarizing current step leads to a fast transient burst-discharge of action potentials. When the membrane potential is relatively depolarized, the same current step will result in a repetitive tonic-discharge throughout the depolarizing current step. In tonic discharge, the frequency of the action potentials is linearly related to the magnitude of the current step (Contreras et al., 1992; Deschenes et al., 1984; Huguenard and Prince, 1992; Jahnsen and Llinás, 1984b). Tonic firing is most often observed in alert animals, while burst firing is predominate during sleep (Domich et al., 1986; Llinás and Steriade, 2006). Several studies have also observed burst discharge during awake states during changes in attentional state or locomotion. (Bezudnaya et al., 2006; Hartings et al., 2003; Marlinski and Beloozerova, 2014).

The thalamus is known for containing many burst producing neurons, however TRN neurons are unique for having exceptionally longer bursts when compared to those of other thalamic region (Huguenard and Prince, 1992). Thalamic burst discharge is comprised of a crown of transient fast action potentials over a low-threshold spike (LTS), which is driven by the activation of T-type voltage dependent low-threshold calcium channels (T-channels). Huguenard and Prince (1992) found that t-type calcium current (I_T) in TRN often remained activated for twice the duration (220 msec) of the I_T underlying the burst in ventrobasal nucleus neurons (110 msec). Additionally, they found that changes in ventrobasal nucleus neuron membrane potentials altered the rate of decay of the burst, however the TRN burst was insensitive to membrane potential changes.

The magnitude and duration of TRN-mediated thalamic inhibition varies based upon these action potential discharge modes. Thalamic inhibition mediated by persistent, tonic action potentials will result in the activation of short-acting GABA_A receptors, while the inhibition mediated by bursts of fast action potentials may additionally activate longer-lasting GABA_B receptors (Cox et al., 1997; Jahnsen and Llinás, 1984b; Kim et al., 1997; Kim and McCormick, 1998). GABA_A and GABA_B receptor activation initiates a chloride conductance (GABA_A) or a potassium conductance (GABA_B), which ultimately decreases membrane excitability of downstream neuron. In the case of GABA released from TRN axons, it inhibits the thalamocortical circuit output. In consideration of burst properties, it should also be noted that while TRN bursts directly cause strong thalamocortical inhibition, the subsequent release of that inhibition can lead to an indirect delayed, post-inhibitory excitation in the thalamocortical cell. The release of the thalamocortical cell from the GABA_A- and/or GABA_B-receptor mediated inhibition, along with

the activation of hyperpolarization-activated cyclic nucleotide-gated (HCN) cation channels, causes repolarization of the thalamocortical cell membrane (McCormick and Pape, 1990). This may elicit a rebound activation of T-channel mediated current, which can ultimately lead to a rebound burst discharge. This mechanism suggests that a larger amplitude GABA-receptor conductance could cause post-inhibitory excitation within the thalamocortical relay neurons, indirectly allowing the TRN to exert thalamocortical inhibition and subsequent excitation in a temporally segregated manner.

Burst discharge in the thalamus is shaped by many factors such as T-channel subunit composition, intrinsic properties, and modulatory inputs. An additional factor that may have a significant impact on burst morphology is the distribution of dendritic T-channels. TRN neurons are known for having long, thin dendrites, and a distinguishing feature of TRN neurons is a distribution of T-channels along the extent of the dendrite that may be more concentrated distally (Cueni et al., 2008b; Destexhe, 1996; Kovács et al., 2010). A study of rat TRN found the largest calcium activity in response to a somatic burst was located at more distal dendrites while in contrast, activity in ventrobasal and dorsal lateral geniculate nucleus neurons was more uniform along the somatodendritic axis (Crandall et al., 2010). This unique distribution pattern has implications on pathway-specific synaptic integration because it suggests that synaptic inputs at more distal locations is preferentially amplified when the cell is in burst mode. This aspect is significant considering that neocortical afferents preferentially synapse onto distal dendrites and may be preferentially amplified over thalamic inputs, which tend to innervate more proximal dendrites of TRN neurons (Liu et al., 1995; Liu and Jones, 1999a; Van Horn and Sherman, 2004). In combination with distal signal amplification in TRN neurons, this spatial synaptic distribution

suggests that location-dependent signal integration could underlie specific functions of corticothalamic and thalamocortical pathways in processing sensory information.

T-type calcium channels in the TRN

There are three subtypes of T-channels underlying thalamic bursts: $Ca_v3.1$ (expressed from the $\alpha1G$ transcript), $Ca_v3.2$ (expressed from the $\alpha1H$ transcript), and $Ca_v3.3$ (expressed from the $\alpha1I$ transcript) (Perez-Reyes, 2003). While $Ca_v3.1$ and $Ca_v3.2$ are expressed in multiple tissues throughout the body, $Ca_v3.1$ is located only in the brain (Perez-Reyes, 2003). All three subtypes of T-channels are expressed in the thalamus, however in most thalamic nuclei, $Ca_v3.1$ is more common. In the TRN, however, despite some debate depending on the organism of study, it appears that all three subtypes may contribute to burst discharge with $Ca_v3.3$ appearing most prominently on distal dendrites (Cain and Snutch, 2010; Cueni et al., 2008a; Joksovic et al., 2005; Kovács et al., 2010; Pellegrini et al., 2016; Talley et al., 1999). The location, density, and channel subtypes comprising I_T will influence the synaptic integration and properties of the burst. $Ca_v3.3$, which is found more densely on distal dendrites, activates more slowly and for a longer duration than $Ca_v3.2$ and $Ca_v3.1$, however the peak current of activation of $Ca_v3.3$ is smaller than the other subtypes (Cain and Snutch, 2010). $Ca_v3.3$ also activates at a threshold that is 10 mV more depolarized than $Ca_v3.2$ and $Ca_v3.1$ and inactivates at a threshold that is 5 mV more depolarized (Cain and Snutch, 2010; Talley et al., 1999).

An additional aspect of T-current (I_T) that must be considered is the developmental age at which the channels mature. Large changes in I_T -related functions occur until postnatal day 21, and smaller developmental changes may continue for weeks past this point (Huntsman and Huguenard, 2000; Murata and Colonnese, 2019; Pirchio et al., 1990; Tennigkeit et al., 1998;

Warren and Jones, 1997). Mouse TRN neurons do not gain the ability to fire multi-spike bursts until approximately three weeks of age and functional sleep spindles do not appear until this time as well (Warren and Jones, 1997). Findings in younger animals are important to understanding developmental processes, however with many studies focusing on younger animals there are still many questions about the properties of the adult TRN where burst discharge is still important to many key functions.

Ion channels in the TRN

Many different ion channels mediate the voltage state-dependent functions of the TRN. Of specific interest to this work are the T-type calcium channels detailed above. These channels are located throughout the dendritic arbors and are responsible for the large, robust bursts produced by TRN neurons. These channels de-inactivate at hyperpolarized potentials allowing for an influx of Ca^{2+} to facilitate state-dependent responses to afferent synaptic excitation. Small conductance calcium-activated potassium channels (SK), specifically type 2 in TRN, are also dispersed along the dendritic arbors and are strongly activated by the low threshold spike (Cueni et al., 2008b; Kleiman-Weiner et al., 2009; Ying and Goldstein, 2005). SK channel-mediated current (I_{SK}) activation typically shortens the burst discharge by rapidly hyperpolarizing the membrane. Blocking I_{SK} enhances the burst in TRN neurons, but has no effect on the burst characteristics of thalamocortical relay neurons (Kleiman-Weiner et al., 2009). This synergistic co-activation of I_{SK} and I_{T} in TRN contributes to the regulation of the variety of inter-burst frequencies that are necessary for rhythmic bursting activities (Barrionuevo et al., 1981; Cueni et al., 2008b).

Several high voltage-activated Ca^{2+} channels are also important to TRN function. L-type high-voltage Ca^{2+} channels are found most densely at the soma in TRN neurons, whereas in thalamocortical cells they are more densely distributed at the dendritic base (Budde et al., 1998; Huguenard and Prince, 1992). In the TRN, L-type channels appear to be comprised of mainly subtype $\text{Ca}_v1.2$. High-voltage Ca^{2+} channel types P/Q ($\text{Ca}_v2.1$), N ($\text{Ca}_v2.2$), and R-type ($\text{Ca}_v2.3$) are also widely distributed within the TRN (Kanyshkova et al., 2014). The final ion channel that will be discussed is the Ca^{2+} activated non-selective cation channels mediating I_{CAN} . This channel is also gradually activated with burst discharge and is responsible for the slow after-depolarization that often presents as a trail of tonic action potentials subsequent to the burst discharge (Bal and McCormick, 1993).

TRN neuron subtypes

For many years the TRN was thought to contain a physiologically homogeneous population of neurons based on their propensity to reliably produce large burst discharges in a hyperpolarized state. In 1992 Contreras et al. challenged this by reporting an additional subset on neurons that appeared to be incapable of producing any burst like discharge even at hyperpolarized states. These neurons, termed Type II cells, or non-bursting neurons as they will be referred to in this text, have been observed by several additional studies (Brunton and Charpak, 1997.; Clemente-Perez et al., 2017; Contreras et al., 1992; Lee et al., 2007). Non-bursting neurons not only lack a robust burst discharge but are reported to lack the underlying I_T mediated LTS. Given this information, there are two likely explanations; 1) that these neurons possess fewer T-channels, or 2) the distribution of T-channels is more distal causing degradation of the LTS signal strength before it reaches the soma to drive a large burst captured via whole

cell recordings. One goal of this work is to investigate this question of how dendritic calcium channel distribution relates to burst frequency.

In addition to non-bursting neurons, Lee et. al. (2007) also reported an electrophysiologically distinctive subtype of TRN neurons termed atypically bursting neurons in rat TRN. This subset was located largely in the dorsal TRN along with non-bursting neurons, whereas typically bursting neurons were found more ventrally. These neurons appeared to fire an initial typical action potential followed by several smaller, wider action potentials. In recordings not detailed in this work, atypically bursting neurons were identified in TRN in mice aged 13 and 14 postnatal days, however at the older time points used in this set of work, no atypically bursting neurons were identified. It is possible that atypically bursting neurons are not a feature of rat versus mouse TRN, but instead are a developmental stage of neurons. Recently, a study in slightly older animals (PND 22-34) reported that a population of more slowly bursting somatostatin-positive neurons occupy the medial and lateral edges of TRN in mid sections, and comprise the vast majority of neurons in more dorsal regions (Martinez-Garcia et al., 2020).

Evidence of electrophysiologically distinct TRN cell types in adult animals has been limited, however the implications of neurons with specific firing patterns, intrinsic properties, and/or synaptic afferents or efferents would add crucial insight to the functioning of the region. Uncovering the function of non-bursting or lower frequency bursting neurons in particular could fill an important knowledge gap, since many of the studied TRN functions rely on burst discharge. Future investigations will further clarify how these apparent neuronal subtypes are integrated into the TRN network and whether electrophysiological properties relate to their development and connectivity.

During slow-wave sleep, reciprocal interplay and activation of TRN and thalamocortical neurons produce oscillatory burst discharges which manifest as sleep spindles (Bazhenov et al., 2000; Destexhe et al., 1994). During awake states as well as non-rapid eye movement (non-REM) sleep, tonic firing is the dominant mode of action potential discharge the nucleus (Pellegrini et al., 2016; Steriade, 2005). Sleep spindles, which occur during the early stages of sleep, can be occur in TRN and are important for initiating and maintaining sleep states. In addition to participating in sleep rhythms, thalamic burst firing is thought to increase the efficiency of communication within the thalamocortical circuit, and it appears that timing of action potentials within a burst may have a significant role in the downstream outcomes (Reinagel et al., 1999; Swadlow and Gusev, 2001). Several *ex vivo* brain slice studies have reported heterogeneous intrinsic TRN burst properties (Brunton and Charpak, 1997.; Contreras et al., 1992; Lee et al., 2007), and studies *in vivo* have further supported a functional diversity of burst patterns. In one example during locomotion, several different patterns of action potential discharge were observed within an *in vivo* burst in TRN that varied with the modality of movement from single-unit extracellular recordings in awake and sleeping cats (Marlinski and Beloozerova, 2014). Bursting neurons were also found to respond robustly to induced nociception, while non-bursting neurons had very little changes in response (Huh and Cho, 2016). Intriguingly, one study found that during a simultaneous recording of two neighboring TRN neurons within the same sector, which in theory received the similar inputs and projected similar outputs, the firing of the cells was very different. This finding may suggest that intrinsic properties of the neurons may have a bigger influence on cell firing patterns than afferent activity (Pinault and Deschênes, 1992).

Together, these data support that the TRN is neither a homogenous nor bimodal region, but likely contains a spectrum of heterogeneous neurons. These neurons have unique intrinsic properties that, when combined with modulatory cholinergic, serotonergic, dopaminergic, histaminergic, and adrenergic influences, may shift their responses to stimuli thus influencing the modulation of thalamocortical circuits.

Synapses Within The TRN

Afferent and efferent chemical synapses

The main sources of synaptic inputs to the TRN are the glutamatergic inputs of axons projecting from either neocortical layer VI or thalamic nuclei. Although fewer overall, other modulatory inputs also supply the region that modify the excitability of the TRN neurons (Liu et al., 1995; Pinault and Deschênes, 1998; Warren et al., 1994). Cholinergic inputs from the ascending reticular system of the brainstem, basal forebrain, and nucleus basalis can provide initially excitatory inputs (via nicotinic receptors) followed by inhibitory modulation (via muscarinic receptors) (Hallanger et al., 1987; Lee and McCormick, 1995; McCormick, 1989; McCormick and Prince, 1986; Mesulam et al., 1983; Sokhadze et al., 2019; Sun et al., 2013). GABAergic inputs from the globus pallidus (Asanuma, 1994; Gandia et al., 1993; Hazrati and Parent, 1991), basal forebrain (Asanuma, 1989; Asanuma and Porter, 1990; Bickford et al., 1994), substantia nigra pars reticulata (Paré et al., 1990), zona incerta (Çavdar et al., 2006), and local TRN neurons supply the region with inhibitory modulation. Dopaminergic inputs from substantia nigra pars compacta, and basal forebrain generally enhance excitation (Govindaiah et al., 2010; Lee and McCormick, 1996; McCormick and Prince, 1986; Mrzljak et al., 1996; Pinault, 2004; Sun

et al., 2013) as do serotonergic and noradrenergic inputs from the dorsal raphe nucleus and suprallemniscal nucleus, and locus coeruleus, respectively (Cropper et al., 1984; McCormick and Wang, 1991; Rodríguez et al., 2011).

Cortical afferents, referred to as corticothalamic inputs, arise largely from axonal fibers of cells located in layer VI of the neocortex. Axonal fibers from these cortical regions send branches that synapse onto TRN cells as they make their way towards their target thalamic nucleus (Guillery and Sherman 2002). These synapses are smaller, individually weaker, and exhibit the paired pulse facilitation: all consistent with a modulatory framework (Liu and Jones, 1999a; Reichova and Sherman, 2004). Notably, activity-dependent plasticity in the TRN has been found at these synapses, which contain group 1 mGluRs in addition to AMPA and *N*-methyl-D-aspartate (NMDA) receptors (Fernandez et al., 2017). Thalamic afferents, referred to as thalamocortical inputs, arise from axonal fibers of thalamic nuclei that send synaptic offshoots as they traverse the TRN on their way to the cortex. These primarily first-order synapses are physically larger and lack the group 1 mGluR component of the corticothalamic synapses. Thalamocortical synapses also exhibit stronger activation and paired-pulse depression, consistent with the primary driver framework (Liu and Jones, 1999a; Reichova and Sherman, 2004). Corticothalamic synapses comprise the majority of TRN inputs (Guillery, 1967; Liu and Jones, 1999b). These inputs are preferentially distributed on distal dendritic locations (60% of synapses) over more proximal dendritic locations (50% of synapses). Conversely, thalamocortical synapses are thought to comprise 30-40% of proximal synapses and only 20% of distal synapses (Deleuze and Huguenard, 2016; Liu et al., 1995; Liu and Jones, 1999a).

The distal preference for corticothalamic synapses in TRN is significant because distal TRN dendrites also contain the many low-threshold calcium channels, which may act as selective amplifiers for distal synapses (Crandall et al., 2010; Kovács et al., 2010). When comparing the responses to corticothalamic fiber stimulation in TRN and thalamocortical relay neurons, TRN neurons experienced over double the quantal excitation and contained more synaptic contacts (Golshani et al., 2001). Further elucidation of functional corticothalamic and thalamocortical synapse contribution utilizing an optogenetic approach found that activation of corticothalamic synapses results in robust TRN excitation that is 3-4x stronger than the response in the ventrobasal nucleus (Cruikshank et al., 2010).

Electrical synapses

In addition to chemical synapses, the TRN also communicates via electrical synapses. These synapses, mostly formed by connexin36 encoded gap junctions, enable couplings between neighboring neurons (Landisman et al., 2002; Zolnik and Connors, 2016). Electrical synapses appear to be prominent components of TRN network communication and may facilitate synchronized activity during rhythmically oscillating states. These electrical synapses also participate in synaptic plasticity revealing them to be a dynamic and active participants in TRN function (Deleuze and Huguenard, 2006; Long et al., 2004).

Synaptic plasticity in the TRN

Neuroplasticity refers to the ability of neurons to enhance or diminish network transmissions in an experience-dependent manner. Most often associated with learning and memory, there are many forms of synaptic plasticity; long-term or short-term, electrical, or chemical are just a few of many distinctions. From the electrophysiological perspective of this

dissertation, plasticity is the ability of a neuron to enhance or diminish synaptic transmission in an experience- or activity-dependent manner. Only recently has this phenomenon been described within the TRN. Mechanisms of TRN neuron plasticity are not fully characterized, however studies have shown involvement of mGluRs and NMDARs (Fernandez et al., 2017), as well as Ca_v3.3 (Astori and Lüthi, 2013). TRN neurons display plasticity of chemical synapses in response to synaptic stimulation occurring concurrently with the high-calcium environment during the burst discharge. Long-term potentiation (LTP) can be induced through activation of Ca_v3.3 at thalamocortical synapses onto TRN neurons when NMDARs are activated concurrently with a burst discharge (Astori and Lüthi, 2013). In a following study, TRN excitability and burst discharge were augmented when corticothalamic inputs were selectively activated by slow trains of optogenetically-evoked excitatory postsynaptic potentials (EPSPs; Fernandez et al., 2017). In addition to plasticity of corticothalamic and thalamocortical synapses, one study reported evidence of potentiation of cholinergic synaptic strength that was dependent upon corticothalamic group 1 mGluR activation (Sun et al., 2016).

At electrical synapses, long-term depression (LTD) has been reported following coupled burst discharge in electrically paired neurons, and with group 1 mGluR activation. Burst-induced LTP in particular was found to be calcium-dependent and the effects were completely abolished by the calcium chelator BAPTA (Haas et al., 2011; Sevetson et al., 2017). LTD can also be electrically elicited by tetanic stimulation from cortical afferents, which induces plasticity via mGluR activation. In contrast to the burst paired induction for coupled neurons, this mGluR-dependent electrical plasticity induces plasticity in a calcium-independent manner (Landisman, 2005; Sevetson et al., 2017). In addition to LTD, selective activation of group 2 mGluRs induced

LTP at TRN electrical synapses (Wang et al., 2015). There is clear evidence of several forms of plasticity at several prominent TRN inputs: electrical, corticothalamic, thalamocortical and cholinergic. However, future studies will clarify how these unique mechanisms of plasticity work together to maintain appropriate TRN function.

Concluding Remarks

More than half a century of study has illuminated many intriguing aspects of the TRN and its role in the thalamocortical circuit. The TRN is an integral contributor to sensory processing, sleep, and attentional gating within the brain, however there are still many functional aspects that remain less clear. For example, the relative contributions of intrinsic properties versus extrinsic neuromodulatory inputs in shaping state and activity-dependent burst discharge has not yet been clearly characterized. Debate also remains regarding whether TRN neurons are homogeneous versus heterogeneous in morphology and electrophysiology. If the neuron population is composed of more heterogeneous neuron types, the relative participation of these groups in modulating different subnetwork activity between different sensory and motor modalities would require further investigation. The goal of this dissertation is to begin to answer these questions by examining how intrinsic properties of TRN neurons contribute to the signal integration and selective output patterns that characterize functionality of the nucleus. The TRN continues to be an area of interest for studies of several disease states such as autism, epilepsy, and schizophrenia. These studies aim to characterize how TRN composition, cellular properties, synaptic integration, and modes of output interact to facilitate appropriate sensory processing, and to better understand how pathology may contribute to associated disease states.

REFERENCES

REFERENCES

- Ahlsén, G., Lindström, S., 1982. Mutual inhibition between perigeniculate neurones. *Brain Res.* 236, 482–486. [https://doi.org/10.1016/0006-8993\(82\)90731-4](https://doi.org/10.1016/0006-8993(82)90731-4)
- Arcelli, P., Frasconi, C., Regondi, M.C., Biasi, S.D., Spreafico, R., 1997. GABAergic Neurons in Mammalian Thalamus: A Marker of Thalamic Complexity? *Brain Res. Bull.* 42, 27–37. [https://doi.org/10.1016/S0361-9230\(96\)00107-4](https://doi.org/10.1016/S0361-9230(96)00107-4)
- Asanuma, C., 1994. GABAergic and pallidal terminals in the thalamic reticular nucleus of squirrel monkeys. *Exp. Brain Res.* 101. <https://doi.org/10.1007/BF00227337>
- Asanuma, C., 1989. Axonal arborizations of a magnocellular basal nucleus input and their relation to the neurons in the thalamic reticular nucleus of rats. *Proc. Natl. Acad. Sci.* 86, 4746–4750. <https://doi.org/10.1073/pnas.86.12.4746>
- Asanuma, C., Porter, L.L., 1990. Light and electron microscopic evidence for a GABAergic projection from the caudal basal forebrain to the thalamic reticular nucleus in rats. *J. Comp. Neurol.* 302, 159–172. <https://doi.org/10.1002/cne.903020112>
- Astori, S., Lüthi, A., 2013. Synaptic Plasticity at Intrathalamic Connections via CaV3.3 T-type Ca²⁺ Channels and GluN2B-Containing NMDA Receptors. *J. Neurosci.* 33, 624–630. <https://doi.org/10.1523/JNEUROSCI.3185-12.2013>
- Avanzini, G., de Curtis, M., Marescaux, C., Panzica, F., Spreafico, R., Vergnes, M., 1992. Role of the thalamic reticular nucleus in the generation of rhythmic thalamo-cortical activities subserving spike and waves, in: Marescaux, C., Vergnes, M., Bernasconi, R. (Eds.), *Generalized Non-Convulsive Epilepsy: Focus on GABA-B Receptors*, Journal of Neural Transmission. Springer, Vienna, pp. 85–95. https://doi.org/10.1007/978-3-7091-9206-1_6
- Avanzini, G., Vergnes, M., Spreafico, R., Marescaux, C., 1993. Calcium-Dependent Regulation of Genetically Determined Spike and Waves by the Reticular Thalamic Nucleus of Rats. *Epilepsia* 34, 1–7. <https://doi.org/10.1111/j.1528-1157.1993.tb02369.x>
- Bal, T., McCormick, D.A., 1993 Mechanisms of oscillatory activity in guinea-pig nucleus reticularis thalami in vitro: a mammalian pacemaker. *J. Physiol.* 468, 669–691. <https://doi.org/10.1113/jphysiol.1993.sp019794>
- Barrionuevo, G., Benoit, O., Tempier, P., 1981. Evidence for two types of firing pattern during the sleep-waking cycle in the reticular thalamic nucleus of the cat. *Exp. Neurol.* 72, 486–501. [https://doi.org/10.1016/0014-4886\(81\)90238-7](https://doi.org/10.1016/0014-4886(81)90238-7)

- Bazhenov, M., Timofeev, I., Steriade, M., Sejnowski, T., 2000. Spiking-Bursting Activity in the Thalamic Reticular Nucleus Initiates Sequences of Spindle Oscillations in Thalamic Networks. *J. Neurophysiol.* 84, 1076–1087. <https://doi.org/10.1152/jn.2000.84.2.1076>
- Bezdudnaya, T., Cano, M., Bereshpolova, Y., Stoelzel, C.R., Alonso, J.-M., Swadlow, H.A., 2006. Thalamic Burst Mode and Inattention in the Awake LGNd. *Neuron* 49, 421–432. <https://doi.org/10.1016/j.neuron.2006.01.010>
- Bickford, M.E., Günlük, A.E., Horn, S.C. van, Sherman, S.M., 1994. GABAergic projection from the basal forebrain to the visual sector of the thalamic reticular nucleus in the cat. *J. Comp. Neurol.* 348, 481–510. <https://doi.org/10.1002/cne.903480402>
- Bourassa, J., Desche[^]nes, M., 1995. Corticothalamic projections from the primary visual cortex in rats: a single fiber study using biocytin as an anterograde tracer. *Neuroscience* 66, 253–263. [https://doi.org/10.1016/0306-4522\(95\)00009-8](https://doi.org/10.1016/0306-4522(95)00009-8)
- Bovenkamp-Janssen, M.C. van de, Scheenen, W.J.J.M., Kuijpers-Kwant, F.J., Kozicz, T., Veening, J.G., Luijtelaar, E.L.J.M. van, McEnery, M.W., Roubos, E.W., 2004. Differential expression of high voltage-activated Ca²⁺ channel types in the rostral reticular thalamic nucleus of the absence epileptic WAG/Rij rat. *J. Neurobiol.* 58, 467–478. <https://doi.org/10.1002/neu.10291>
- Broicher, T., Kanyshkova, T., Meuth, P., Pape, H.-C., Budde, T., 2008. Correlation of T-channel coding gene expression, IT, and the low threshold Ca²⁺ spike in the thalamus of a rat model of absence epilepsy. *Mol. Cell. Neurosci.* 39, 384–399. <https://doi.org/10.1016/j.mcn.2008.07.012>
- Brunton, J., Charpak, S., 1992 HETEROGENEITY OF CELL FIRING PROPERTIES AND OPIOID SENSITIVITY IN THE THALAMIC RETICULAR NUCLEUS 5.
- Budde, T., Munsch, T., Pape, H.-C., 1998. Distribution of L-type calcium channels in rat thalamic neurones. *Eur. J. Neurosci.* 10, 586–597. <https://doi.org/10.1046/j.1460-9568.1998.00067.x>
- Cain, S.M., Snutch, T.P., 2010. Contributions of T-type calcium channel isoforms to neuronal firing. *Channels* 4, 475–482. <https://doi.org/10.4161/chan.4.6.14106>
- Çavdar, S., Onat, F., Çakmak, Y.Ö., Saka, E., Yananlı, H.R., Aker, R., 2006. Connections of the zona incerta to the reticular nucleus of the thalamus in the rat. *J. Anat.* 209, 251–258. <https://doi.org/10.1111/j.1469-7580.2006.00600.x>
- Chen, Y., Parker, W.D., Wang, K., 2014. The Role of T-Type Calcium Channel Genes in Absence Seizures. *Front. Neurol.* 5. <https://doi.org/10.3389/fneur.2014.00045>

- Chen, Z., Wimmer, R.D., Wilson, M.A., Halassa, M.M., 2016. Thalamic Circuit Mechanisms Link Sensory Processing in Sleep and Attention. *Front. Neural Circuits* 9. <https://doi.org/10.3389/fncir.2015.00083>
- Cicirata, F., Angaut, P., Serapide, M.F., Panto, M.R., 1990. Functional organization of the direct and indirect projection via the reticularis thalami nuclear complex from the motor cortex to the thalamic nucleus ventralis lateralis. *Exp. Brain Res.* 79, 325–337. <https://doi.org/10.1007/BF00608242>
- Clemente-Perez, A., Makinson, S.R., Higashikubo, B., Brovarney, S., Cho, F.S., Urry, A., Holden, S.S., Wimer, M., Dávid, C., Fenno, L.E., Acsády, L., Deisseroth, K., Paz, J.T., 2017. Distinct Thalamic Reticular Cell Types Differentially Modulate Normal and Pathological Cortical Rhythms. *Cell Rep.* 19, 2130–2142. <https://doi.org/10.1016/j.celrep.2017.05.044>
- Coleman, K.A., Mitrofanis, J., 1996. Organization of the Visual Reticular Thalamic Nucleus of the Rat. *European Journal of Neuroscience* 8, 388–404. <https://doi.org/10.1111/j.1460-9568.1996.tb01222.x>
- Contreras, D., Curro Dossi, R., Steriade, M., 1992. Bursting and tonic discharges in two classes of reticular thalamic neurons. *J. Neurophysiol.* 68, 973–977. <https://doi.org/10.1152/jn.1992.68.3.973>
- Cox, C.L., Huguenard, J.R., Prince, D.A., 1997. Nucleus reticularis neurons mediate diverse inhibitory effects in thalamus. *Proc. Natl. Acad. Sci.* 94, 8854–8859. <https://doi.org/10.1073/pnas.94.16.8854>
- Cox, C.L., Huguenard, J.R., Prince, D.A., 1996. Heterogeneous axonal arborizations of rat thalamic reticular neurons in the ventrobasal nucleus. *J. Comp. Neurol.* 366, 416–430. [https://doi.org/10.1002/\(SICI\)1096-9861\(19960311\)366:3<416::AID-CNE4>3.0.CO;2-7](https://doi.org/10.1002/(SICI)1096-9861(19960311)366:3<416::AID-CNE4>3.0.CO;2-7)
- Crabtree, J.W., 2018. Functional Diversity of Thalamic Reticular Subnetworks. *Front. Syst. Neurosci.* 12. <https://doi.org/10.3389/fnsys.2018.00041>
- Crabtree, J.W., 1996. Organization in the somatosensory sector of the cat's thalamic reticular nucleus. *J. Comp. Neurol.* 366, 207–222. [https://doi.org/10.1002/\(SICI\)1096-9861\(19960304\)366:2<207::AID-CNE2>3.0.CO;2-9](https://doi.org/10.1002/(SICI)1096-9861(19960304)366:2<207::AID-CNE2>3.0.CO;2-9)
- Crabtree, J.W., 1992. The Somatotopic Organization Within the Rabbit's Thalamic Reticular Nucleus. *Eur. J. Neurosci.* 4, 1343–1351. <https://doi.org/10.1111/j.1460-9568.1992.tb00159.x>
- Crandall, S.R., Govindaiah, G., Cox, C.L., 2010. Low-Threshold Ca²⁺ Current Amplifies Distal Dendritic Signaling in Thalamic Reticular Neurons. *J. Neurosci.* 30, 15419–15429. <https://doi.org/10.1523/JNEUROSCI.3636-10.2010>

- Crick, F., 1984. Function of the thalamic reticular complex: the searchlight hypothesis. *Proc. Natl. Acad. Sci.* 81, 4586–4590. <https://doi.org/10.1073/pnas.81.14.4586>
- Cropper, E.C., Eisenman, J.S., Azmitia, E.C., 1984. An immunocytochemical study of the serotonergic innervation of the thalamus of the rat. *J. Comp. Neurol.* 224, 38–50. <https://doi.org/10.1002/cne.902240104>
- Cruikshank, S.J., Urabe, H., Nurmikko, A.V., Connors, B.W., 2010. Pathway-Specific Feedforward Circuits between Thalamus and Neocortex Revealed by Selective Optical Stimulation of Axons. *Neuron* 65, 230–245. <https://doi.org/10.1016/j.neuron.2009.12.025>
- Cueni, L., Canepari, M., Adelman, J.P., Lüthi, A., 2008a. Ca²⁺ signaling by T-type Ca²⁺ channels in neurons. *Pflüg. Arch. - Eur. J. Physiol.* 457, 1161. <https://doi.org/10.1007/s00424-008-0582-6>
- Cueni, L., Canepari, M., Luján, R., Emmenegger, Y., Watanabe, M., Bond, C.T., Franken, P., Adelman, J.P., Lüthi, A., 2008b. T-type Ca²⁺ channels, SK2 channels and SERCAs gate sleep-related oscillations in thalamic dendrites. *Nat. Neurosci.* 11, 683–692. <https://doi.org/10.1038/nn.2124>
- David, F., Schmiedt, J.T., Taylor, H.L., Orban, G., Giovanni, G.D., Uebele, V.N., Renger, J.J., Lambert, R.C., Leresche, N., Crunelli, V., 2013. Essential Thalamic Contribution to Slow Waves of Natural Sleep. *J. Neurosci.* 33, 19599–19610. <https://doi.org/10.1523/JNEUROSCI.3169-13.2013>
- Deleuze, C., Huguenard, J.R., 2016. Two classes of excitatory synaptic responses in rat thalamic reticular neurons. *J. Neurophysiol.* 116, 995–1011. <https://doi.org/10.1152/jn.01121.2015>
- Deleuze, C., Huguenard, J.R., 2006. Distinct Electrical and Chemical Connectivity Maps in the Thalamic Reticular Nucleus: Potential Roles in Synchronization and Sensation. *J. Neurosci.* 26, 8633–8645. <https://doi.org/10.1523/JNEUROSCI.2333-06.2006>
- Deschenes, M., Paradis, M., Roy, J.P., Steriade, M., 1984. Electrophysiology of neurons of lateral thalamic nuclei in cat: resting properties and burst discharges. *J. Neurophysiol.* 51, 1196–1219. <https://doi.org/10.1152/jn.1984.51.6.1196>
- Destexhe, A., Contreras, D., Sejnowski, T.J., Steriade, M., 1994. A model of spindle rhythmicity in the isolated thalamic reticular nucleus. *J. Neurophysiol.* 72, 803–818. <https://doi.org/10.1152/jn.1994.72.2.803>
- Destexhe, A., Contreras, D., Steriade, M., Sejnowski, T.J., Huguenard, J.R., 1996. In vivo, in vitro, and computational analysis of dendritic calcium currents in thalamic reticular neurons. *J. Neurosci.* 16, 169–185.

- Domich, L., Oakson, G., Steriade, M., 1986. Thalamic burst patterns in the naturally sleeping cat: a comparison between cortically projecting and reticularis neurones. *J. Physiol.* 379, 429–449. <https://doi.org/10.1113/jphysiol.1986.sp016262>
- Fernandez, L.M., Vantomme, G., Osorio-Forero, A., Cardis, R., Béard, E., Lüthi, A., 2018. Thalamic reticular control of local sleep in mouse sensory cortex. *eLife* 7, e39111. <https://doi.org/10.7554/eLife.39111>
- Fernandez, L.M.J., Pellegrini, C., Vantomme, G., Béard, E., Lüthi, A., Astori, S., 2017. Cortical afferents onto the nucleus Reticularis thalami promote plasticity of low-threshold excitability through GluN2C-NMDARs. *Sci. Rep.* 7, 12271. <https://doi.org/10.1038/s41598-017-12552-8>
- Ferrarelli, F., Tononi, G., 2011. The Thalamic Reticular Nucleus and Schizophrenia. *Schizophr. Bull.* 37, 306–315. <https://doi.org/10.1093/schbul/sbq142>
- Fitzgibbon, T., Tevah, L.V., Sefton, A.J., 1995. Connections between the reticular nucleus of the thalamus and pulvinar-lateralis posterior complex: A WGA-HRP study. *J. Comp. Neurol.* 363, 489–504. <https://doi.org/10.1002/cne.903630311>
- Friedberg, E.B., Ross, D.T., 1993. Degeneration of rat thalamic reticular neurons following intrathalamic domoic acid injection. *Neurosci. Lett.* 151, 115–119. [https://doi.org/10.1016/0304-3940\(93\)90060-X](https://doi.org/10.1016/0304-3940(93)90060-X)
- Gandia, J., De Las Heras, S., García, M., Giménez-Amaya, J.M., 1993. Afferent projections to the reticular thalamic nucleus from the globus pallidus and the substantia nigra in the rat. *Brain Res. Bull.* 32, 351–358. [https://doi.org/10.1016/0361-9230\(93\)90199-L](https://doi.org/10.1016/0361-9230(93)90199-L)
- Golshani, P., Liu, X.-B., Jones, E.G., 2001. Differences in quantal amplitude reflect GluR4-subunit number at corticothalamic synapses on two populations of thalamic neurons. *Proc. Natl. Acad. Sci.* 98, 4172–4177. <https://doi.org/10.1073/pnas.061013698>
- Govindaiah, G., Wang, T., Gillette, M.U., Crandall, S.R., Cox, C.L., 2010. Regulation of Inhibitory Synapses by Presynaptic D4 Dopamine Receptors in Thalamus. *J. Neurophysiol.* 104, 2757–2765. <https://doi.org/10.1152/jn.00361.2010>
- Guillery, R.W., 1967. Patterns of fiber degeneration in the dorsal lateral geniculate nucleus of the cat following lesions in the visual cortex. *J. Comp. Neurol.* 130, 197–221. <https://doi.org/10.1002/cne.901300303>
- Guillery, R.W., Harting, J.K., 2003. Structure and connections of the thalamic reticular nucleus: Advancing views over half a century. *J. Comp. Neurol.* 463, 360–371. <https://doi.org/10.1002/cne.10738>
- Guillery, R.W., Sherman, S.M., 2002. Thalamic Relay Functions and Their Role in Corticocortical

- Communication: Generalizations from the Visual System. *Neuron* 33, 163–175.
[https://doi.org/10.1016/S0896-6273\(01\)00582-7](https://doi.org/10.1016/S0896-6273(01)00582-7)
- Haas, J.S., Zavala, B., Landisman, C.E., 2011. Activity-Dependent Long-Term Depression of Electrical Synapses. *Science* 334, 389–393. <https://doi.org/10.1126/science.1207502>
- Halassa, M.M., Chen, Z., Wimmer, R.D., Brunetti, P.M., Zhao, S., Zikopoulos, B., Wang, F., Brown, E.N., Wilson, M.A., 2014. State-Dependent Architecture of Thalamic Reticular Subnetworks. *Cell* 158, 808–821. <https://doi.org/10.1016/j.cell.2014.06.025>
- Hallanger, A.E., Levey, A.I., Lee, H.J., Rye, D.B., Wainer, B.H., 1987. The origins of cholinergic and other subcortical afferents to the thalamus in the rat. *J. Comp. Neurol.* 262, 105–124. <https://doi.org/10.1002/cne.902620109>
- Hartings, J.A., Temereanca, S., Simons, D.J., 2003. State-Dependent Processing of Sensory Stimuli by Thalamic Reticular Neurons. *J. Neurosci.* 23, 5264–5271. <https://doi.org/10.1523/JNEUROSCI.23-12-05264.2003>
- Hayama, T., Hashimoto, K., Ogawa, H., 1994. Anatomical location of a taste-related region in the thalamic reticular nucleus in rats. *Neuroscience Research* 18, 291–299. [https://doi.org/10.1016/0168-0102\(94\)90165-1](https://doi.org/10.1016/0168-0102(94)90165-1)
- Hazrati, L.-N., Parent, A., 1991. Projection from the external pallidum to the reticular thalamic nucleus in the squirrel monkey. *Brain Res.* 550, 142–146. [https://doi.org/10.1016/0006-8993\(91\)90418-U](https://doi.org/10.1016/0006-8993(91)90418-U)
- Hou, G., Smith, A.G., Zhang, Z.-W., 2016. Lack of Intrinsic GABAergic Connections in the Thalamic Reticular Nucleus of the Mouse. *Journal of Neuroscience* 36, 7246–7252. <https://doi.org/10.1523/JNEUROSCI.0607-16.2016>
- Houser, C.R., Vaughn, J.E., Barber, R.P., Roberts, E., 1980. GABA neurons are the major cell type of the nucleus reticularis thalami. *Brain Res.* 200, 341–354. [https://doi.org/10.1016/0006-8993\(80\)90925-7](https://doi.org/10.1016/0006-8993(80)90925-7)
- Huguenard, J., Prince, D., 1992. A novel T-type current underlies prolonged Ca(2+)-dependent burst firing in GABAergic neurons of rat thalamic reticular nucleus. *J. Neurosci.* 12, 3804–3817. <https://doi.org/10.1523/JNEUROSCI.12-10-03804.1992>
- Huh, Y., Cho, J., 2016. Differential Responses of Thalamic Reticular Neurons to Nociception in Freely Behaving Mice. *Front. Behav. Neurosci.* 10. <https://doi.org/10.3389/fnbeh.2016.00223>
- Huntsman, M.M., Huguenard, J.R., 2000. Nucleus-Specific Differences in GABA_A-Receptor-Mediated Inhibition Are Enhanced During Thalamic Development. *J. Neurophysiol.* 83, 350–358. <https://doi.org/10.1152/jn.2000.83.1.350>

- Huntsman, M.M., Porcello, D.M., Homanics, G.E., DeLorey, T.M., Huguenard, J.R., 1999. Reciprocal Inhibitory Connections and Network Synchrony in the Mammalian Thalamus. *Science* 283, 541–543. <https://doi.org/10.1126/science.283.5401.541>
- Iossifov, I., Ronemus, M., Levy, D., Wang, Z., Hakker, I., Rosenbaum, J., Yamrom, B., Lee, Y., Narzisi, G., Leotta, A., Kendall, J., Grabowska, E., Ma, B., Marks, S., Rodgers, L., Stepansky, A., Troge, J., Andrews, P., Bekritsky, M., Pradhan, K., Ghiban, E., Kramer, M., Parla, J., Demeter, R., Fulton, L.L., Fulton, R.S., Magrini, V.J., Ye, K., Darnell, J.C., Darnell, R.B., Mardis, E.R., Wilson, R.K., Schatz, M.C., McCombie, W.R., Wigler, M., 2012. De Novo Gene Disruptions in Children on the Autistic Spectrum. *Neuron* 74, 285–299. <https://doi.org/10.1016/j.neuron.2012.04.009>
- Jahnsen, H., Llinás, R., 1984a. Ionic basis for the electro-responsiveness and oscillatory properties of guinea-pig thalamic neurones in vitro. *J. Physiol.* 349, 227–247. <https://doi.org/10.1113/jphysiol.1984.sp015154>
- Jahnsen, H., Llinás, R., 1984b. Electrophysiological properties of guinea-pig thalamic neurones: an in vitro study. *J. Physiol.* 349, 205–226. <https://doi.org/10.1113/jphysiol.1984.sp015153>
- Joksovic, P.M., Bayliss, D.A., Todorovic, S.M., 2005. Different kinetic properties of two T-type Ca²⁺ currents of rat reticular thalamic neurones and their modulation by enflurane. *J. Physiol.* 566, 125–142. <https://doi.org/10.1113/jphysiol.2005.086579>
- Jones, E.G., 1975. Some aspects of the organization of the thalamic reticular complex. *J. Comp. Neurol.* 162, 285–308. <https://doi.org/10.1002/cne.901620302>
- Kanyshkova, T., Ehling, P., Cerina, M., Meuth, P., Zobeiri, M., Meuth, S.G., Pape, H.-C., Budde, T., 2014. Regionally specific expression of high-voltage-activated calcium channels in thalamic nuclei of epileptic and non-epileptic rats. *Mol. Cell. Neurosci.* 61, 110–122. <https://doi.org/10.1016/j.mcn.2014.06.005>
- Kim, U., McCormick, D.A., 1998. The Functional Influence of Burst and Tonic Firing Mode on Synaptic Interactions in the Thalamus. *J. Neurosci.* 18, 9500–9516. <https://doi.org/10.1523/JNEUROSCI.18-22-09500.1998>
- Kim, U., Sanchez-Vives, M.V., McCormick, D.A., 1997. Functional Dynamics of GABAergic Inhibition in the Thalamus. *Science* 278, 130–134. <https://doi.org/10.1126/science.278.5335.130>
- Kleiman-Weiner, M., Beenhakker, M.P., Segal, W.A., Huguenard, J.R., 2009. Synergistic Roles of GABAA Receptors and SK Channels in Regulating Thalamocortical Oscillations. *J. Neurophysiol.* 102, 203–213. <https://doi.org/10.1152/jn.91158.2008>

- Kolmac, C.I., Mitrofanis, J., 1997. Organisation of the reticular thalamic projection to the intralaminar and midline nuclei in rats. *J. Comp. Neurol.* 377, 165–178. [https://doi.org/10.1002/\(SICI\)1096-9861\(19970113\)377:2<165::AID-CNE2>3.0.CO;2-1](https://doi.org/10.1002/(SICI)1096-9861(19970113)377:2<165::AID-CNE2>3.0.CO;2-1)
- Kovács, K., Sík, A., Ricketts, C., Timofeev, I., 2010. Subcellular distribution of low-voltage activated T-type Ca²⁺ channel subunits (Cav3.1 and Cav3.3) in reticular thalamic neurons of the cat. *J. Neurosci. Res.* 88, 448–460. <https://doi.org/10.1002/jnr.22200>
- Krol, A., Wimmer, R.D., Halassa, M.M., Feng, G., 2018. Thalamic Reticular Dysfunction as a Circuit Endophenotype in Neurodevelopmental Disorders. *Neuron* 98, 282–295. <https://doi.org/10.1016/j.neuron.2018.03.021>
- Lam, Y.-W., Sherman, S.M., 2011. Functional Organization of the Thalamic Input to the Thalamic Reticular Nucleus. *J. Neurosci. Off. J. Soc. Neurosci.* 31, 6791–6799. <https://doi.org/10.1523/JNEUROSCI.3073-10.2011>
- Lamar, K.-M.J., Carvill, G.L., 2018. Chromatin Remodeling Proteins in Epilepsy: Lessons From CHD2-Associated Epilepsy. *Front. Mol. Neurosci.* 11. <https://doi.org/10.3389/fnmol.2018.00208>
- Landisman, C.E., 2005. Long-Term Modulation of Electrical Synapses in the Mammalian Thalamus. *Science* 310, 1809–1813. <https://doi.org/10.1126/science.1114655>
- Landisman, C.E., Long, M.A., Beierlein, M., Deans, M.R., Paul, D.L., Connors, B.W., 2002. Electrical Synapses in the Thalamic Reticular Nucleus. *J. Neurosci.* 22, 1002–1009. <https://doi.org/10.1523/JNEUROSCI.22-03-01002.2002>
- Lee, K.H., McCormick, D.A., 1996. Abolition of Spindle Oscillations by Serotonin and Norepinephrine in the Ferret Lateral Geniculate and Perigeniculate Nuclei In Vitro. *Neuron* 17, 309–321. [https://doi.org/10.1016/S0896-6273\(00\)80162-2](https://doi.org/10.1016/S0896-6273(00)80162-2)
- Lee, K.H., McCormick, D.A., 1995. Acetylcholine excites GABAergic neurons of the ferret perigeniculate nucleus through nicotinic receptors. *J. Neurophysiol.* 73, 2123–2128. <https://doi.org/10.1152/jn.1995.73.5.2123>
- Lee, S.-H., Govindaiah, G., Cox, C.L., 2007. Heterogeneity of firing properties among rat thalamic reticular nucleus neurons. *J. Physiol.* 582, 195–208. <https://doi.org/10.1113/jphysiol.2007.134254>
- Lee, S.M., Friedberg, M.H., Ebner, F.F., 1994. The role of GABA-mediated inhibition in the rat ventral posterior medial thalamus. I. Assessment of receptive field changes following thalamic reticular nucleus lesions. *Journal of Neurophysiology* 71, 1702–1715. <https://doi.org/10.1152/jn.1994.71.5.1702>

- Letinic, K., Rakic, P., 2001. Telencephalic origin of human thalamic GABAergic neurons. *Nat. Neurosci.* 4, 931–936. <https://doi.org/10.1038/nn0901-931>
- Liu, X.-B., Jones, E.G., 1999a. Predominance of corticothalamic synaptic inputs to thalamic reticular nucleus neurons in the rat. *J. Comp. Neurol.* 414, 67–79. [https://doi.org/10.1002/\(SICI\)1096-9861\(19991108\)414:1<67::AID-CNE6>3.0.CO;2-Z](https://doi.org/10.1002/(SICI)1096-9861(19991108)414:1<67::AID-CNE6>3.0.CO;2-Z)
- Liu, X.-B., Jones, E.G., 1999b. Predominance of corticothalamic synaptic inputs to thalamic reticular nucleus neurons in the rat. *J. Comp. Neurol.* 414, 67–79. [https://doi.org/10.1002/\(SICI\)1096-9861\(19991108\)414:1<67::AID-CNE6>3.0.CO;2-Z](https://doi.org/10.1002/(SICI)1096-9861(19991108)414:1<67::AID-CNE6>3.0.CO;2-Z)
- Liu, X.B., Warren, R.A., Jones, E.G., 1995. Synaptic distribution of afferents from reticular nucleus in ventroposterior nucleus of cat thalamus. *J. Comp. Neurol.* 352, 187–202. <https://doi.org/10.1002/cne.903520203>
- Liu, Z., Vergnes, M., Depaulis, A., Marescaux, C., 1992. Involvement of intrathalamic GABA_B neurotransmission in the control of absence seizures in the rat. *Neuroscience* 48, 87–93. [https://doi.org/10.1016/0306-4522\(92\)90340-8](https://doi.org/10.1016/0306-4522(92)90340-8)
- Llinás, R.R., Steriade, M., 2006. Bursting of Thalamic Neurons and States of Vigilance. *J. Neurophysiol.* 95, 3297–3308. <https://doi.org/10.1152/jn.00166.2006>
- Long, M.A., Landisman, C.E., Connors, B.W., 2004. Small Clusters of Electrically Coupled Neurons Generate Synchronous Rhythms in the Thalamic Reticular Nucleus. *J. Neurosci.* 24, 341–349. <https://doi.org/10.1523/JNEUROSCI.3358-03.2004>
- Lozsádi, D.A., 1994. Organization of cortical afferents to the rostral, limbic sector of the rat thalamic reticular nucleus. *J. Comp. Neurol.* 341, 520–533. <https://doi.org/10.1002/cne.903410408>
- Lübke, J., 1993. Morphology of neurons in the thalamic reticular nucleus (TRN) of mammals as revealed by intracellular injections into fixed brain slices. *J. Comp. Neurol.* 329, 458–471. <https://doi.org/10.1002/cne.903290404>
- Marlinski, V., Beloozerova, I.N., 2014. Burst firing of neurons in the thalamic reticular nucleus during locomotion. *J. Neurophysiol.* 112, 181–192. <https://doi.org/10.1152/jn.00366.2013>
- Martinez-Garcia, R.I., Voelcker, B., Zaltsman, J.B., Patrick, S.L., Stevens, T.R., Connors, B.W., Cruikshank, S.J., 2020. Two dynamically distinct circuits drive inhibition in the sensory thalamus. *Nature* 583, 813–818. <https://doi.org/10.1038/s41586-020-2512-5>
- McAlonan, K., Cavanaugh, J., Wurtz, R.H., 2006. Attentional Modulation of Thalamic Reticular Neurons. *J. Neurosci.* 26, 4444–4450. <https://doi.org/10.1523/JNEUROSCI.5602-05.2006>

- McCormick, D.A., 1989. Cholinergic and noradrenergic modulation of thalamocortical processing. *Trends Neurosci.* 12, 215–221. [https://doi.org/10.1016/0166-2236\(89\)90125-2](https://doi.org/10.1016/0166-2236(89)90125-2)
- McCormick, D.A., Pape, H.C., 1990. Properties of a hyperpolarization-activated cation current and its role in rhythmic oscillation in thalamic relay neurones. *The Journal of Physiology* 431, 291–318. <https://doi.org/10.1113/jphysiol.1990.sp018331>
- McCormick, D.A., Prince, D.A., 1986. Acetylcholine induces burst firing in thalamic reticular neurones by activating a potassium conductance. *Nature* 319, 402–405. <https://doi.org/10.1038/319402a0>
- McCormick, D.A., Wang, Z., 1991. Serotonin and noradrenaline excite GABAergic neurones of the guinea-pig and cat nucleus reticularis thalami. *J. Physiol.* 442, 235–255. <https://doi.org/10.1113/jphysiol.1991.sp018791>
- Mesulam, M.-M., Mufson, E.J., Wainer, B.H., Levey, A.I., 1983. Central cholinergic pathways in the rat: An overview based on an alternative nomenclature (Ch1–Ch6). *Neuroscience* 10, 1185–1201. [https://doi.org/10.1016/0306-4522\(83\)90108-2](https://doi.org/10.1016/0306-4522(83)90108-2)
- Mrzljak, L., Bergson, C., Pappy, M., Huff, R., Levenson, R., Goldman-Rakic, P.S., 1996. Localization of dopamine D4 receptors in GABAergic neurons of the primate brain. *Nature* 381, 245–248. <https://doi.org/10.1038/381245a0>
- Mulle, C., Madariaga, A., Deschenes, M., 1986. Morphology and electrophysiological properties of reticularis thalami neurons in cat: in vivo study of a thalamic pacemaker. *J. Neurosci.* 6, 2134–2145. <https://doi.org/10.1523/JNEUROSCI.06-08-02134.1986>
- Murata, Y., Colonnese, M.T., 2019. Thalamic inhibitory circuits and network activity development. *Brain Res.* 1706, 13–23. <https://doi.org/10.1016/j.brainres.2018.10.024>
- Noor, A., Whibley, A., Marshall, C.R., Gianakopoulos, P.J., Piton, A., Carson, A.R., Orlic-Milacic, M., Lionel, A.C., Sato, D., Pinto, D., Drmic, I., Noakes, C., Senman, L., Zhang, X., Mo, R., Gauthier, J., Crosbie, J., Pagnamenta, A.T., Munson, J., Estes, A.M., Fiebig, A., Franke, A., Schreiber, S., Stewart, A.F.R., Roberts, R., McPherson, R., Guter, S.J., Cook, E.H., Dawson, G., Schellenberg, G.D., Battaglia, A., Maestrini, E., Autism Genome Project Consortium, Jeng, L., Hutchison, T., Rajcan-Separovic, E., Chudley, A.E., Lewis, S.M.E., Liu, X., Holden, J.J., Fernandez, B., Zwaigenbaum, L., Bryson, S.E., Roberts, W., Szatmari, P., Gallagher, L., Stratton, M.R., Gecz, J., Brady, A.F., Schwartz, C.E., Schachar, R.J., Monaco, A.P., Rouleau, G.A., Hui, C. -c., Lucy Raymond, F., Scherer, S.W., Vincent, J.B., 2010. Disruption at the PTCHD1 Locus on Xp22.11 in Autism Spectrum Disorder and Intellectual Disability. *Science Translational Medicine* 2, 49ra68-49ra68. <https://doi.org/10.1126/scitranslmed.3001267>

- Ohara, P.T., Havton, L.A., 1996. Dendritic arbors of neurons from different regions of the rat thalamic reticular nucleus share a similar orientation. *Brain Res.* 731, 236–240. [https://doi.org/10.1016/0006-8993\(96\)00706-8](https://doi.org/10.1016/0006-8993(96)00706-8)
- Pare´, D., Hazrati, L.-N., Parent, A., Steriade, M., 1990. Substantia nigra pars reticulata projects to the reticular thalamic nucleus of the cat: a morphological and electrophysiological study. *Brain Res.* 535, 139–146. [https://doi.org/10.1016/0006-8993\(90\)91832-2](https://doi.org/10.1016/0006-8993(90)91832-2)
- Pellegrini, C., Lecci, S., Lüthi, A., Astori, S., 2016. Suppression of Sleep Spindle Rhythmogenesis in Mice with Deletion of CaV3.2 and CaV3.3 T-type Ca²⁺ Channels. *Sleep* 39, 875–885. <https://doi.org/10.5665/sleep.5646>
- Perez-Reyes, E., 2003. Molecular Physiology of Low-Voltage-Activated T-type Calcium Channels. *Physiol. Rev.* 83, 117–161. <https://doi.org/10.1152/physrev.00018.2002>
- Pinault, D., 2004. The thalamic reticular nucleus: structure, function and concept. *Brain Res. Rev.* 46, 1–31. <https://doi.org/10.1016/j.brainresrev.2004.04.008>
- Pinault, D., Deschênes, M., 1992. Voltage-dependent 40-Hz oscillations in rat reticular thalamic neurons in vivo. *Neuroscience* 51, 245–258. [https://doi.org/10.1016/0306-4522\(92\)90312-P](https://doi.org/10.1016/0306-4522(92)90312-P)
- Pinault, D., Deschênes, M., 1998. Projection and innervation patterns of individual thalamic reticular axons in the thalamus of the adult rat: A three-dimensional, graphic, and morphometric analysis. *J. Comp. Neurol.* 391, 180–203. [https://doi.org/10.1002/\(SICI\)1096-9861\(19980209\)391:2<180::AID-CNE3>3.0.CO;2-Z](https://doi.org/10.1002/(SICI)1096-9861(19980209)391:2<180::AID-CNE3>3.0.CO;2-Z)
- Pirchio, M., Lightowler, S., Crunelli, V., 1990. Postnatal development of the T calcium current in cat thalamocortical cells. *Neuroscience* 38, 39–45. [https://doi.org/10.1016/0306-4522\(90\)90372-B](https://doi.org/10.1016/0306-4522(90)90372-B)
- Pratt, J.A., Morris, B.J., 2015. The thalamic reticular nucleus: A functional hub for thalamocortical network dysfunction in schizophrenia and a target for drug discovery. *J. Psychopharmacol. (Oxf.)* 29, 127–137. <https://doi.org/10.1177/0269881114565805>
- Reichova, I., Sherman, S.M., 2004. Somatosensory Corticothalamic Projections: Distinguishing Drivers From Modulators. *Journal of Neurophysiology* 92, 2185–2197. <https://doi.org/10.1152/jn.00322.2004>
- Reinagel, P., Godwin, D., Sherman, S.M., Koch, C., 1999. Encoding of Visual Information by LGN Bursts. *J. Neurophysiol.* 81, 2558–2569. <https://doi.org/10.1152/jn.1999.81.5.2558>
- Rodríguez, J.J., Noristani, H.N., Hoover, W.B., Linley, S.B., Vertes, R.P., 2011. Serotonergic projections and serotonin receptor expression in the reticular nucleus of the thalamus in the rat. *Synapse* 65, 919–928. <https://doi.org/10.1002/syn.20920>

- Scheibel, M.E., Scheibel, A.B., 1966. The organization of the nucleus reticularis thalami: A golgi study. *Brain Res.* 1, 43–62. [https://doi.org/10.1016/0006-8993\(66\)90104-1](https://doi.org/10.1016/0006-8993(66)90104-1)
- Seabrook, T.A., Krahe, T.E., Govindaiah, G., Guido, W., 2013. Interneurons in the mouse visual thalamus maintain a high degree of retinal convergence throughout postnatal development. *Neural Develop.* 8, 24. <https://doi.org/10.1186/1749-8104-8-24>
- Sevetson, J., Fittro, S., Heckman, E., Haas, J.S., 2017. A calcium-dependent pathway underlies activity-dependent plasticity of electrical synapses in the thalamic reticular nucleus. *J. Physiol.* 595, 4417–4430. <https://doi.org/10.1113/JP274049>
- Sherman, S.M., 2001. Tonic and burst firing: dual modes of thalamocortical relay. *Trends in Neurosciences* 24, 122–126. [https://doi.org/10.1016/S0166-2236\(00\)01714-8](https://doi.org/10.1016/S0166-2236(00)01714-8)
- Shosaku, A., Kayama, Y., Sumitomo, I., 1984. Somatotopic organization in the rat thalamic reticular nucleus. *Brain Res.* 311, 57–63. [https://doi.org/10.1016/0006-8993\(84\)91398-2](https://doi.org/10.1016/0006-8993(84)91398-2)
- Sohal, V.S., Huguenard, J.R., 2003. Inhibitory Interconnections Control Burst Pattern and Emergent Network Synchrony in Reticular Thalamus. *J. Neurosci.* 23, 8978–8988. <https://doi.org/10.1523/JNEUROSCI.23-26-08978.2003>
- Sokhadze, G., Campbell, P.W., Guido, W., 2019 Postnatal development of cholinergic input to the thalamic reticular nucleus of the mouse. *Eur. J. Neurosci.* 0. <https://doi.org/10.1111/ejn.13942>
- Spreafico, R., Battaglia, G., Frassoni, C., 1991. The reticular thalamic nucleus (RTN) of the rat: Cytoarchitectural, Golgi, immunocytochemical, and horseradish peroxidase study. *J. Comp. Neurol.* 304, 478–490. <https://doi.org/10.1002/cne.903040311>
- Spreafico, R., de Curtis, M., Frassoni, C., Avanzini, G., 1988. Electrophysiological characteristics of morphologically identified reticular thalamic neurons from rat slices. *Neuroscience* 27, 629–638. [https://doi.org/10.1016/0306-4522\(88\)90294-1](https://doi.org/10.1016/0306-4522(88)90294-1)
- Steriade, M., Contreras, D., Dossi, R.C., Nunez, A., 1993. The slow (< 1 Hz) oscillation in reticular thalamic and thalamocortical neurons: scenario of sleep rhythm generation in interacting thalamic and neocortical networks. *J. Neurosci.* 13, 3284–3299. <https://doi.org/10.1523/JNEUROSCI.13-08-03284.1993>
- Steriade, M., Domich, L., Oakson, G., 1986. Reticularis thalami neurons revisited: activity changes during shifts in states of vigilance. *J. Neurosci.* 6, 68–81. <https://doi.org/10.1523/JNEUROSCI.06-01-00068.1986>
- Steriade, M., 2005. Sleep, epilepsy and thalamic reticular inhibitory neurons. *Trends Neurosci., INMED/TINS special issue: Multiple facets of GABAergic synapses* 28, 317–324. <https://doi.org/10.1016/j.tins.2005.03.007>

- Steullet, P., Cabungcal, J.-H., Bukhari, S.A., Ardelt, M.I., Pantazopoulos, H., Hamati, F., Salt, T.E., Cuenod, M., Do, K.Q., Berretta, S., 2017. The thalamic reticular nucleus in schizophrenia and bipolar disorder: role of parvalbumin-expressing neuron networks and oxidative stress. *Mol. Psychiatry*. <https://doi.org/10.1038/mp.2017.230>
- Sun, Q.-Q., Huguenard, J.R., Prince, D.A., 2002. Somatostatin Inhibits Thalamic Network Oscillations In Vitro: Actions on the GABAergic Neurons of the Reticular Nucleus. *J. Neurosci.* 22, 5374–5386. <https://doi.org/10.1523/JNEUROSCI.22-13-05374.2002>
- Sun, Y.-G., Pita-Almenar, J.D., Wu, C.-S., Renger, J.J., Uebele, V.N., Lu, H.-C., Beierlein, M., 2013. Biphasic Cholinergic Synaptic Transmission Controls Action Potential Activity in Thalamic Reticular Nucleus Neurons. *J. Neurosci.* 33, 2048–2059. <https://doi.org/10.1523/JNEUROSCI.3177-12.2013>
- Sun, Y.-G., Rupprecht, V., Zhou, L., Dasgupta, R., Seibt, F., Beierlein, M., 2016. mGluR1 and mGluR5 Synergistically Control Cholinergic Synaptic Transmission in the Thalamic Reticular Nucleus. *J. Neurosci.* 36, 7886–7896. <https://doi.org/10.1523/JNEUROSCI.0409-16.2016>
- Swadlow, H.A., Gusev, A.G., 2001. The impact of “bursting” thalamic impulses at a neocortical synapse. *Nat. Neurosci.* 4, 402–408. <https://doi.org/10.1038/86054>
- Talley, E.M., Cribbs, L.L., Lee, J.-H., Daud, A., Perez-Reyes, E., Bayliss, D.A., 1999. Differential Distribution of Three Members of a Gene Family Encoding Low Voltage-Activated (T-Type) Calcium Channels. *J. Neurosci.* 19, 1895–1911. <https://doi.org/10.1523/JNEUROSCI.19-06-01895.1999>
- Tennigkeit, F., Schwarz, D.W.F., Puil, E., 1998. Postnatal development of signal generation in auditory thalamic neurons. *Dev. Brain Res.* 109, 255–263. [https://doi.org/10.1016/S0165-3806\(98\)00056-X](https://doi.org/10.1016/S0165-3806(98)00056-X)
- Tsakiridou, E., Bertollini, L., Curtis, M. de, Avanzini, G., Pape, H.C., 1995. Selective increase in T-type calcium conductance of reticular thalamic neurons in a rat model of absence epilepsy. *J. Neurosci.* 15, 3110–3117. <https://doi.org/10.1523/JNEUROSCI.15-04-03110.1995>
- Van Horn, S.C., Sherman, S.M., 2004. Differences in projection patterns between large and small corticothalamic terminals. *J. Comp. Neurol.* 475, 406–415. <https://doi.org/10.1002/cne.20187>
- Wang, Z., Neely, R., Landisman, C.E., 2015. Activation of Group I and Group II Metabotropic Glutamate Receptors Causes LTD and LTP of Electrical Synapses in the Rat Thalamic Reticular Nucleus. *J. Neurosci.* 35, 7616–7625. <https://doi.org/10.1523/JNEUROSCI.3688-14.2015>

- Warren, R.A., Agmon, A., Jones, E.G., 1994. Oscillatory synaptic interactions between ventroposterior and reticular neurons in mouse thalamus in vitro. *J. Neurophysiol.* 72, 1993–2003. <https://doi.org/10.1152/jn.1994.72.4.1993>
- Warren, R.A., Jones, E.G., 1997. Maturation of Neuronal Form and Function in a Mouse Thalamo-Cortical Circuit. *J. Neurosci.* 17, 277–295. <https://doi.org/10.1523/JNEUROSCI.17-01-00277.1997>
- Wells, M.F., Wimmer, R.D., Schmitt, L.I., Feng, G., Halassa, M.M., 2016. Thalamic reticular impairment underlies attention deficit in *Ptchd1*^{Y/-} mice. *Nature* 532, 58–63. <https://doi.org/10.1038/nature17427>
- Williams, D., 1953. A study of thalamic and cortical rhythms in petit mal. *Brain* 76, 50–69. <https://doi.org/10.1093/brain/76.1.50>
- Yen, C.-T., Jones, E.G., 1983. Intracellular staining of physiologically identified neurons and axons in the somatosensory thalamus of the cat. *Brain Res.* 280, 148–154. [https://doi.org/10.1016/0006-8993\(83\)91183-6](https://doi.org/10.1016/0006-8993(83)91183-6)
- Ying, S.-W., Goldstein, P.A., 2005. Propofol-Block of SK Channels in Reticular Thalamic Neurons Enhances GABAergic Inhibition in Relay Neurons. *J. Neurophysiol.* 93, 1935–1948. <https://doi.org/10.1152/jn.01058.2004>
- Zhang, L., Jones, E.G., 2004. Corticothalamic Inhibition in the Thalamic Reticular Nucleus. *J. Neurophysiol.* 91, 759–766. <https://doi.org/10.1152/jn.00624.2003>
- Zikopoulos, B., Barbas, H., 2007. Circuits for multisensory integration and attentional modulation through the prefrontal cortex and the thalamic reticular nucleus in primates. *Rev. Neurosci.* 18, 417–438.
- Zolnik, T.A., Connors, B.W., 2016. Electrical synapses and the development of inhibitory circuits in the thalamus. *J. Physiol.* 594, 2579–2592. <https://doi.org/10.1113/JP271880>

CHAPTER 2: HETEROGENEITY OF BURST DISCHARGE IN THE THALAMIC RETICULAR NUCLEUS

Abstract

Long studied for its role in sensory processing, sleep rhythms, and attentional gating, the activities of the thalamic reticular nucleus (TRN) significantly impact the information flow between the thalamus and neocortex. The TRN receives synaptic inputs from both neocortical and thalamic regions and based upon this information it provides feedback and feedforward inhibition of thalamic neurons. TRN neurons typically discharge action potentials in two distinct modes: burst mode consisting of a transient, high frequency action potential discharge from a hyperpolarized membrane potential, and tonic mode consisting of repetitive action potential discharge from a relatively depolarized state. Previous studies have classified a burst discharge as distinct transient high frequency (> 250 Hz) trains of multiple action potentials however, these studies identified a broad range of frequencies of burst discharge in adult animals ranging from 3-342 Hz. In neurons with higher frequency discharge (> 100 Hz), the burst was composed of many action potentials. These cells had higher input resistances, higher action potential firing thresholds, narrower action potentials, and larger somata. The amplitude of the transient low threshold spike and the magnitude of the calcium current that underlies the burst discharge, was positively correlated with the burst discharge frequency and the number of action potentials per burst. Considering the vast array of functions carried out by the TRN, examination of the diversity of these neurons could provide insight into how intrinsic properties may relate to its various network activities.

Introduction

The TRN lies at an anatomical and physiological interface between the neocortex and thalamus. With this unique placement, TRN receives glutamatergic synaptic afferents from both corticothalamic and thalamocortical cell axons as they traverse the nucleus (Lam and Sherman, 2011; Pinault and Deschênes, 1998). As these corticothalamic and thalamocortical fibers traverse the TRN, they give rise to collaterals that provide excitatory afferent inputs to TRN neurons. The TRN neurons integrate this information and send efferent fibers to inhibit downstream thalamocortical neurons. While the TRN receives inputs from motor and limbic afferents, the focus of this study is on the sensory regions of TRN (Sokhadze et al., 2019; Zikopoulos and Barbas, 2007). Synaptic contacts from thalamocortical and corticothalamic afferents transmitting information from specific sensory modalities are not random, but topographically distributed throughout the TRN in discrete sectors (Crabtree, 1996, 1992; Lam and Sherman, 2011). As TRN neurons synapse onto downstream thalamocortical neuron targets, they may form closed or open circuits. The closed circuit in this case refers to TRN efferents synapsing with the same neurons that they receive inputs from, and in open circuits, the efferents may synapse with neurons of different thalamic nuclei. The open-circuit scenario could function to increase crosstalk among sensory modalities, since the thalamocortical inhibition from TRN, which is impacted by afferent inputs, will be potentially received by cells that process information within a different modality. It is clear from the variety of synaptic inputs, complex organization, and distribution of thalamic outputs, that the TRN is not a single modality output circuit. Instead, the TRN is a multi-modal nucleus that modulates information from nearly all sensory systems by balancing the activity of these circuits through thalamic inhibition.

The TRN has several roles in addition to modulation of sensory processing. Burst discharge exchanges between neocortex, thalamus, and TRN functions to generate and maintain sleep rhythms, such as the sleep spindles seen in early sleep stages and the slow wave rhythms of non-REM sleep (David et al., 2013; Pellegrini et al., 2016; Steriade, 2005). A pathologic condition which results from abnormal TRN burst discharge and has been especially tied to abnormal T-type calcium channel (T-channel) expression within the TRN is absence epilepsy (Bovenkamp-Janssen et al., 2004; Broicher et al., 2008; Ekonomou et al., 1998).

TRN neurons communicate with thalamic neurons via two distinct modes of action potential output: burst and tonic modes. Burst mode is characterized by a transient, high frequency discharge of action potentials (> 250 Hz) requiring the activation of voltage dependent low-threshold T-channels (Guido and Weyand, 1995; Lee et al., 2007; Lu et al., 1992). At relatively hyperpolarized potentials the T-channels are de-inactivated, allowing depolarization of the membrane potential to activate T-channels. This activation characteristically produces a transient membrane depolarization, referred to as a low-threshold spike (LTS), which is crowned by a transient, high frequency discharge of multiple action potentials. At relatively depolarized membrane potentials, T-channels are largely inactivated. Suprathreshold depolarization of the membrane in tonic mode will trigger action potential firing in which the frequency of action potential discharge is linearly related to the magnitude of the membrane depolarization (Contreras et al., 1992; Zhan et al., 1999). While all TRN neurons fire tonically at depolarized membrane states, a previously reported subset of TRN neurons, termed non-bursting neurons, continue to only discharge tonic action potentials during burst mode (Contreras et al., 1992; Lee et al., 2007). From a functional aspect, burst vs. tonic action potential discharge can have

significantly different impact on downstream thalamocortical neurons. In terms of inhibition, burst discharge engages both GABA_A and GABA_B receptor dependent inhibition, whereas tonic discharge predominantly engages GABA_A receptor dependent inhibition (Kim et al., 1997; Kim and McCormick, 1998).

For TRN neurons to maintain repetitive burst rhythms, small-conductance calcium-activated potassium channels (SK) are synergistically activated by the calcium influx of the burst. SK channels create a strong after-hyperpolarization potential (AHP) following the burst, which rapidly hyperpolarizes the cell and allows the T-channels to recover and more quickly be prepared to mediate another burst (Cueni et al., 2008; Kleiman-Weiner et al., 2009). While SK channels are strongly activated in TRN, it is unknown whether the distribution of SK channels is uniform along the dendrites of all TRN neurons. If densities of SK channels are not uniformly distributed, they could act as a selective burst modulator in which synaptic inputs at certain locations would result in a burst with strong SK-attenuation, while others could activate only T-channels resulting in a longer duration burst.

Intrinsic properties of individual TRN neurons are likely to play a significant role in TRN function. While there are several exogenous neuromodulatory molecules that can alter how a neuron responds to afferent inputs through changes in membrane state (Cox et al., 1995; Funke and Eysel, 1993; McCormick and Prince, 1986), this type of modulation would not be expected to change the downstream frequency-related output in TRN neurons that do not experience a voltage-dependent change in firing pattern in burst mode (i.e., non-bursting neurons).

A broad survey of TRN neurons identified a surprisingly wide distribution of burst frequencies for TRN neurons. The experiments within this study are designed to determine

potential mechanisms underlying these heterogeneous burst properties. Findings from this study are aimed to improve characterization of TRN function and classify how intrinsic physiology of these neurons relates to the diverse functions of the TRN.

Materials and Methods

Slice preparation

All animals were housed at the Michigan State University animal facilities and experimental procedures were conducted in accordance with the Institutional Animal Care and Use Committee (IACUC). Adult female and male C57BL/6J (WT), and SOM-IRES-Cre (Jackson Laboratories #013044) (Taniguchi et al., 2011) x Ai14 (Jackson Laboratories #007914) (Madisen et al., 2010) mice were utilized within these experiments (Average 42 ± 12 days old, range 30 to 111 days old). Animals were deeply anesthetized (3% isoflurane, 97% O₂) and in some cases perfused with the cold (4°C) oxygenated (95% O₂, 5% CO₂) slicing solution containing (in mM): 2.5 KCl, 1.25 NaH₂PO₄, 10.0 MgSO₄, 0.5 CaCl₂, 26.0 NaHCO₃, 10.0 glucose, and 234.0 sucrose. Horizontal brain slices (300 μm thickness) were made using a vibrating tissue slicer in a bath of the cold (4°C), oxygenated (95% O₂, 5% CO₂) slicing solution. Slices were hemisected and transferred to a warmed holding chamber (35°C) of oxygenated (95% O₂, 5% CO₂) artificial cerebrospinal fluid (ACSF) solution containing (in mM): 126.0 NaCl, 2.5 KCl, 1.25 NaH₂PO₄, 2.0 MgCl₂, 2.0 CaCl₂, 26.0 NaHCO₃, and 10.0 glucose. After 30 minutes, chamber temperature was returned to room temperature and slices incubated for a minimum of 60 minutes prior to recording.

Electrophysiology

Borosilicate glass micropipettes (4-6 M Ω resistance) were used to perform whole-cell TRN neuron recordings. Micropipettes were filled with a solution of (in mM): 117 K-gluconate, 13 KCl, 1.0 MgCl₂, 0.07 CaCl₂, 0.1 EGTA, 10 HEPES, 2.0 ATP, and 0.4 GTP. All experiments utilized a Zeiss microscope equipped with DIC optics (Thorndale, NY). TRN was located using a low power 5x objective, and individual neurons were identified using a high-power, water immersion 63x objective. Following break-in, cells were allowed to stabilize for at least five minutes prior to starting experiments. Only cells with an input resistance greater than 100 M Ω , resting membrane potential more negative than -50 mV, lack of spontaneous action potential firing, and evoked action potential peak > +0 mV were included for analyses. Data were obtained using a MultiClamp 700b amplifier, sampled at 20 kHz, and filtered at 10 kHz (Digidata 1440a, Molecular Devices, San Jose, CA). Reported voltages are corrected for an 8 mV liquid junction potential. PClamp software (Molecular Devices, Inc.) was used for data acquisition and analysis.

Pharmacology

All pharmaceutical agents were purchased from either Sigma-Aldrich Inc. or Tocris Bioscience (Bio-Techne). Concentrated stock solutions were prepared and diluted to final concentrations in ACSF prior to experimentation. All antagonist agents were bath applied for at least 10 minutes prior to commencing experiment. For experiments using agonists, these compounds were applied via syringe pump where the concentration of the drug within syringe was equal to 4x the final concentration, or 20-40 μ M, which resulted in a bath concentration of 5-10 μ M (Cox et al., 1995).

Morphology

Soma volume was calculated from z-stack images spanning the entire depth of the neuron. Alexa-594 (25 μ M) was included in the internal solution to visualize neurons, and neurons were allowed to fill for at least thirty minutes prior to image acquisition. Images were obtained using a two-photon laser scanning microscope (Ultima, Bruker). Data were acquired using Prairie View (Bruker). To calculate soma volume, images spanning the z-depth of the soma were imported into FIJI (NIH open source) (Solé et al., 2007).

Data Analysis

Analysis of general intrinsic properties were calculated using Clampfit (Molecular Devices). Either Mathematica or Microsoft Excel were used for statistical analyses. All values are reported as mean \pm standard deviation. Burst frequencies were calculated from the average frequency of the intervals of each action potential in a discrete burst cluster. If no discrete burst cluster was present the first two action potentials were used for analysis. Action potential threshold was calculated as the voltage at which the first derivative surpasses 10 mV/ms. Rheobase was measured as the lowest intensity current step (20 pA intervals, 1 s duration) to elicit an action potential from holding membrane potential of -60 mV. Half-width of the action potential was defined as the duration of the action potential at half amplitude, measured from the threshold. Input resistance was measured from the linear slope of a current-voltage relationship protocol. Measurements were taken from 1-4 points above and below 0 mV during the last 200ms of a series of 1 second duration current pulses with Δ 10-20 pA step sizes.

Results

Heterogeneous burst frequencies in the TRN

Whole-cell recordings were obtained from 264 TRN neurons to assess burst discharge characteristics. Neurons were held at -80 mV in current clamp, and burst discharge was elicited from depolarizing current steps (20 pA increments, 1s duration). Burst frequency was calculated from the average discharge frequency of all action potentials within the first burst response to the lowest intensity current step that produced a short latency, transient action potential discharge of ≥ 2 action potentials. If no discrete cluster of action potentials were present, the frequency of the first two action potentials was calculated. In a subset of 78 neurons (with > 100 Hz bursts and > 2 APs), the frequency of the first inter-spike-interval was compared to the average burst frequency and the two values were found to be highly correlated ($P < 0.001$, $r = 0.808$, $n = 78$).

Surprisingly, the average burst frequencies of TRN neurons were distributed across a broad range of frequencies (3-342 Hz; Figure 2.0 A, B). Based on prior studies (Brunton and Charpak, 1992.; Contreras et al., 1992; Guido and Weyand, 1995; Huguenard and Prince, 1992; Lee et al., 2007) a clear demarcation of high-frequency burst discharge was expected, and lower frequency discharges that would closely resemble tonic discharge, however this was not observed. As illustrated in Figure 2.0 C, most neurons with average burst frequencies of ≤ 100 Hz discharged only 2 action potentials (see methods for calculation) in burst mode (86/123 cells). In contrast, the vast majority of neurons with burst averages > 100 Hz fired 3 or more action potentials per burst (126/141 cells).

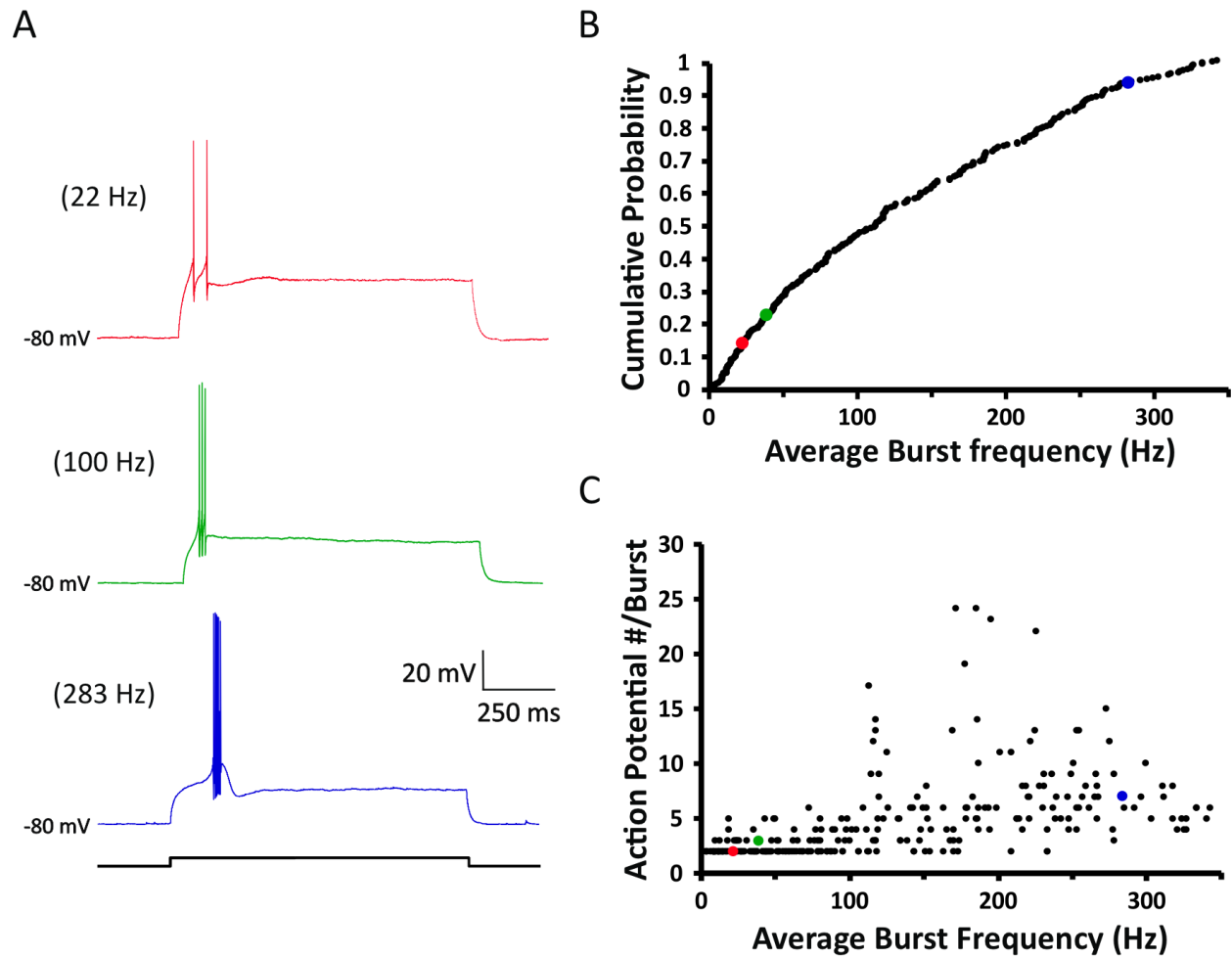


Figure 2.0: Burst characteristics of TRN neurons. (A) Representative traces of the three colored data points in B and C exemplifying neurons bursting at 22 Hz (red, top), 100 Hz (green, middle), and 283 Hz (blue, lower). (B) Depicts the range of action potential firing frequencies at -80 mV (burst mode) within the TRN represented as a cumulative probability. (C) Shows the number of action potentials in the initial burst as it relates to the burst frequency.

Synaptically evoked bursts

The characterization of burst discharge in our study was based on the response to a one second duration current step. Given prior studies indicating distribution of T-channels along the dendritic extent of TRN neurons (Crandall et al., 2010; Kovács et al., 2010), it is plausible that non-bursting neurons, and perhaps lower frequency bursting neurons identified in this study, have a greater distal dendritic distribution of T-channels. If lower frequency bursting neurons have more distally located T-channels, the decrease in frequency could be due to incomplete activation of the dendritic T-channels since they are activated via a somatic current injection. Therefore, electrical stimulation of synaptic inputs was utilized to provide activation of dendrites as opposed to somatic current injection.

To activate afferent synaptic inputs to TRN, a monopolar stimulating electrode was placed within the internal capsule. The membrane potential was held at -80 mV and stimulus voltage was gradually increased (50-400 μ A, 100 μ s) to elicit a burst discharge. Correlation analysis of somatically versus synaptically evoked burst frequencies revealed a strong positive correlation (Figure 2.1 B; r = of 0.929, p < 0.001, n = 13) between somatically evoked and synaptically evoked burst discharge. Interestingly, 10 of the 13 tested neurons discharged higher frequency synaptically evoked action potentials, possibly indicating greater activation of distal I_T , however this difference was not statistically significant (P = 0.081, n = 13, *paired T-test*). In addition, it is important to note that the lower burst frequency characteristic of individual cells was consistent by either method of activation suggesting the lower burst frequency is a characteristic of the neuron, and not an artifact of the activation protocol.

In addition to comparing frequencies of the burst mode discharge, action potential number per discharge was also compared between synaptic stimulation and somatic current injection. The number of action potentials elicited via either method was significantly positively correlated (Figure 2.1 C; $n = 16$; $r = 0.785$, $P < 0.001$), and there was no significant difference between the number of action potentials generated via either group ($P = 0.072$, *paired T-test*, $n = 16$).

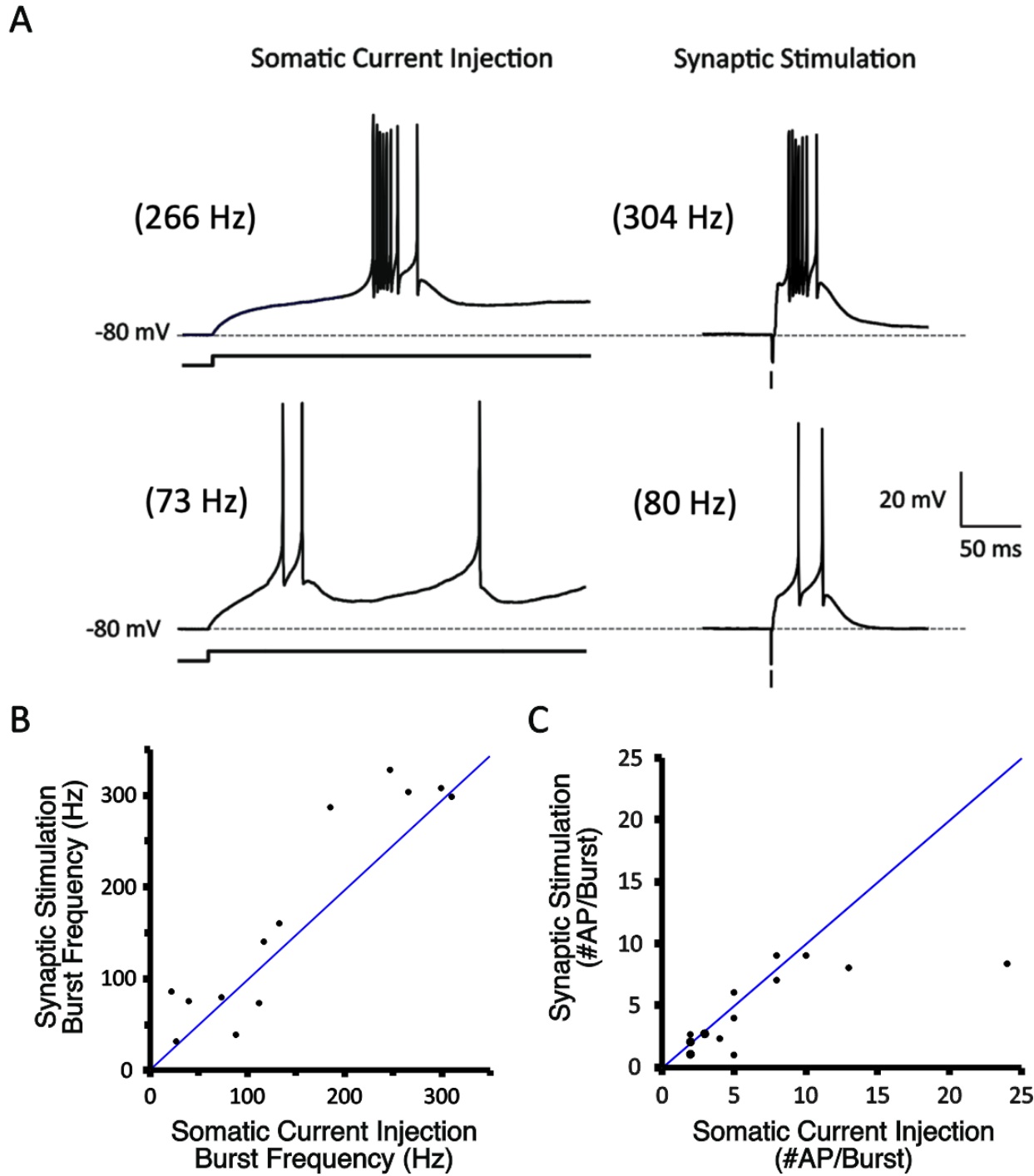


Figure 2.1: Comparison of synaptic vs. somatic activation of a burst in TRN neurons. (A) Example traces of burst discharge evoked by somatic current injection (left) and minimal electrical stimulation of synaptic afferents (right) in a higher frequency bursting (top) and a lower

Figure 2.1 (cont'd)

frequency bursting (bottom) neuron. (B) Comparison of average burst frequency produced by somatic current steps and synaptic activation. (C) Number of action potentials/burst for somatically evoked and synaptically-evoked burst discharges from 16 TRN neurons. Each of the three enlarged data points represent two identical overlapping data points.

Intrinsic properties of high and low frequency bursting TRN neurons

Several intrinsic properties of the TRN neurons were measured to discern whether burst discharge frequencies were related to differences in overall intrinsic properties. Apparent input resistance and membrane potential were measured from resting membrane potential; number of action potentials per burst and average burst frequency were measured from -80 mV; action potential half-width, threshold, and rheobase were measured from a membrane potential of -60 mV to prevent activation of T-channel current. Initial correlation analyses revealed that several intrinsic properties were positively correlated with the average burst frequency (Table 2.0). The number of action potentials per burst ($r = 0.502$, $P < 0.001$) and rheobase ($r = 0.285$, $P = 0.003$) were positively correlated with average burst frequency. In contrast, the average burst frequency was negatively correlated with input resistance ($r = -0.262$, $P < 0.001$) and action potential half-width ($r = -0.409$, $P < 0.001$). There was no significant correlation of resting membrane potential ($r = 0.015$, $P = 0.834$) or action potential threshold ($r = -0.181$, $P = 0.066$) with the frequency of the burst.

To further assess the intrinsic differences between higher and lower frequency bursting neurons, neurons were grouped by those with average burst frequencies at or below 100 Hz, and

those with frequencies above 100 Hz. This cut-off was selected based upon the propensity for most neurons with burst frequencies less than 100 Hz to fire only two action potentials per burst. Input resistance (Table 2.0; ≤ 100 Hz: 359.1 ± 308.8 M Ω , > 100 Hz: 263.6 ± 149.5 M Ω , $P = 0.012$), number of action potentials per burst (≤ 100 Hz: 2.5 ± 0.9 action potentials, > 100 Hz: 6.7 ± 4.3 action potentials, $P < 0.001$), action potential half-width (≤ 100 Hz: 0.28 ± 0.06 ms, > 100 Hz: 0.25 ± 0.05 ms, $P < 0.001$), and action potential threshold (≤ 100 Hz: -39.3 ± 12.8 mV, > 100 Hz: -43.6 ± 5.4 mV, $P = 0.012$) were significantly different between the two groups. Resting membrane potential (≤ 100 Hz: -76.6 ± 14.5 mV, > 100 Hz: -76.2 ± 15.4 mV, $P = 0.012$) and rheobase (≤ 100 Hz: 55.2 ± 39.7 pA, > 100 Hz: 69.5 ± 47.4 pA, $P = 0.012$) did not vary between the higher and lower frequency bursting neuron groups.

	≤ 100 Hz		> 100 Hz		P-Value <i>U</i> -test	Correlation with burst frequency (<i>r</i>)	P-Value (Correlation)
	Average \pm Standard Deviation	n	Average \pm Standard Deviation	n			
Resting Membrane Potential (mV)	-76.6 ± 14.5	106	-76.2 ± 15.4	112	0.720	0.015	0.834
Input Resistance (M Ω)	359.1 ± 308.8	105	263.6 ± 149.5	118	0.012	-0.262	<0.001
Burst AP Number	2.5 ± 0.9	123	6.7 ± 4.3	141	<0.001	0.502	<0.001
AP Half-Width (ms)	0.28 ± 0.06	43	0.25 ± 0.05	61	<0.001	-0.409	<0.001
AP Threshold (mV)	-39.3 ± 12.8	43	-43.6 ± 5.4	61	0.012	0.181	0.066
Rheobase (pA)	55.2 ± 39.7	43	69.5 ± 47.4	61	0.128	0.285	0.003

Table 2.0: Intrinsic properties of higher and lower frequency bursting TRN neurons. The frequency at which TRN neurons discharge action potentials in burst mode (-80 mV) is negatively correlated with cellular input resistance and action potential half-width. Burst frequency is positively correlated with the number of action potentials per burst discharge and the threshold of the action potentials. TRN neurons producing discharging action potentials at ≤ 100 Hz and $>$

Table 2.0 (cont'd)

100 Hz had significantly different input resistances, action potentials per burst discharge, action potential half-widths and action potential firing thresholds.

Morphologic study of TRN neurons

Several studies suggest that TRN somatic morphology is not homogeneous and there are multiple subtypes (Lübke, 1993; Spreafico et al., 1991, 1988). It is unclear if the different soma morphologies are associated with different intrinsic properties or function. Soma morphology was analyzed in a subgroup of TRN neurons to determine if the morphology was related to the average burst frequency of these cells. Soma volume was calculated from 72 fluorescently filled neurons (Alexa 594) with burst frequencies ranging from 3-324 Hz. Soma volume was positively correlated with average burst frequency (Figure 2.2 A (left); $n = 72$, $r = 0.49$, $P < 0.001$). The average soma size of the lower frequency bursting neurons (Figure 2.2 A (right), ≤ 100 Hz: $1423 \pm 610 \mu\text{m}^3$, $n = 30$) was significantly smaller than the higher frequency bursting neurons (Figure 2.2 A (right), > 100 Hz: $1992 \pm 799 \mu\text{m}^3$, $n = 42$; $P = 0.002$, *Mann-Whitney U-test*).

In addition to soma volume, the number of primary dendrites was also calculated from the z-stack images. Previous studies have found that TRN neuron dendritic arborizations may vary: some cells were found to have bipolar dendrites while others appeared to have more multipolar diffuse arbors (Lübke, 1993; Spreafico et al., 1988). Our findings indicate that there is no correlation of burst frequency and primary dendrite number (Figure 2.2 B (left), $n = 72$, $r = 0.003$, $P = 0.645$) and no statistical difference in the number of primary dendrites of higher frequency

bursting neurons (Figure 2.2 B (right), > 100 Hz: 5.1 ± 1.6 , $n = 42$) and lower frequency bursting TRN neurons (Figure 2.2 B (right), ≤ 100 Hz: 5.2 ± 1.3 , $n = 30$; $P = 0.888$, *Mann-Whitney U-test*).

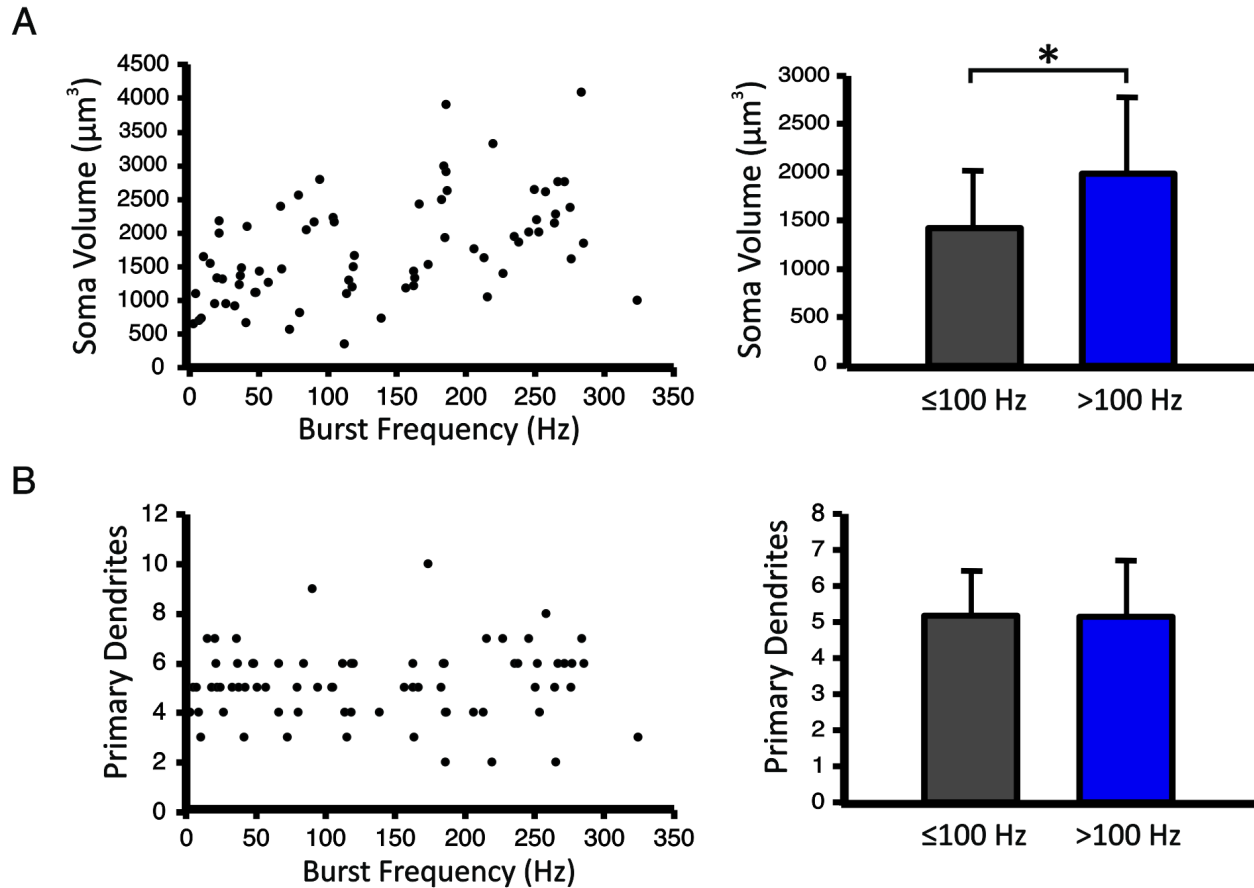


Figure 2.2: Morphologic comparison of higher and lower frequency bursting TRN neurons. (A) Graph of soma volume as it relates to burst frequency (left, $n = 72$, $r = 0.49$, $P < 0.001$). Histogram depicting soma volumes for ≤ 100 Hz and > 100 Hz groups (right, $P = 0.002$). (B) Graph of proximal dendritic branch sites as it relates to burst frequency (left). Histogram depicting number of proximal branch sites for ≤ 100 Hz and > 100 Hz groups (right). * Denotes $P < 0.05$.

Low threshold spike properties in high and low frequency bursting neurons

A distinct feature of the robust burst discharge in TRN neurons is the relatively large, voltage-dependent, T-type calcium channel-mediated low-threshold spike (LTS) which underlies the fast action potential discharge (Figure 2.3 A; Coulter et al., 1989; Destexhe et al., 1998; Zhan et al., 1999). In our previous study of rat TRN neurons, burst discharges were associated with a large, consistent amplitude LTS; whereas non-bursting neurons, which lack burst discharge at hyperpolarized membrane potentials, in many cases had no apparent LTS (Lee et. al., 2007). In this current study of adult mice, in the presence of tetrodotoxin (TTX, 1 μ M), nearly all neurons (44 of 45 neurons) produced an LTS of various amplitudes, regardless of the average burst frequency (Figure 2.3 B). The LTS peak amplitude was positively correlated with average burst frequency ($r = 0.714$, $P < 0.001$) and the peak amplitude of the LTS was significantly larger in higher vs lower frequency bursting neurons (Figure 2.3 B; ≤ 100 Hz: 9.2 ± 5.5 mV; > 100 Hz: 18.1 ± 9.7 mV, $n = 49$, $P = 0.002$, *Mann-Whitney U-test*). With this finding that TRN neurons bursting at lower frequencies produce a significantly smaller yet visible LTS, it was next tested whether this smaller LTS could be due to initial partial activation of I_T . If I_T was being only partially activated, the peak would be expected to grow with increasing current injections. A series of current steps ($\Delta 20$ pA) were injected and the LTS peak was measured relative to the steady-state ohmic step at each current step eliciting a short-latency depolarization. Results revealed that for both higher and lower frequency bursting neurons, the LTS did not increase in magnitude with increasing activating current (Figure 2.3 C).

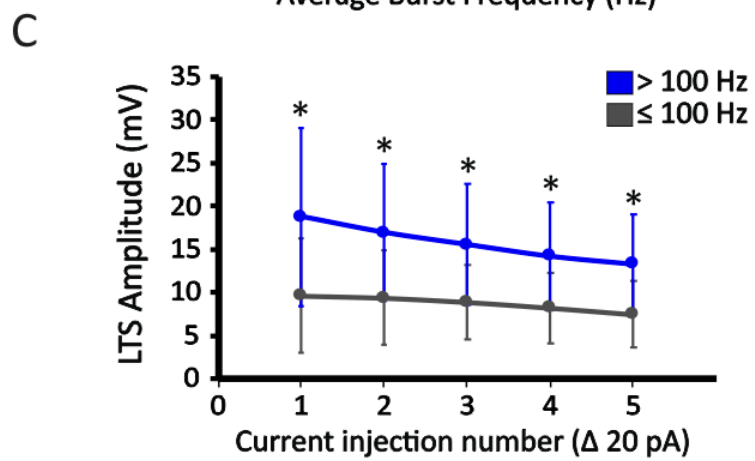
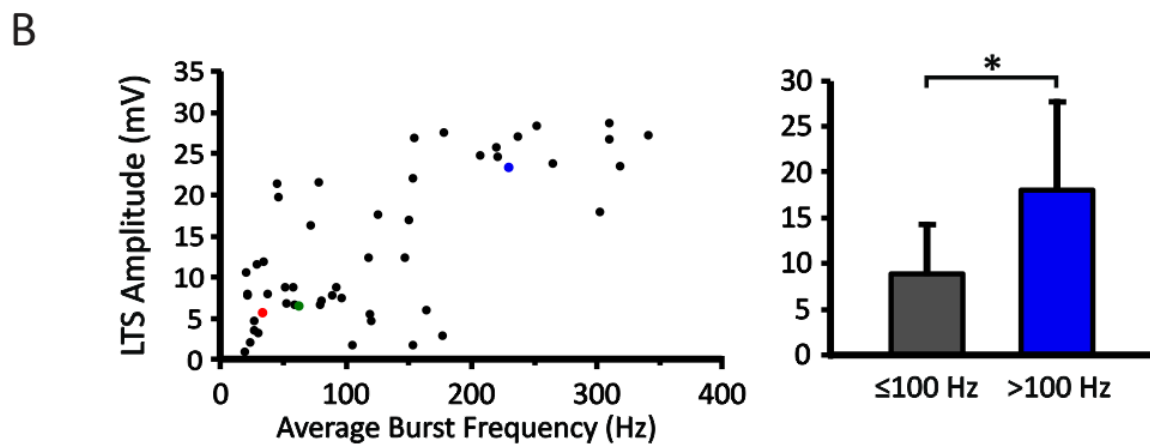
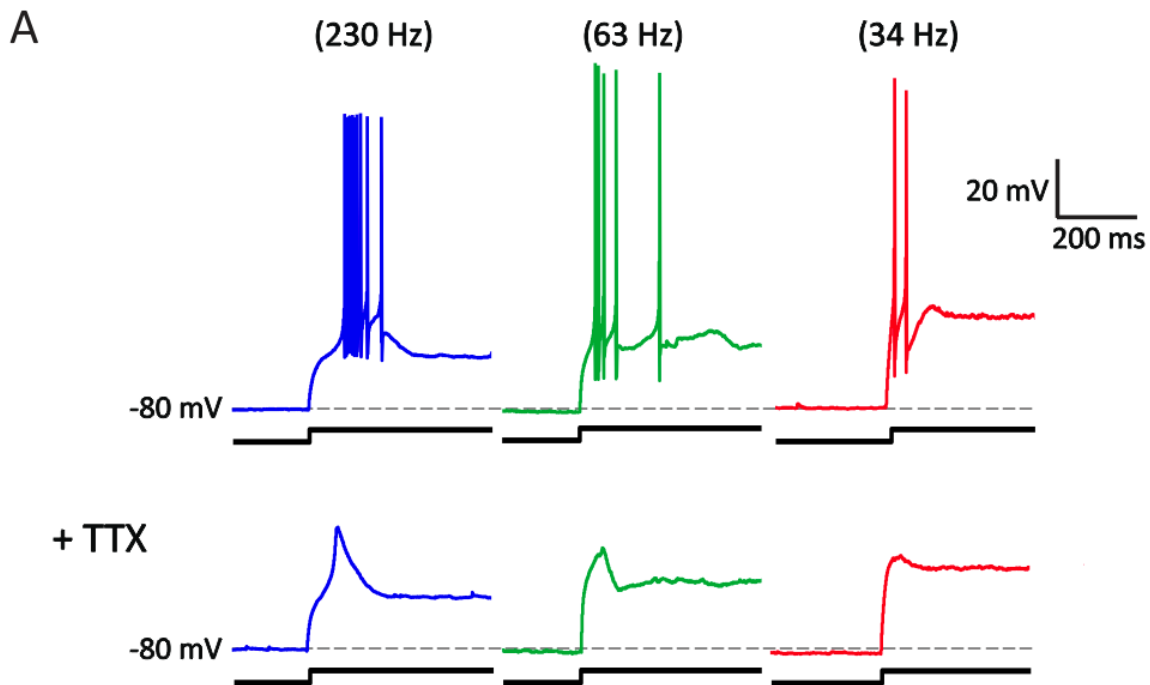


Figure 2.3: LTS amplitude is correlated with burst frequency.

Figure 2.3 (cont'd)

(A) Representative examples of different burst discharges in TRN neurons (blue, 230 Hz, 60 pA step; green, 63 Hz, 100 pA step; red, 34 Hz, 80 pA step). In the presence of TTX (1 mM), the action potentials are blocked, thereby unmasking the underlying LTS. (B) *Left*, Relationship of LTS amplitude and burst frequency. Data points from the three example cells are designated by respective color-coded data points. *Right*, histogram illustrating average LTS amplitude in high (> 100 Hz, blue) and low bursting (\leq 100 Hz, gray) frequency subgroups. (C) LTS amplitude in response to increasing stimulus intensity for higher (blue) and lower frequency (gray) bursting neurons. Depolarization 1 is defined as the lowest intensity to elicit a clear LTS. Depolarizations 2-5 represent the peak LTS measurements at subsequent increases in intensity (20 pA increments). * Denotes $P < 0.05$.

T-type calcium current in high and low frequency bursting neurons

Prior studies have shown that a voltage dependent T-current underlies the LTS observed in current clamp recordings (Coulter et al., 1989; Huguenard and Prince, 1992). To evoke the low-threshold, transient T-current in the TRN neurons an inactivation protocol was conducted in voltage clamp in the presence of 1 μ M TTX (Figure 2.4 A). In all 25 neurons tested, which ranged from 17 to 326 Hz average burst frequency prior to the voltage clamp recordings in TTX, a measurable transient inward current was successfully evoked. The peak of the inward current (absolute value) was positively correlated with the average burst frequency pre-TTX (Figure 2.4 B; $n = 25$; $r = 0.879$, $P < 0.001$). Lower frequency bursting neurons (\leq 100 Hz) have a significantly smaller peak current amplitude (190.5 ± 59.8 pA, $n = 15$) compared to the higher frequency bursting neurons (448.5 ± 204.5 pA, $n = 10$; $P < 0.001$, *Mann-Whitney U-test*). Furthermore, the

halfwidth of the inward current also significantly differed between these two groups (Figure 2.4 C: ≤ 100 Hz: 31.4 ± 14.7 ms, $n = 15$; > 100 Hz: 18.9 ± 5.0 ms, $n = 8$; $P = 0.001$, *Mann-Whiney U-test*). In a subgroup of neurons, both the LTS (in current clamp) and transient inward current (voltage clamp) were recorded from the same neurons. In these cells, the peak inward currents were positively correlated with the peak amplitude of the LTS (Figure 2.4 D: $n = 16$, $r = 0.875$, $p < 0.001$). The next aim was to confirm whether this transient inward current was a calcium current, as is the I_T mediating the LTS in high frequency bursting neurons. At relatively low concentrations ($100 \mu\text{M}$), NiCl_2 preferentially blocks T-type low-threshold calcium currents (Huguenard and Prince, 1992). The voltage step required to evoke the maximum inward current in the neuron was measured utilizing an inactivation protocol. Peak inward current amplitude was measured before and after $100 \mu\text{M}$ NiCl_2 application (Figure 2.5 A). The inward current was significantly attenuated by NiCl_2 in all neurons tested regardless of initial inward current amplitude (Figure 2.5 A, B; control: 310.0 ± 200.0 pA; NiCl_2 : 109.8 ± 115.3 pA, $n = 19$; $P < 0.001$, *paired T-test*).

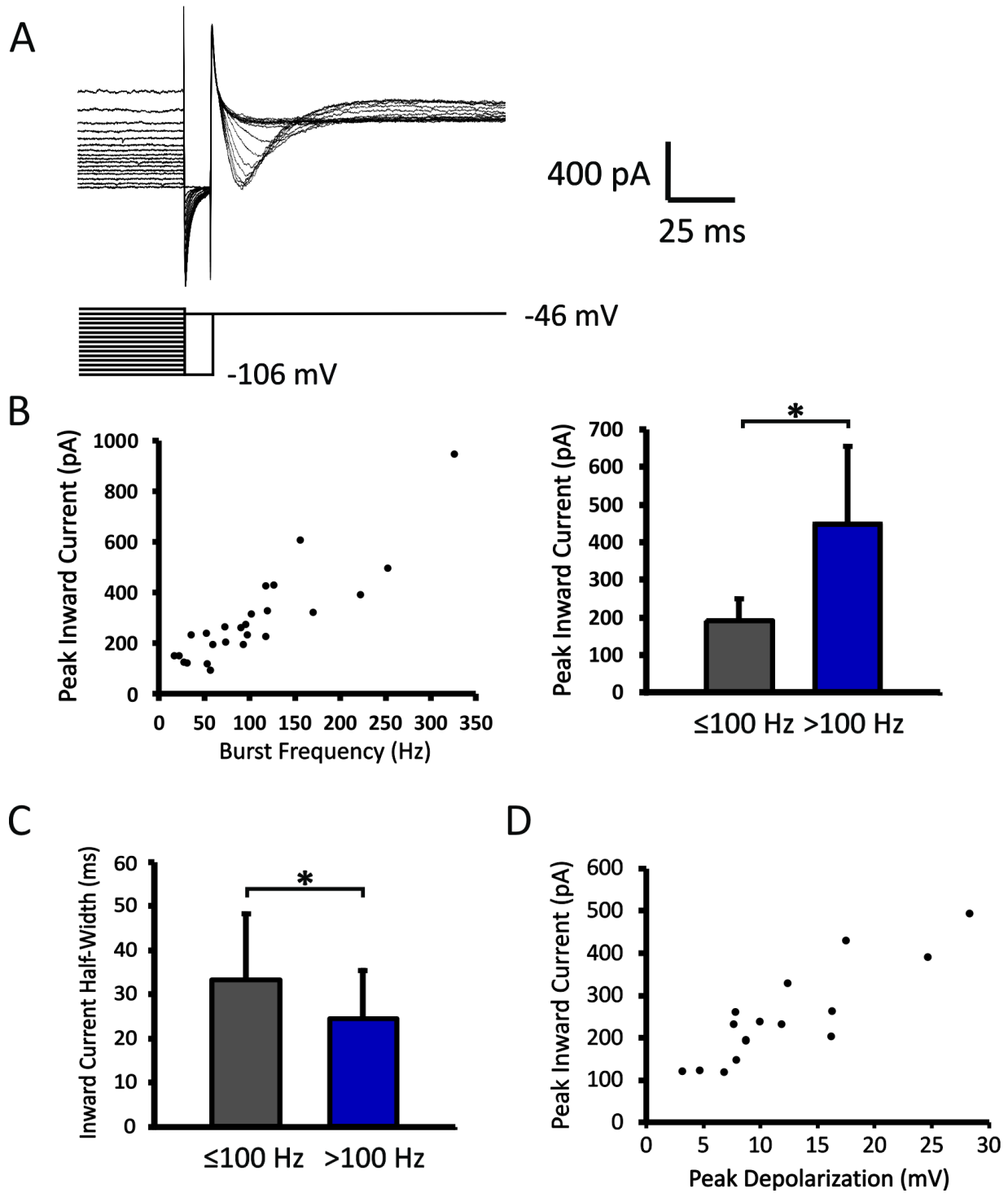


Figure 2.4: Calcium mediated low-threshold current underlies the low-threshold depolarization in all TRN neurons. (A) Example T-current activation protocol. (B) Inward current correlation with

Figure 2.4 (cont'd)

burst frequency (left) and corresponding histogram showing peak values of lower frequency (gray) and higher frequency blue) bursting neurons (right; $n = 25$; $r = 0.879$, $P < 0.001$). (C) Histogram depicting the half-width of the inward current in lower frequency (grey) and higher frequency (blue) bursting neurons (448.5 ± 204.5 pA, $n = 10$; $P < 0.001$). (D) Peak inward current (voltage clamp) is positively correlated with the peak depolarization (current clamp) mediating the LTS ($n = 16$, $r = 0.875$, $p < 0.001$). * Denotes $P < 0.05$, *Mann-Whitney U-test*.

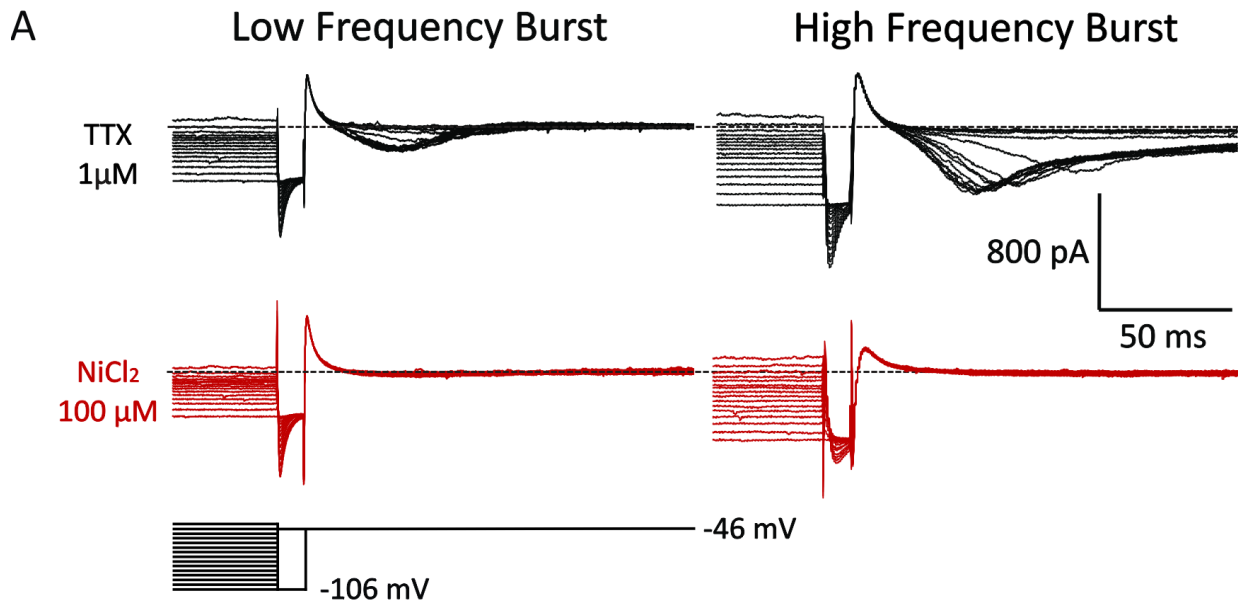
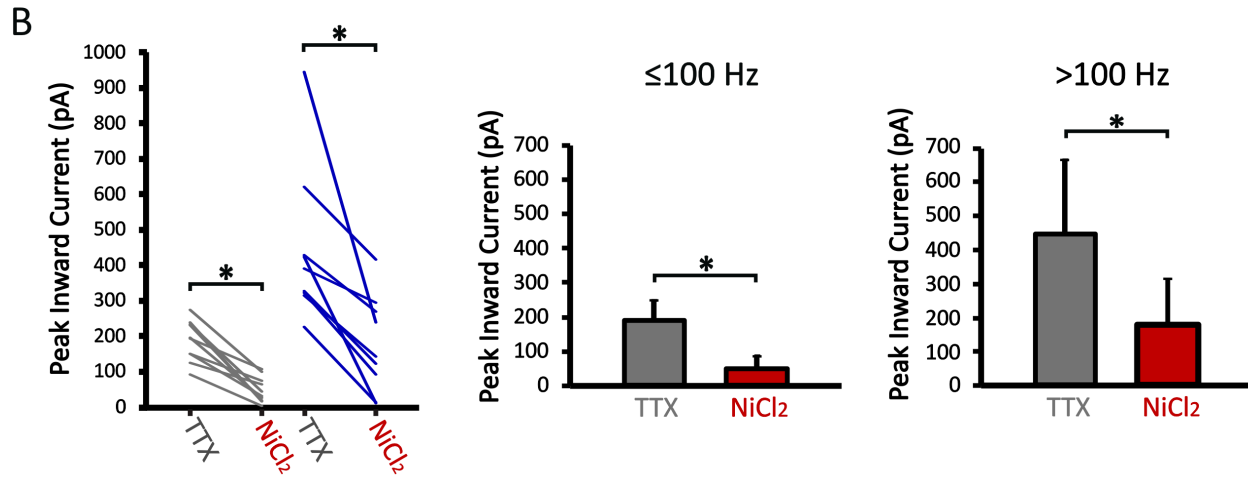


Figure 2.5: Nickel decreases the inward current amplitude in all TRN neurons.

(A) Representative current responses for lower frequency (left) and higher frequency (right) bursting neurons before and after the addition of NiCl_2 (bottom). Current was elicited from a one second hyperpolarizing (-100 mV) de-inactivating current step. Capacitance transient currents are clipped. (B) Effect of NiCl_2 on the burst of higher and lower frequency bursting neurons. Peak amplitudes (absolute value) before and after nickel (left). Gray traces are lower frequency

Figure 2.5 (cont'd)

bursting neurons and blue are higher frequency bursting. Histogram representations of higher and lower frequency groups are depicted on the right. * Denotes $P < 0.05$.



Impact of SK channels on burst discharge of TRN neurons

Small-conductance calcium-activated potassium (SK) channels impact TRN neuron output by rapidly attenuating the burst discharge (Cueni et al., 2008; Sailer et al., 2004). When SK channels are blocked by apamin, excitability of TRN neurons increases while thalamocortical relay neuron activity is subsequently inhibited (Kleiman-Weiner et al., 2009; Ying and Goldstein, 2005). In SK type 2 channel knock out mice, the predominant SK channel subtype in the TRN, there is a reduction in oscillatory activity (Cueni et al., 2008). Electroencephalogram recordings in this transgenic mouse reveal a decrease in slow delta waves and sleep spindles, as well as more awakenings during non-REM sleep (Cueni et al., 2008; Kleiman-Weiner et al., 2009; Ying and Goldstein, 2005). The next experiment was designed to test whether attenuation of SK channels

would differentially affect the burst discharge in higher and lower frequency bursting TRN neurons.

In the presence of apamin (100 nM), the number of action potentials per burst was significantly increased in both higher frequency bursting neurons (Figure 2.6 A, D; control: 6.5 ± 3.2 action potentials, apamin: 25.8 ± 19.5 APs; $n = 11$; $P = 0.008$, *paired t-test*) and lower frequency bursting neurons (control: 2.5 ± 1.2 APs; apamin: 11.2 ± 8.9 APs; $n = 14$, $P = 0.002$, *paired t-test*). The average burst frequency was also significantly increased by apamin in both higher frequency bursting neurons (Figure 2.6 A, D; control: 207.8 ± 59.9 Hz, apamin: 303.4 ± 104.3 Hz, $n = 11$; $P = 0.002$ *paired t-test*) and lower frequency bursting neurons (control: 38.3 ± 23.8 Hz; apamin: 159.0 ± 108.6 Hz, $n = 14$; $p < 0.001$; *paired t-test*). The next goal was to unmask the underlying LTS by adding TTX (1 mM) to determine whether apamin was directly affecting the LTS properties. In these conditions, the half-width of the LTS was significantly increased in the lower frequency bursting neurons (Figure 2.6 B, D; control: 53.8 ± 12.52 ms, apamin: 94.3 ± 39.2 ms, $n = 9$; $P = 0.02$, *paired t-test*), which is consistent with the longer bursts observed. Our dataset with fast bursting neurons all showed an increase as well, but the data is skewed because in two cells there was a long-lasting plateau potential that prevented measurement of the width (> 100 Hz control: 31.3 ± 10.8 ms, apamin: 97.9 ± 65.7 ms, $n = 4$, $P = 0.170$).

To avoid the potential activation of high threshold calcium currents that could underlie the plateau potential observed in current clamp recordings, the effect of apamin on the transient inward current was next examined. In voltage clamp recordings, the peak amplitude of the inward current was not altered in the presence of apamin (Figure 2.6 C, D; ≤ 100 Hz: control: 195.1 ± 53.8 pA; apamin: 173.7 ± 76.2 pA, $n = 12$, $P = 0.330$, *paired t-test*; > 100 Hz: control: 517.0

± 21.0 pA, apamin: 436.8 ± 124.2 pA, $n = 4$, $P = 0.071$, *paired t-test*). However, similarly to the current clamp LTS half-width measurements, the half-widths of the peak transient inward current were significantly widened by apamin in lower frequency bursting neurons (Figure 2.6 D; control: 32.3 ± 16.1 ms, apamin: 51.4 ± 18.3 ms, $n = 12$; $P = 0.022$, *paired t-test*) but not higher frequency bursting neurons (control: 22.1 ± 13.4 ms, apamin: 37.1 ± 15.8 ms, $n = 5$; $P = 0.060$, *paired t-test*).

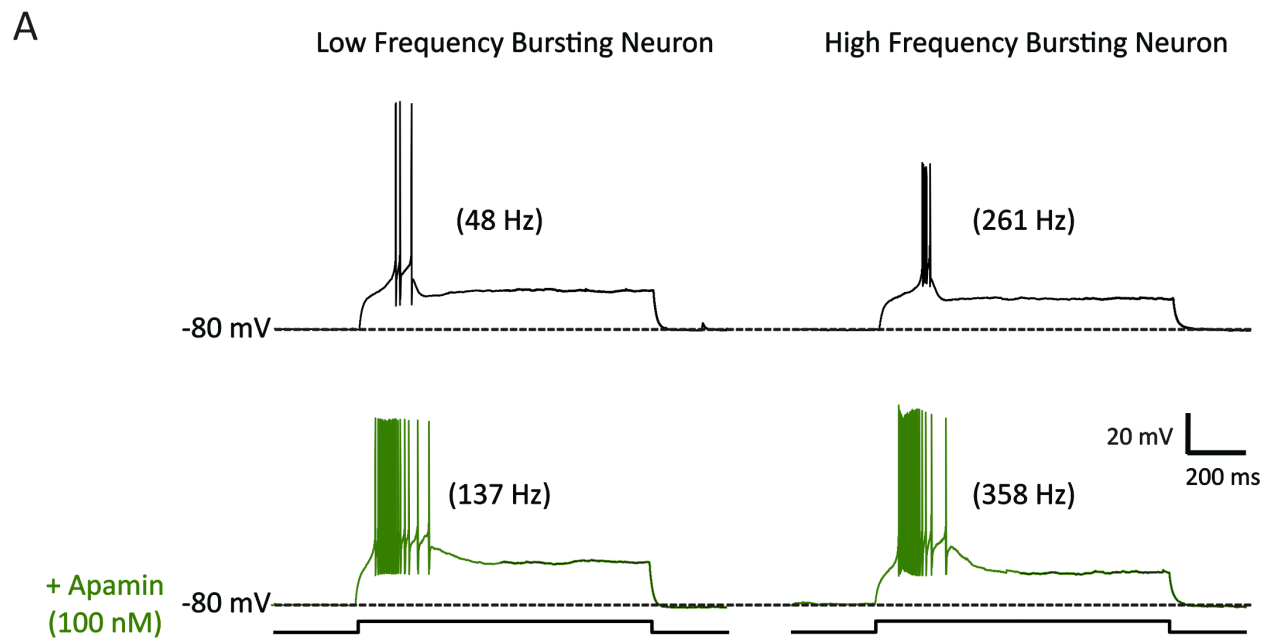


Figure 2.6: Apamin prolongs burst discharge in TRN neurons.

(A) Representative traces of a lower frequency (48 Hz, 60 pA step) and higher frequency (261 Hz, 100 pA step) bursting neuron before and after the application of apamin (100 nM). Post apamin frequencies are “spike matched” to the number of action potentials in the initial burst. (B) Current clamp recordings from representative lower frequency bursting (78 Hz) and higher frequency bursting (252 Hz) neurons in the presence of TTX (1 μ M) revealing the underlying LTS.

Figure 2.6 (cont'd)

Following the addition of apamin (100 nM), the LTS is lengthened in both neurons (C) Same cells as in B, in voltage clamp recordings. (D) In burst mode in the presence of apamin, nearly all TRN neurons discharge more action potentials (left), at higher frequencies (right). (E) Although sample size of the higher frequency bursting neurons in voltage clamp is limited, the duration of the LTS underlying the burst (left) becomes significantly increased in lower frequency bursting neurons, as does the associated calcium-mediated inward current (right). * Denotes $P < 0.05$.

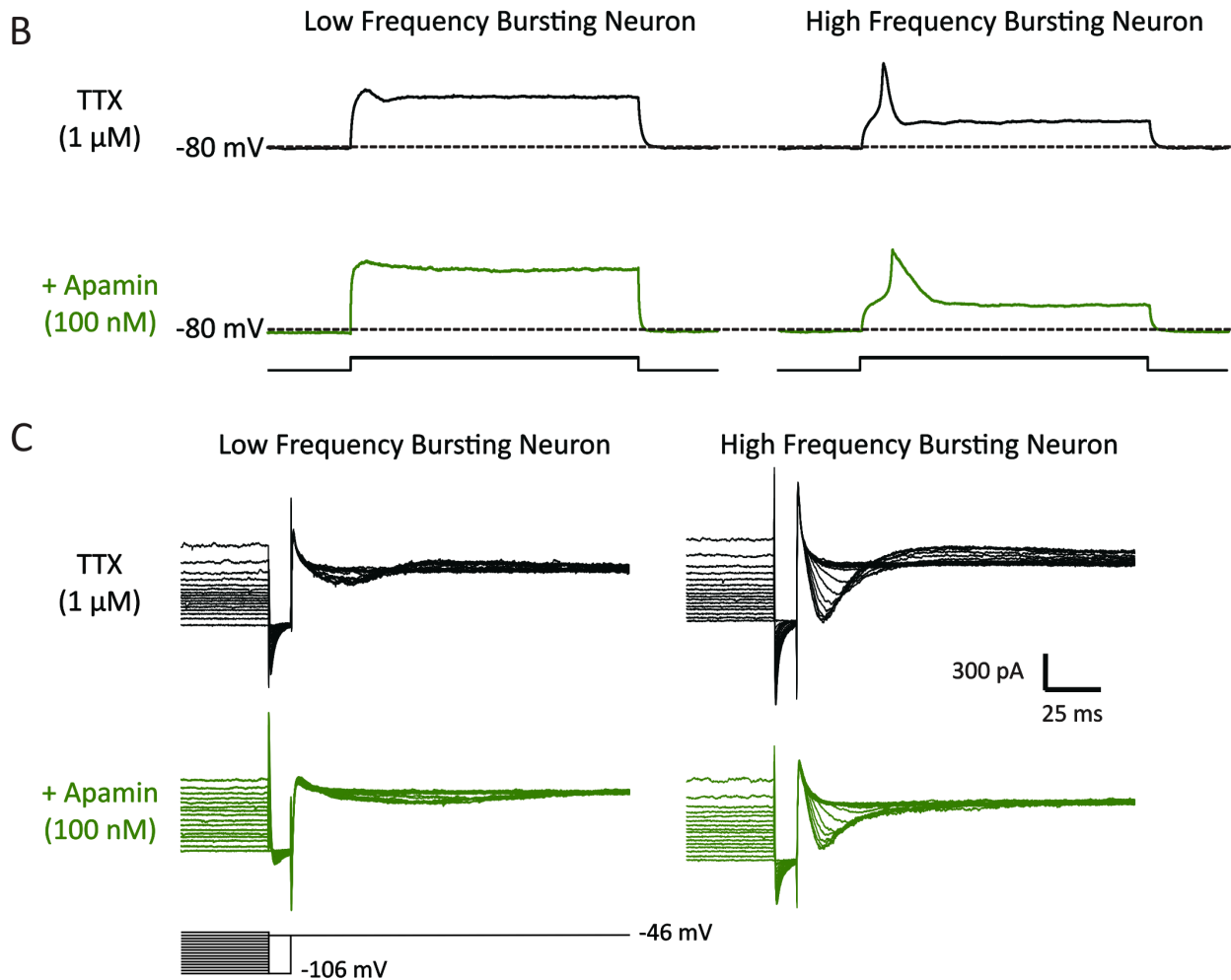
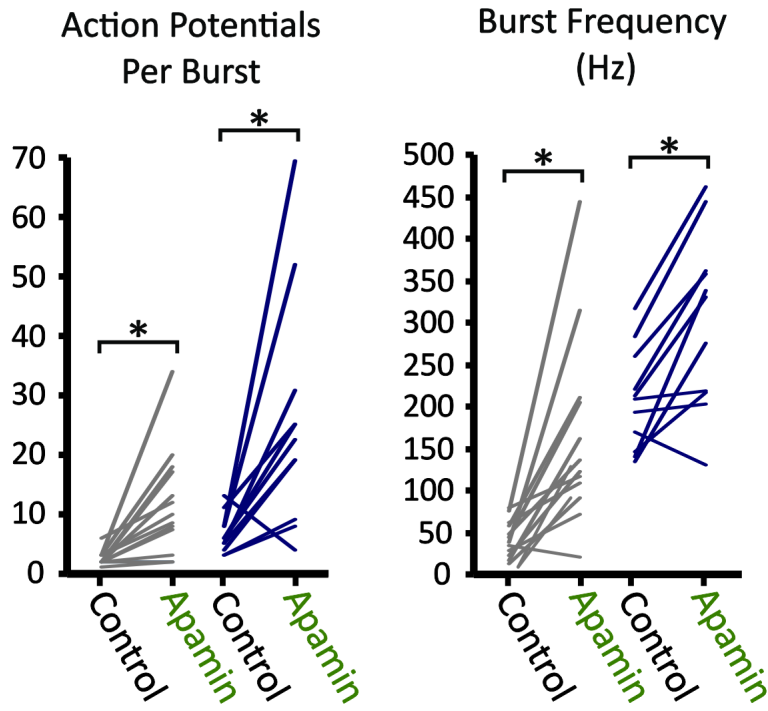
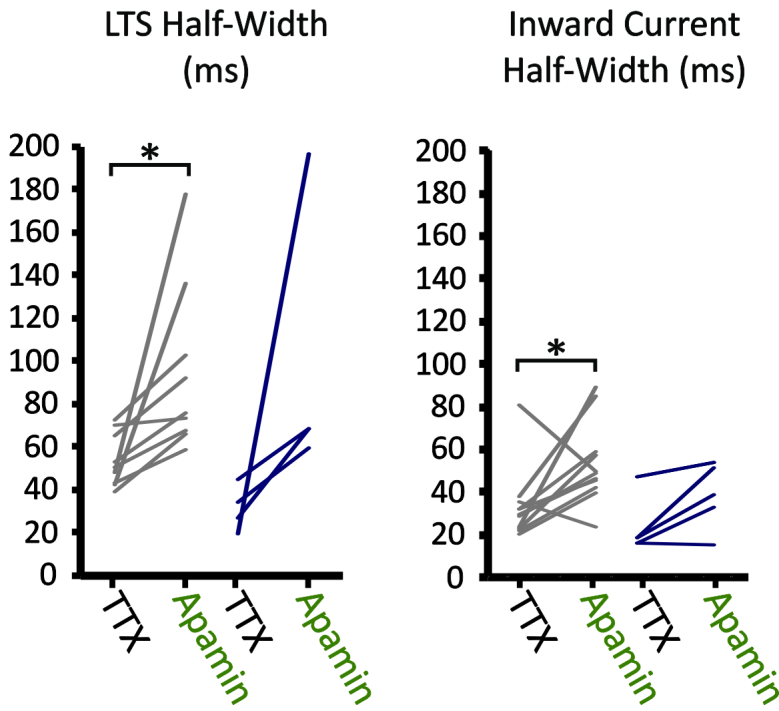


Figure 2.6 (cont'd)

D



E



Lower frequency bursting TRN neurons cannot be identified by SOM-Cre fluorescent labeling within the SOM⁺/Ai32 transgenic animal

A previous study correlated somatostatin-containing (SOM⁺) TRN neurons with a lower frequency bursting phenotype in a SOM-Cre mouse model in older (PND 30-180) mice (Clemente-Perez et al., 2017). In an attempt to determine whether the lower frequency bursting neurons identified in these studies were SOM⁺ neurons, fluorescently labeled neurons were recorded within a genetic SOM-Cre/Ai14 mouse line. Surprisingly, several recorded fluorescently labeled SOM⁺ neurons within the TRN of this animal model produced robust burst discharges and it was determined that the somatostatin-containing neurons do not appear to be associated with lower frequency bursts (Figure 2.7 A-B, n = 11).

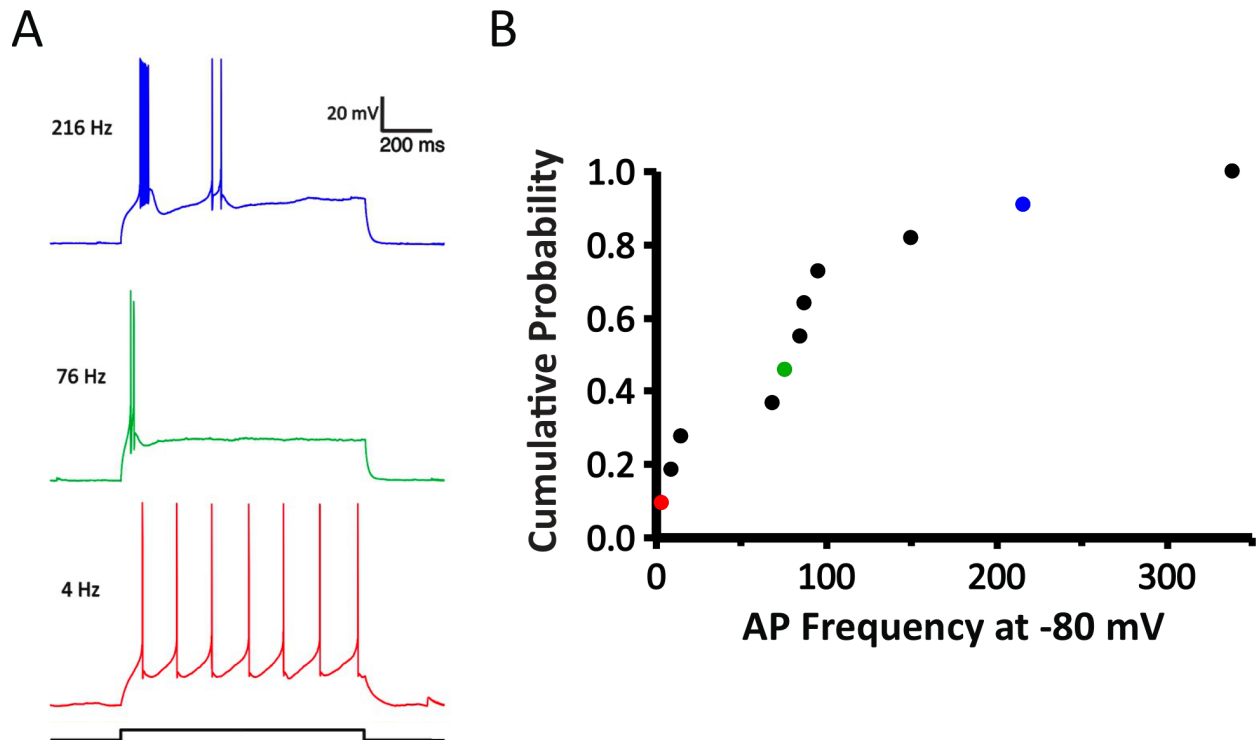


Figure 2.7: Burst discharge frequencies of fluorescently labeled SOM+ neurons. (A) Example traces of SOM⁺ fluorescent neurons illustrating that fluorescently labeled neurons within the SOM⁺ transgenic mouse are both higher and lower frequency bursting neurons. (B) Burst frequencies of SOM⁺ neurons expressed as a cumulative probability.

Phenylephrine increases the burst frequency of TRN neurons

SK channels have been widely studied in TRN, yet it remains unclear whether endogenous neuromodulators may be able to selectively inhibit or enhance I_{SK} . Apamin, a component of bee venom, is known to block these channels, but the possibility of endogenous modulation would represent an intriguing mechanism of tuning up or down the burst frequency. One possible modulator candidate is the adrenergic α_1 agonist phenylephrine, which has previously been

found to excite TRN neurons (McCormick and Wang, 1991). Bolus injections of phenylephrine were applied and the subsequent effects on the burst discharge were evaluated.

A burst discharge was elicited from > 100 Hz bursting neurons by injecting one second current impulses of 20 pA increments. Once baseline characteristics were obtained, phenylephrine (5-10 μ M) was applied for 30 seconds. A series of burst discharges were elicited and measurements of action potential number and burst frequency were measured at the peak effect of the phenylephrine. The number of action potentials per burst was not significantly affected by the application of phenylephrine (Figure 2.8 A-B: control: 11.9 ± 7.1 action potentials, phenylephrine: 10.7 ± 8.5 action potentials, $n = 9$, $p = 0.577$, *paired t-test*). The burst frequency was also not affected by phenylephrine (Figure 2.8 C: control: $198.8 \text{ Hz} \pm 53.3 \text{ Hz}$, phenylephrine: $228.5 \pm 43.5 \text{ Hz}$, $n = 11$, $P = 0.165$, *paired t-test*). In 12 out of 14 cells, phenylephrine did have the effect of depolarizing the membrane, which was compensated for by a manual current clamp prior to recording burst discharge characteristics.

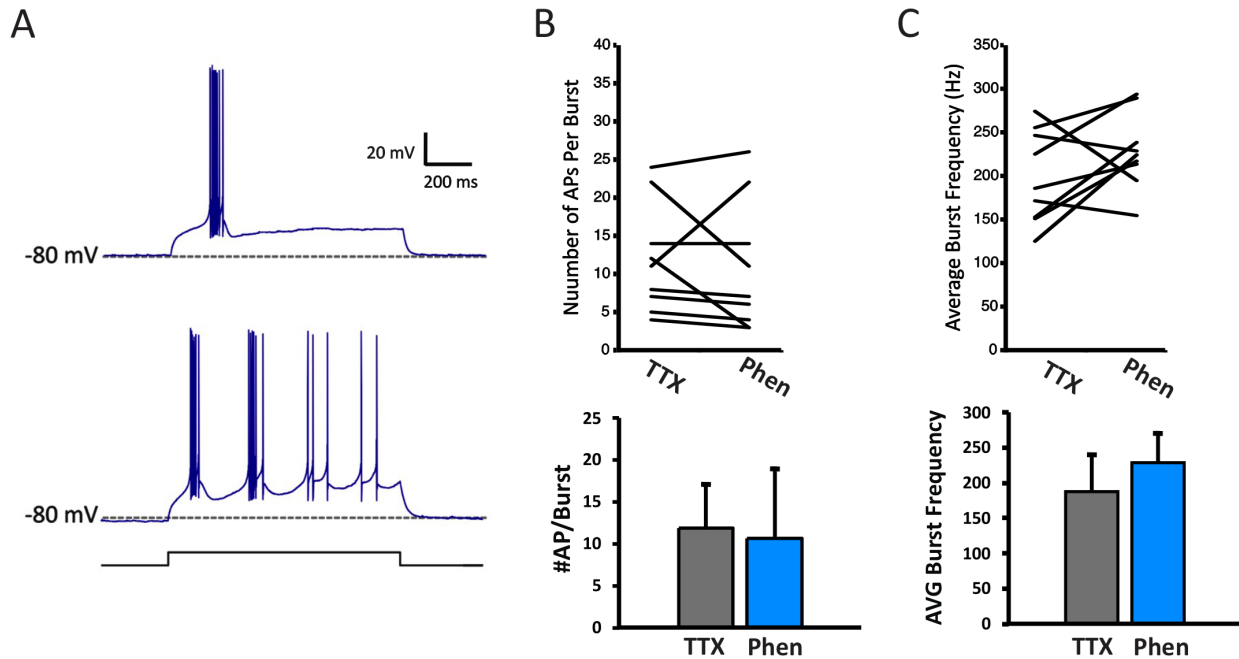


Figure 2.8: Phenylephrine does not affect TRN neuron burst frequency or action potential number. (A) Example traces of before (top), and at maximal phenylephrine effect (bottom). (B) Application of phenylephrine increased the frequency of the burst in the population ($n = 11$, $P = 0.04$, *paired T-test*). (C) Phenylephrine did not change the number of action potentials per burst ($P = 0.129$, $n = 11$, *paired T-test*).

Discussion

In contrast to the traditional presumption that burst discharge is a high frequency (> 250 Hz) transient discharge of many action potentials, the burst discharge of TRN neurons is quite variable. Our data shows that in adult mice, this variable burst discharge frequency is also related to multiple differences of intrinsic properties that may bring useful context to future studies of possible structural or functional subtypes. Neurons at either end of this variable burst frequency spectrum vary significantly in action potentials per burst, input resistance, soma size, action

potential threshold, and action potential half-width. Distinctions between neurons within the middle of the spectrum are often very gradual and there is not clear subtype grouping based upon the described properties.

Recent genetic analysis performed on TRN neurons (Li et al., 2020) found that two identified gene profiles were expressed in a somewhat mutually exclusive manner. These genetic profiles, which included genes for GABA transporters (*Slc6a1*) and T-type calcium channels (*Cacna1i*), could not be used to distinctly split TRN neurons into distinct subgroups. As one profile increased in expression, however, the other appeared to decrease reciprocally. In consideration of our reported findings, it is possible that TRN neurons exhibit a shifting spectrum of these described gene expression profiles, where neurons that highly express one profile have distinct electrophysiological properties from neurons with lower expression of the same profile.

A recent study identified that TRN neurons located within the “core” and “edge” regions of the nucleus may be functionally distinct. Calbindin-containing core cells were found to receive inputs from first-order primary sensory relay of the ventroposterior nucleus, while the SOM-containing edge cells received inputs from the higher-order posterior medial thalamic nucleus (Martinez-Garcia et al., 2020). Neurons at the edges of the nucleus also tended to fire lower frequency bursts than core cells. A limitation of our study is that the recorded TRN neurons were sampled widely from the nucleus and the location of the neurons within this study were not recovered. Further examination will be needed to determine the degree to which the lower frequency bursting neurons may be associated with this anatomical distribution within the nucleus.

Another previous study reported that SOM⁺ neurons have weaker bursts compared to parvalbumin containing neurons (Clemente-Perez et al., 2017). To determine whether lower frequency bursting neurons may represent a distinct subset of SOM⁺ neurons, recordings were made from fluorescently tagged neurons within the SOM-Cre x Ai14 transgenic animal. Findings revealed that the burst frequencies of these neurons were similar to the non-labeled neurons. Martinez-Garcia et al. (2020) reported that in a similar SOM-Cre mouse line, many fluorescent cells were located throughout the nucleus, whereas when they utilized specific local viral injections to label SOM⁺ cells, they were largely confined to the edge regions. They postulated that in the SOM-Cre line, Cre recombination may occur early on in development when some more central neurons may produce SOM before a possible developmental loss in this expression (Hu et al., 2013). Further studies will be needed to determine how SOM⁺ cells may be related to lower frequency bursting neurons.

One curious finding from these data was a lack of previously reported atypically bursting neurons (Lee et al., 2007). Previously, in addition to a subset of bursting and non-bursting neurons, a third class of atypically bursting neurons were identified. These neurons produced a burst with an initial typical action potential followed by action potentials with lower amplitudes and longer half-widths. Atypically bursting neurons were localized to the more dorsal portions of the TRN along with non-bursting neurons, while typically bursting neurons were found more ventrally. Two possible reasons for our lack of atypical neurons are the age of the animals, as well as possible differences between mouse and rat models. The entirety of this work utilizes mouse TRN from animals aged 30 postnatal days or greater, while Lee et. al. (2007) based their studies in the TRN of rats aged 10-28 postnatal days. In recordings of mouse TRN (PND 13) not reported

in this study, two atypically bursting neurons were identified. It is possible that the atypical burst phenotype is a developmental stage within the TRN, and if so, it would be interesting to know if they are late maturing bursting neurons or perhaps may represent a precursor to slowly bursting neurons.

An additional aspect of our study that varied from previous studies, was the range in somata volumes reported. Our study found that mouse TRN somata volumes ranged from 360-4090 μm^3 , whereas a previous study comparing soma volumes of rat, cat, and rabbit, reported were much smaller (150-860 μm^3 ; Lübke, 1993). The method used to evaluate the somata may account for these differences. Two-photon microscopy was utilized to create z-stacked images spanning the depth of the neuron to calculate soma volume. Our slices were also not dehydrated prior to imaging and decreasing likelihood of soma shrinkage. Additionally, the patch electrode pipette was not removed before imaging the neurons, because in practice it was observed that this sometimes has the effect of distorting the membrane and thus soma shape. In two separate blinded analyses of these data, soma size was positively correlated with burst frequency.

Observations from these studies revealed that the neurons of the TRN cannot easily be separated into discrete populations based on electrophysiological or morphological properties. However, neurons at either end of this broad spectrum vary significantly in their intrinsic properties and the magnitude and duration of the burst-mode output. GABA_B receptors are strongly activated by fast tetanic action potentials, as produced by high frequency burst discharge, whereas lower frequency bursting neurons may only be able to activate faster acting GABA_A receptors. This suggests that higher and lower frequency bursting neurons may occupy distinct physiologic roles in their patterns of thalamic inhibition.

Burst discharge is the predominant firing mode during sleep, however there is evidence that bursts may be important to facilitate specific signal transmissions or changes in attention (Bezudnaya et al., 2006; Guido and Weyand, 1995; Hartings et al., 2003; Ramcharan et al., 2000). While high frequency bursting neurons are known to play a large role in sleep, the lower frequency bursting neurons are unlikely to participate in the large, rhythmic bursts of slow-wave sleep patterns and would instead have a different role. A drawback of this study is the lack of specific locations of the neurons, the recordings were conducted through a wide range and the vast majority likely fall within the sensory TRN. One possible role of lower frequency bursting neurons in sensory processing could be to provide longer lasting, lower levels of thalamic inhibition to more finely modulate the sensory circuit. While higher frequency burst neurons are firing in a phasic “on or off” pattern, the lower frequency bursting neurons would act as a dimmer switch to maintain a lower level of inhibition that may more closely resemble a tonic or phasic pattern.

SK channel activation plays a critical role in shaping burst mode output in both higher and lower frequency bursting neurons. Blocking I_{SK} increased the frequency and number of action potentials per burst, making lower frequency bursting neurons more physiologically similar to higher frequency bursting neurons. Attempts to identify endogenous neuromodulators of I_{SK} , have been largely unsuccessful (Liegeois et al., 2003). Our investigation into a possible adrenergic mechanism utilizing phenylephrine was also not successful. Differences in I_{SK} activity do not appear to account for the variable burst discharge characteristics, however determination of an endogenous neuromodulator of I_{SK} would provide an additional mode of input-specific signal integration and modulation of thalamocortical inhibition.

The TRN has time and time again proven itself to be a highly organized hub of modulatory subnetworks which integrate complex sensory information and regulate thalamocortical excitation. Further characterization of network connectivity and thalamocortical output of higher and lower frequency bursting neurons will clarify the functional role of this broad spectrum of burst properties within the TRN.

REFERENCES

REFERENCES

- Bovenkamp-Janssen, M.C. van de, Scheenen, W.J.J.M., Kuijpers-Kwant, F.J., Kozicz, T., Veening, J.G., Luijtelaar, E.L.J.M. van, McEnery, M.W., Roubos, E.W., 2004. Differential expression of high voltage-activated Ca²⁺ channel types in the rostral reticular thalamic nucleus of the absence epileptic WAG/Rij rat. *J. Neurobiol.* 58, 467–478. <https://doi.org/10.1002/neu.10291>
- Bezdudnaya, T., Cano, M., Bereshpolova, Y., Stoelzel, C.R., Alonso, J.-M., Swadlow, H.A., 2006. Thalamic Burst Mode and Inattention in the Awake LGNd. *Neuron* 49, 421–432. <https://doi.org/10.1016/j.neuron.2006.01.010>
- Broicher, T., Kanyshkova, T., Meuth, P., Pape, H.-C., Budde, T., 2008. Correlation of T-channel coding gene expression, IT, and the low threshold Ca²⁺ spike in the thalamus of a rat model of absence epilepsy. *Mol. Cell. Neurosci.* 39, 384–399. <https://doi.org/10.1016/j.mcn.2008.07.012>
- Brunton, J., Charpak, S., 1992. Heterogeneity of cell firing properties and opioid sensitivity in the thalamic reticular nucleus 5.
- Clemente-Perez, A., Makinson, S.R., Higashikubo, B., Brovarney, S., Cho, F.S., Urry, A., Holden, S.S., Wimer, M., Dávid, C., Fenno, L.E., Acsády, L., Deisseroth, K., Paz, J.T., 2017. Distinct Thalamic Reticular Cell Types Differentially Modulate Normal and Pathological Cortical Rhythms. *Cell Rep.* 19, 2130–2142. <https://doi.org/10.1016/j.celrep.2017.05.044>
- Contreras, D., Curro Dossi, R., Steriade, M., 1992. Bursting and tonic discharges in two classes of reticular thalamic neurons. *J. Neurophysiol.* 68, 973–977. <https://doi.org/10.1152/jn.1992.68.3.973>
- Coulter, D.A., Huguenard, J.R., Prince, D.A., 1989. Calcium currents in rat thalamocortical relay neurones: kinetic properties of the transient, low-threshold current. *J. Physiol.* 414, 587–604. <https://doi.org/10.1113/jphysiol.1989.sp017705>
- Cox, C.L., Huguenard, J.R., Prince, D.A., 1995. Cholecystokinin depolarizes rat thalamic reticular neurons by suppressing a K⁺ conductance. *J. Neurophysiol.* 74, 990–1000. <https://doi.org/10.1152/jn.1995.74.3.990>
- Crabtree, J.W., 1996. Organization in the somatosensory sector of the cat's thalamic reticular nucleus. *J. Comp. Neurol.* 366, 207–222. [https://doi.org/10.1002/\(SICI\)1096-9861\(19960304\)366:2<207::AID-CNE2>3.0.CO;2-9](https://doi.org/10.1002/(SICI)1096-9861(19960304)366:2<207::AID-CNE2>3.0.CO;2-9)
- Crabtree, J.W., 1992. The Somatotopic Organization Within the Rabbit's Thalamic Reticular Nucleus. *Eur. J. Neurosci.* 4, 1343–1351. <https://doi.org/10.1111/j.1460-9568.1992.tb00159.x>

- Crandall, S.R., Govindaiah, G., Cox, C.L., 2010. Low-Threshold Ca²⁺ Current Amplifies Distal Dendritic Signaling in Thalamic Reticular Neurons. *J. Neurosci.* 30, 15419–15429. <https://doi.org/10.1523/JNEUROSCI.3636-10.2010>
- Cueni, L., Canepari, M., Luján, R., Emmenegger, Y., Watanabe, M., Bond, C.T., Franken, P., Adelman, J.P., Lüthi, A., 2008. T-type Ca²⁺ channels, SK2 channels and SERCAs gate sleep-related oscillations in thalamic dendrites. *Nat. Neurosci.* 11, 683–692. <https://doi.org/10.1038/nn.2124>
- David, F., Schmiedt, J.T., Taylor, H.L., Orban, G., Giovanni, G.D., Uebele, V.N., Renger, J.J., Lambert, R.C., Leresche, N., Crunelli, V., 2013. Essential Thalamic Contribution to Slow Waves of Natural Sleep. *J. Neurosci.* 33, 19599–19610. <https://doi.org/10.1523/JNEUROSCI.3169-13.2013>
- Destexhe, A., Neubig, M., Ulrich, D., Huguenard, J., 1998. Dendritic Low-Threshold Calcium Currents in Thalamic Relay Cells. *J. Neurosci.* 18, 3574–3588. <https://doi.org/10.1523/JNEUROSCI.18-10-03574.1998>
- Domich, L., Oakson, G., Steriade, M., 1986. Thalamic burst patterns in the naturally sleeping cat: a comparison between cortically projecting and reticularis neurones. *The Journal of Physiology* 379, 429–449. <https://doi.org/10.1113/jphysiol.1986.sp016262>
- Ekonomou, A., Angelatou, F., Vergnes, M., Kostopoulos, G., 1998. Lower density of A1 adenosine receptors in nucleus reticularis thalami in rats with genetic absence epilepsy: *NeuroReport* 9, 2135–2140. <https://doi.org/10.1097/00001756-199806220-00042>
- Funke, K., Eysel, U.T., 1993. Modulatory effects of acetylcholine, serotonin and noradrenaline on the activity of cat perigeniculate neurons. *Exp. Brain Res.* 95, 409–420. <https://doi.org/10.1007/BF00227133>
- Guido, W., Weyand, T., 1995. Burst responses in thalamic relay cells of the awake behaving cat. *J. Neurophysiol.* 74, 1782–1786. <https://doi.org/10.1152/jn.1995.74.4.1782>
- Hartings, J.A., Temereanca, S., Simons, D.J., 2003. State-Dependent Processing of Sensory Stimuli by Thalamic Reticular Neurons. *J. Neurosci.* 23, 5264–5271. <https://doi.org/10.1523/JNEUROSCI.23-12-05264.2003>
- Hu, H., Cavendish, J.Z., Agmon, A., 2013. Not all that glitters is gold: off-target recombination in the somatostatin–IRES–Cre mouse line labels a subset of fast-spiking interneurons. *Front. Neural Circuits* 7. <https://doi.org/10.3389/fncir.2013.00195>
- Huguenard, J.R., Prince, D.A., 1992. A novel T-type current underlies prolonged Ca²⁺-dependent burst firing in GABAergic neurons of rat thalamic reticular nucleus. *J. Neurosci.* 12, 3804–3817. <https://doi.org/10.1523/JNEUROSCI.12-10-03804.1992>

- Jacobsen, R.B., Ulrich, D., Huguenard, J.R., 2001. GABAB and NMDA Receptors Contribute to Spindle-Like Oscillations in Rat Thalamus In Vitro. *J. Neurophysiol.* 86, 1365–1375. <https://doi.org/10.1152/jn.2001.86.3.1365>
- Kim, U., McCormick, D.A., 1998. The Functional Influence of Burst and Tonic Firing Mode on Synaptic Interactions in the Thalamus. *J. Neurosci.* 18, 9500–9516. <https://doi.org/10.1523/JNEUROSCI.18-22-09500.1998>
- Kim, U., Sanchez-Vives, M.V., McCormick, D.A., 1997. Functional Dynamics of GABAergic Inhibition in the Thalamus. *Science* 278, 130–134. <https://doi.org/10.1126/science.278.5335.130>
- Kleiman-Weiner, M., Beenhakker, M.P., Segal, W.A., Huguenard, J.R., 2009. Synergistic Roles of GABAA Receptors and SK Channels in Regulating Thalamocortical Oscillations. *J. Neurophysiol.* 102, 203–213. <https://doi.org/10.1152/jn.91158.2008>
- Kovács, K., Sík, A., Ricketts, C., Timofeev, I., 2010. Subcellular distribution of low-voltage activated T-type Ca²⁺ channel subunits (Cav3.1 and Cav3.3) in reticular thalamic neurons of the cat. *J. Neurosci. Res.* 88, 448–460. <https://doi.org/10.1002/jnr.22200>
- Lam, Y.-W., Sherman, S.M., 2011. Functional Organization of the Thalamic Input to the Thalamic Reticular Nucleus. *J. Neurosci. Off. J. Soc. Neurosci.* 31, 6791–6799. <https://doi.org/10.1523/JNEUROSCI.3073-10.2011>
- Lee, S.-H., Govindaiah, G., Cox, C.L., 2007. Heterogeneity of firing properties among rat thalamic reticular nucleus neurons. *J. Physiol.* 582, 195–208. <https://doi.org/10.1113/jphysiol.2007.134254>
- Li, Y., Lopez-Huerta, V.G., Adiconis, X., Levandowski, K., Choi, S., Simmons, S.K., Arias-Garcia, M.A., Guo, B., Yao, A.Y., Blosser, T.R., Wimmer, R.D., Aida, T., Atamian, A., Naik, T., Sun, X., Bi, D., Malhotra, D., Hession, C.C., Shema, R., Gomes, M., Li, T., Hwang, E., Krol, A., Kowalczyk, M., Peça, J., Pan, G., Halassa, M.M., Levin, J.Z., Fu, Z., Feng, G., 2020. Distinct subnetworks of the thalamic reticular nucleus. *Nature* 583, 819–824. <https://doi.org/10.1038/s41586-020-2504-5>
- Liegeois, J., Mercier, F., Graulich, A., Graulich-Lorge, F., Scuvee-Moreau, J., Seutin, V., 2003. Modulation of Small Conductance Calcium-Activated Potassium (SK) Channels: A New Challenge in Medicinal Chemistry. *Curr. Med. Chem. Schiph.* 10, 625–47. <http://dx.doi.org/10.2174/0929867033457908>
- Lu, S.M., Guido, W., Sherman, S.M., 1992. Effects of membrane voltage on receptive field properties of lateral geniculate neurons in the cat: contributions of the low-threshold Ca²⁺ conductance. *J. Neurophysiol.* 68, 2185–2198. <https://doi.org/10.1152/jn.1992.68.6.2185>

- Lübke, J., 1993. Morphology of neurons in the thalamic reticular nucleus (TRN) of mammals as revealed by intracellular injections into fixed brain slices. *J. Comp. Neurol.* 329, 458–471. <https://doi.org/10.1002/cne.903290404>
- Madisen, L., Zwingman, T.A., Sunkin, S.M., Oh, S.W., Zariwala, H.A., Gu, H., Ng, L.L., Palmiter, R.D., Hawrylycz, M.J., Jones, A.R., Lein, E.S., Zeng, H., 2010. A robust and high-throughput Cre reporting and characterization system for the whole mouse brain. *Nat. Neurosci.* 13, 133–140. <https://doi.org/10.1038/nn.2467>
- Marlinski, V., Beloozerova, I.N., 2014. Burst firing of neurons in the thalamic reticular nucleus during locomotion. *J. Neurophysiol.* 112, 181–192. <https://doi.org/10.1152/jn.00366.2013>
- Martinez-Garcia, R.I., Voelcker, B., Zaltsman, J.B., Patrick, S.L., Stevens, T.R., Connors, B.W., Cruikshank, S.J., 2020. Two dynamically distinct circuits drive inhibition in the sensory thalamus. *Nature* 583, 813–818. <https://doi.org/10.1038/s41586-020-2512-5>
- McCormick, D.A., Prince, D.A., 1986. Acetylcholine induces burst firing in thalamic reticular neurones by activating a potassium conductance. *Nature* 319, 402–405. <https://doi.org/10.1038/319402a0>
- McCormick, D.A., Wang, Z., 1991. Serotonin and noradrenaline excite GABAergic neurones of the guinea-pig and cat nucleus reticularis thalami. *J. Physiol.* 442, 235–255. <https://doi.org/10.1113/jphysiol.1991.sp018791>
- Pellegrini, C., Lecci, S., Lüthi, A., Astori, S., 2016. Suppression of Sleep Spindle Rhythmogenesis in Mice with Deletion of CaV3.2 and CaV3.3 T-type Ca²⁺ Channels. *Sleep* 39, 875–885. <https://doi.org/10.5665/sleep.5646>
- Pinault, D., Deschênes, M., 1998. Projection and innervation patterns of individual thalamic reticular axons in the thalamus of the adult rat: A three-dimensional, graphic, and morphometric analysis. *J. Comp. Neurol.* 391, 180–203. [https://doi.org/10.1002/\(SICI\)1096-9861\(19980209\)391:2<180::AID-CNE3>3.0.CO;2-Z](https://doi.org/10.1002/(SICI)1096-9861(19980209)391:2<180::AID-CNE3>3.0.CO;2-Z)
- Ramcharan, E.J., Cox, C.L., Zhan, X.J., Sherman, S.M., Gnadt, J.W., 2000. Cellular Mechanisms Underlying Activity Patterns in the Monkey Thalamus During Visual Behavior. *Journal of Neurophysiology* 84, 1982–1987. <https://doi.org/10.1152/jn.2000.84.4.1982>
- Sailer, C.A., Kaufmann, W.A., Marksteiner, J., Knaus, H.-G., 2004. Comparative immunohistochemical distribution of three small-conductance Ca²⁺-activated potassium channel subunits, SK1, SK2, and SK3 in mouse brain. *Mol. Cell. Neurosci.* 26, 458–469. <https://doi.org/10.1016/j.mcn.2004.03.002>
- Sokhadze, G., Campbell, P.W., Guido, W., 2019. Postnatal development of cholinergic input to the thalamic reticular nucleus of the mouse. *Eur. J. Neurosci.* 0. <https://doi.org/10.1111/ejn.13942>

- Solé, A., Mas, J., Esteve, I., 2007. A new method based on image analysis for determining cyanobacterial biomass by CLSM in stratified benthic sediments. *Ultramicroscopy* 107, 669–673. <https://doi.org/10.1016/j.ultramic.2007.01.007>
- Spreafico, R., Battaglia, G., Frassoni, C., 1991. The reticular thalamic nucleus (RTN) of the rat: Cytoarchitectural, Golgi, immunocytochemical, and horseradish peroxidase study. *J. Comp. Neurol.* 304, 478–490. <https://doi.org/10.1002/cne.903040311>
- Spreafico, R., de Curtis, M., Frassoni, C., Avanzini, G., 1988. Electrophysiological characteristics of morphologically identified reticular thalamic neurons from rat slices. *Neuroscience* 27, 629–638. [https://doi.org/10.1016/0306-4522\(88\)90294-1](https://doi.org/10.1016/0306-4522(88)90294-1)
- Steriade, M., 2005. Sleep, epilepsy and thalamic reticular inhibitory neurons. *Trends Neurosci., INMED/TINS special issue: Multiple facets of GABAergic synapses* 28, 317–324. <https://doi.org/10.1016/j.tins.2005.03.007>
- Steriade, M., Domich, L., Oakson, G., 1986. Reticularis thalami neurons revisited: activity changes during shifts in states of vigilance. *J. Neurosci.* 6, 68–81. <https://doi.org/10.1523/JNEUROSCI.06-01-00068.1986>
- Taniguchi, H., He, M., Wu, P., Kim, S., Paik, R., Sugino, K., Kvitsiani, D., Kvitsani, D., Fu, Y., Lu, J., Lin, Y., Miyoshi, G., Shima, Y., Fishell, G., Nelson, S.B., Huang, Z.J., 2011. A resource of Cre driver lines for genetic targeting of GABAergic neurons in cerebral cortex. *Neuron* 71, 995–1013. <https://doi.org/10.1016/j.neuron.2011.07.026>
- Warren, R.A., Golshani, P., Jones, E.G., 1997. GABA_B-Receptor-Mediated Inhibition in Developing Mouse Ventral Posterior Thalamic Nucleus. *J. Neurophysiol.* 78, 550–553. <https://doi.org/10.1152/jn.1997.78.1.550>
- Warren, R.A., Jones, E.G., 1997. Maturation of Neuronal Form and Function in a Mouse Thalamo-Cortical Circuit. *J. Neurosci.* 17, 277–295. <https://doi.org/10.1523/JNEUROSCI.17-01-00277.1997>
- Ying, S.-W., Goldstein, P.A., 2005. Propofol-Block of SK Channels in Reticular Thalamic Neurons Enhances GABAergic Inhibition in Relay Neurons. *J. Neurophysiol.* 93, 1935–1948. <https://doi.org/10.1152/jn.01058.2004>
- Zhan, X.J., Cox, C.L., Rinzel, J., Sherman, S.M., 1999. Current Clamp and Modeling Studies of Low-Threshold Calcium Spikes in Cells of the Cat's Lateral Geniculate Nucleus. *J. Neurophysiol.* 81, 2360–2373. <https://doi.org/10.1152/jn.1999.81.5.2360>
- Zikopoulos, B., Barbas, H., 2007. Circuits for multisensory integration and attentional modulation through the prefrontal cortex and the thalamic reticular nucleus in primates. *Rev. Neurosci.* 18, 417–438.

CHAPTER 3: DENDRITIC CALCIUM CHANNEL ACTIVITY AND DISTRIBUTION IN HETEROGENEOUS TRN NEURONS

Abstract

Neurons within the thalamic reticular nucleus (TRN) are critical modulators of sensory processing within the brain. Their significant contribution to thalamocortical inhibition allows them to appropriately modulate sensory afferents as they are processed between the thalamus and cortex. TRN neurons distinctly discharge action potentials in two modes: burst and tonic mode. In Chapter 2, burst discharge from TRN neurons was shown to vary greatly in the action potential frequency during this transient discharge. Such variability could have important implications on the functional output of these different TRN neurons. Prior studies suggest that T-type calcium channels are distributed throughout the dendrites in TRN neurons with high frequency burst discharge. Considering that a significant population of TRN neurons have a lower frequency burst discharge, the distribution of calcium responses along the proximal-distal extent of TRN dendrites was next examined. Using two-photon laser scanning microscopy, it was found that calcium signals were significantly smaller in lower frequency bursting neurons at all intermediate and distal dendritic regions relative to higher frequency bursting neurons. Subsequent blocking of small conductance calcium-activated potassium channels (SK) unmasked a larger calcium response at proximal and intermediate locations for higher frequency bursting neurons, but mainly at proximal locations for lower frequency bursting neurons. These data reveal that heterogeneous TRN burst discharge frequencies may represent a diverse cell population with different dendritic ion channel composition and distribution.

Introduction

The thalamic reticular nucleus (TRN) is a GABAergic nucleus that serves as a major source of inhibition onto thalamocortical neurons that affect sensory circuits (Cox et al., 1997). As ascending sensory information enters the thalamus, it must be relayed to the appropriate neocortical region for subsequent processing. The TRN is uniquely situated in that thalamocortical and corticothalamic axons give rise to collateral afferents onto TRN neurons as they traverse the region. The synaptic integration of these collaterals serves to “inform” TRN neurons of the state of excitation within the thalamocortical and corticothalamic pathways (Guillery and Harting, 2003). TRN neurons integrate this information to perform appropriate thalamocortical inhibition in response, and thus they play an important role in the modulation and likely regulation of sensory transmission from the thalamus to the neocortex.

TRN neurons produce action potentials in two distinct modes: burst and tonic mode. When a TRN neuron is in burst mode, the membrane potential is relatively hyperpolarized, allowing incoming excitatory postsynaptic potentials (EPSPs) to activate a transient T-type calcium channel-mediated LTS of varying sizes (Kim and McCormick, 1998; Hartings et al., 2003). This LTS can then generate a burst of multiple Na⁺-dependent action potentials at a relatively high frequency. In tonic mode, action potentials are discharged at a roughly consistent rate that is related to the magnitude of afferent synaptic excitation.

While most TRN neurons produce high-frequency bursts of action potentials at hyperpolarized membrane potentials, a subset of non-bursting neurons appears to be incapable of producing burst discharge. Instead, they fire action potentials in a tonic pattern in response to membrane depolarizations, regardless of membrane potential (Contreras et al., 1992; Lee et al.,

2007). While non-bursting neurons may have fewer T-type calcium (T-)channels or have less T-channel current (I_T) activation, it is also possible that they lack the typical robust burst due to a distribution of T-channels that is biased towards distal dendrites with little signal propagation through the more proximal arbors (Chausson et al., 2013). Burst discharge in general is largely determined by the presence of T-channels at the soma and proximal dendrites. A more distal distribution of T-channels in neurons lacking burst discharge could also serve as a voltage state-dependent amplifier of afferent synaptic activity at those distal locations. The differentiation of burst and tonic modes is important to the TRN because the inhibitory output onto thalamocortical neurons is quantitatively different depending on the mode. High frequency bursts of action potentials deliver strong tetanic inhibition, through the activation of both GABA_A and GABA_B receptors, whereas tonic discharge of TRN neurons primarily activates only GABA_A receptors (Kim et al., 1997; Kim and McCormick, 1998).

These studies have previously shown that not only do TRN neurons discharge bursts across a broad range of frequencies, but the amplitude of the I_T -mediated LTS is positively correlated with the burst frequency (Chapter 2). It is not clear whether reduced LTS amplitude is due to a decreased density of T-channels on the soma and proximal dendrites, a lower level of T-channel activation, or a greater distribution of T-channels distally along the dendrites. As previously discussed, it is possible that the lack of typical burst discharge in non-bursting neurons may not necessarily indicate that they lack T-channels, but instead there are a greater density of T-channels on distal dendrites that are not activated by somatic depolarization but could act as synaptic amplifiers in response to afferent synaptic activity at distal sites. While

nearly all TRN neurons can elicit a transient I_T mediated LTS at hyperpolarized states, the distribution of T-channels along the dendritic arbor remains unclear.

The relative location of dendritic T-type calcium channels underlying the LTS is an important feature of the neuron because densities may provide location-specific amplification of afferent signals in burst mode. (Cueni et al., 2008a; Destexhe et al., 1996). The location of T-channels along the dendrites may also impact different characteristics identified in these highly variable burst types, such as LTS amplitude, LTS half-width, and average burst discharge frequency. In addition to T-channels, small conductance calcium-activated potassium (SK) channels have also been shown to have significant influence on burst discharge, however their activity and dendritic distribution in lower frequency bursting is unknown. SK channels are activated during burst discharge in TRN neurons. Rhythmic oscillations in the TRN are maintained by the interplay of I_T , selective sarcoplasmic reticulum calcium ATPase (SERCA) and SK channels, which rapidly uptake calcium to allow T-channels to quickly recover (Cueni et al., 2008b). SK channels are activated by calcium influx, such as during an I_T -mediated burst. Activated SK current (I_{SK}) increases a K^+ conductance, leading to an accelerated repolarization following the LTS, truncating the burst duration and subsequently reducing the inter-burst interval of repetitive bursting TRN neurons (Cueni et al., 2008b; Hallworth et al., 2003; Liegeois et al., 2003). While I_{SK} can contribute to the fast AHP (after hyperpolarization) of single action potentials, the greater impact, and one that directly contributes to TRN maintenance of oscillatory rhythms, comes from their activation the burst discharge calcium influx (Cueni et al., 2008b; Liegeois et al., 2003). It is clear that I_{SK} activation has a prominent role in shaping the burst output of TRN neurons. However, given the potential of dendritic I_T to act as a location- and voltage-dependent amplifier

of local synaptic afferents, location-specific densities of SK channels could also serve to impact the I_T -mediated amplification of afferent synaptic activity.

In earlier findings (Chapter 2), it was found that burst discharge frequencies in TRN neurons vary widely in the frequency and number of action potentials per burst. Because T-channels are responsible for the LTS that underlies a burst discharge, a series of experiments were conducted to measure whether the density and/or distribution of calcium channels along the dendrite were related to the frequency of the burst. Additionally, the I_{SK} inhibitor apamin was applied to investigate whether dendritic I_{SK} may impact I_T in a location-specific manner.

Materials and Methods

Slice preparation

Animals were housed at Michigan State University animal facilities and all experiments were conducted in accordance with the Institutional Animal Care and Use Committee (IACUC). All experiments utilized female and male adult C57BL/6J mice (Postnatal age 42 ± 13 days, range 29-72). For brain slicing procedures, animals were deeply anesthetized (3% isoflurane, 97% O_2) and in some cases perfused with the cold ($4^\circ C$) slicing solution containing (in mM): 2.5 KCl, 1.25 NaH_2PO_4 , 10.0 $MgSO_4$, 0.5 $CaCl_2$, 26.0 $NaHCO_3$, 10.0 glucose, and 234.0 sucrose. Horizontal brain slices (300 μm thickness) were made using a vibrating tissue slicer while immersed in cold ($4^\circ C$), oxygenated (95% O_2 , 5% CO_2) slicing solution. Slices were immediately transferred to a warmed holding chamber ($35^\circ C$) of oxygenated (95% O_2 , 5% CO_2) artificial cerebrospinal fluid (ACSF) solution containing (in mM): 126.0 NaCl, 2.5 KCl, 1.25 NaH_2PO_4 , 2.0 $MgCl_2$, 2.0 $CaCl_2$, 26.0

NaHCO₃, and 10.0 glucose. After 30 minutes, holding chamber temperature was returned to room temperature and slices incubated for a minimum of 60 minutes prior to recording.

Electrophysiology

Glass micropipettes pulled to resistances between 4-6 MΩ were used to perform whole-cell TRN neuron recordings in horizontal brain slices. Micropipettes were filled with an internal solution of (in mM): 117 K-methyl-sulfate, 13 KCl, 1.0 MgCl₂, 0.07 CaCl₂, 10 HEPES, 2.0 ATP, and 0.4 GTP. An Olympus BX-51WI with Dodt gradient contrast optics was utilized to locate the neurons, and cells were recorded in a slice chamber with fresh oxygenated (95% O₂, 5% CO₂) ACSF maintained at 32°C. Only cells with an input resistance greater than 100 MΩ, a resting membrane potential more negative than -50 mV that did not fluctuate > 10 mV throughout the duration of the recording, lacked spontaneous action potential firing, and had an evoked action potential peak > +0 mV were included for analyses. Data were obtained using a MultiClamp 700b amplifier and sampled at a rate of 20 kHz. Data were filtered at 4 kHz using a Digidata 1550a digitizer. All voltages are corrected for an 8 mV liquid junction potential. PClamp software (Molecular Devices, Inc.) was used for electrophysiology.

Pharmacology

All antagonists were bath applied for at least 10 minutes prior to proceeding with experiments. Concentrated stock solutions were created in distilled water and brought to a working concentration in ACSF. Pharmaceutical agents were purchased from either Tocris (Minneapolis, MN) or Sigma-Aldrich Co. (St. Louis, MO).

Calcium imaging

A two-photon laser scanning system was used for cell imaging (Ultima, Bruker). After break-in, the cell was allowed to fill with the calcium-insensitive fluorescent indicator Alexa 594 (25 μM) for at least fifteen minutes before calcium imaging. As illustrated in Figure 3.0 A, calcium influx was measured at three distances from the soma to distal dendrites: proximal (10 μm from the soma), intermediate (75-130 μm from the soma), and distal (150-350 μm from the soma). Rapid linescans (5-7 scans/location) were executed at discrete dendritic locations to measure fluorescent calcium activity using a calcium-sensitive dye (Fluo5-ff, 100 μM) relative to a calcium insensitive indicator, Alexa 594 (Figure 3.0 B). Background subtraction was used to remove non-fluorescent noise from stable calcium recordings obtained from the linescans, and the calcium signal was then averaged over the multiple scans to yield peak ($\Delta\text{G/R}$) or time-integral ($(\Delta\text{G/R})/\text{ms}$) measurements (Figure 3.0 C). Peak $\Delta\text{G/R}$ measurements have been frequently used to report data within calcium imaging studies, however consideration of the potential volumetric limitations of non-linear dye diffusion, especially in thin ($< 1 \mu\text{m}$) distal dendrites of TRN neurons (up to 350 μm from the soma), indicates that the buffering potential of the calcium indicator is likely non-linear throughout the dendritic arbors. Conversely, the heightened buffering potential in more proximal dendrites adds considerable weight to the accuracy of the time-integral based measurements which are unrelated to the K_B of the calcium indicator (Helmchen et al., 1996).

Data Analysis

All electrophysiological analysis was performed using Clampfit (Molecular Devices, San Jose, CA) software. Calcium signals were analyzed using custom code in Mathematica (Wolfram,

Champaign, IL). Statistics were calculated using Microsoft excel and Mathematica and all values are reported as average \pm standard deviation unless otherwise stated.

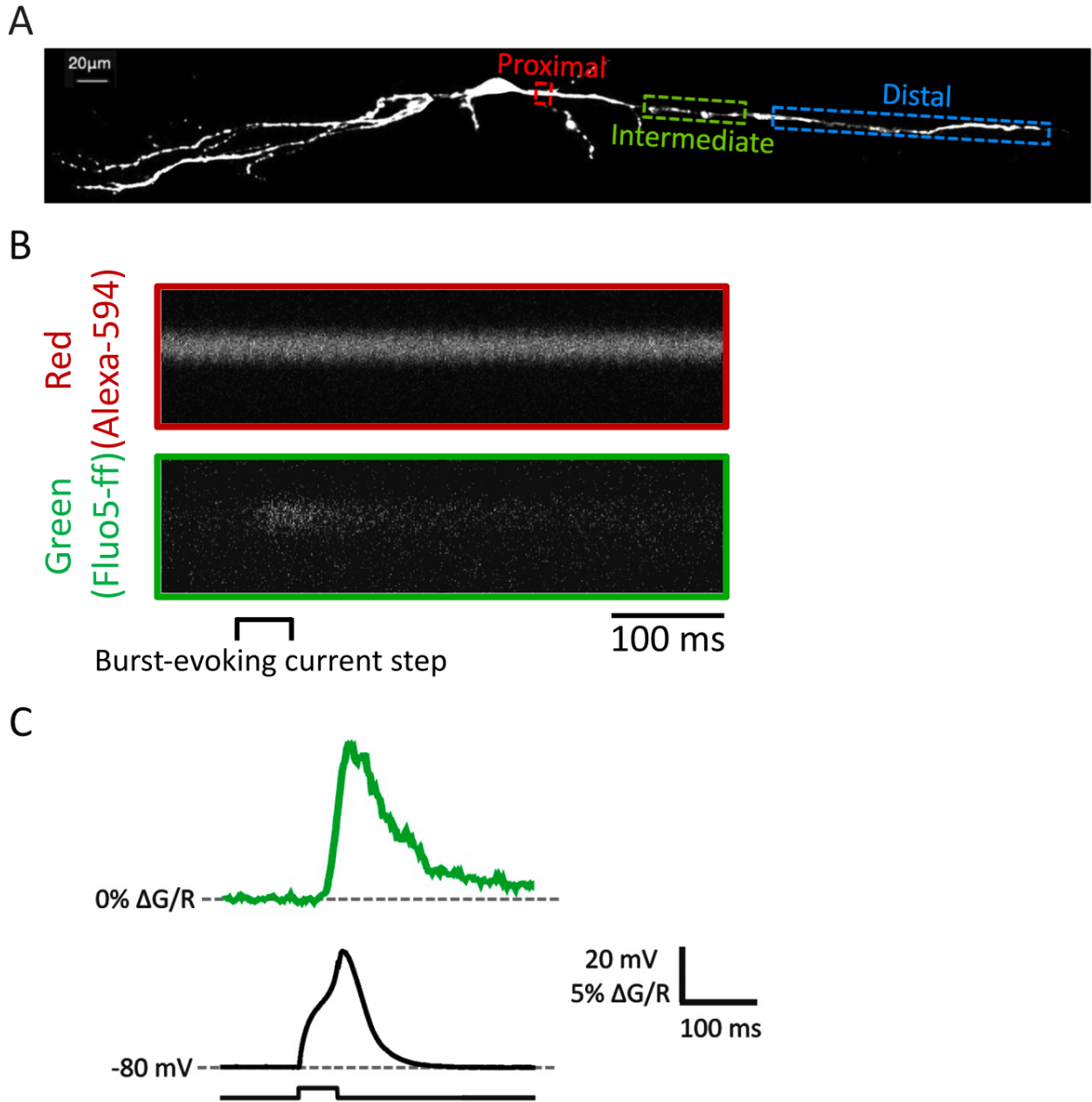


Figure 3.0: Dendritic calcium imaging of TRN neurons. (A) Fluorescently filled TRN neuron with proximal (10 μ m), intermediate (75-130 μ m), and distal (150-350 μ m) ranges of dendritic imaging

Figure 3.0 (cont'd)

locations indicated. (B) Raw linescan images showing the green (Fluo5-ff) and red (Alexa 595) channel fluorescence in response to a somatic burst evoked by a 50 ms current step. (C) Calcium measurements are reported as the change in the green channel over red ($\% \Delta G/R$) as a function of time (top). A representative evoked burst trace is shown below.

Results

Dendritic calcium response to somatically evoked burst discharge in high-frequency bursting neurons

A previous study found that within higher frequency bursting TRN neurons, an LTS generated at the soma will result in calcium signals within the dendrites. These calcium signals were also found to increase in magnitude from proximal to distal dendrites, a phenomenon not observed in thalamocortical neurons (Crandall et al., 2010). To determine whether this distribution is consistent for both lower frequency (≤ 100 Hz) and higher frequency (> 100 Hz) bursting TRN neurons, the next aim was to activate dendritic I_T by evoking a maximal somatic burst that would backpropagate into the dendritic arbors. Short (30-60 ms) current steps of increasing intensities (50 pA intervals) were used to determine the maximally activated somatic burst. TTX (1 μ M) was then applied to block the Na^+ -dependent action potentials, and thereby unmask the LTS.

In the subset of higher frequency bursting neurons, (> 100 Hz), calcium signals could be evoked throughout the length of the dendrites. In response to a short (30-60 ms) current injection, the integral of the calcium signal was largest proximally and decreased at more distal

distances (Figure 3.1 A-B; proximal: 2839 ± 1535 ($\Delta G/R$)/ms), $n = 32D, 32C$; intermediate: 2524 ± 1649 ($\Delta G/R$)/ms, $n = 21D, 21C$; distal: 1741 ± 809 ($\Delta G/R$)/ms, $n = 16D, 16C$). Subsequent statistical analyses did not show a significant difference of the calcium signal at different locations ($F_{2,66} = 3.100$, $P = 0.052$, ANOVA); however, subsequent post hoc Tukey tests indicated significant decrease in calcium activity from proximal to distal regions ($P = 0.040$, Tukey post hoc test). When analyzing the peak calcium signal ($\Delta G/R$), the largest burst-evoked calcium signals occurred in the intermediate (Figure 3.1 C-D; 15.8 ± 7.0 $\Delta G/R$, $n = 21D, 21C$) and distal regions (15.5 ± 6.4 $\Delta G/R$, $n = 16D, 16C$). The signal in the proximal region averaged 12.1 ± 6.0 $\Delta G/R$ ($n = 32D, 32C$). There was no statistical difference between peak calcium signals at any dendritic distance ($F_{2,66} = 2.661$, $P = 0.077$, ANOVA).

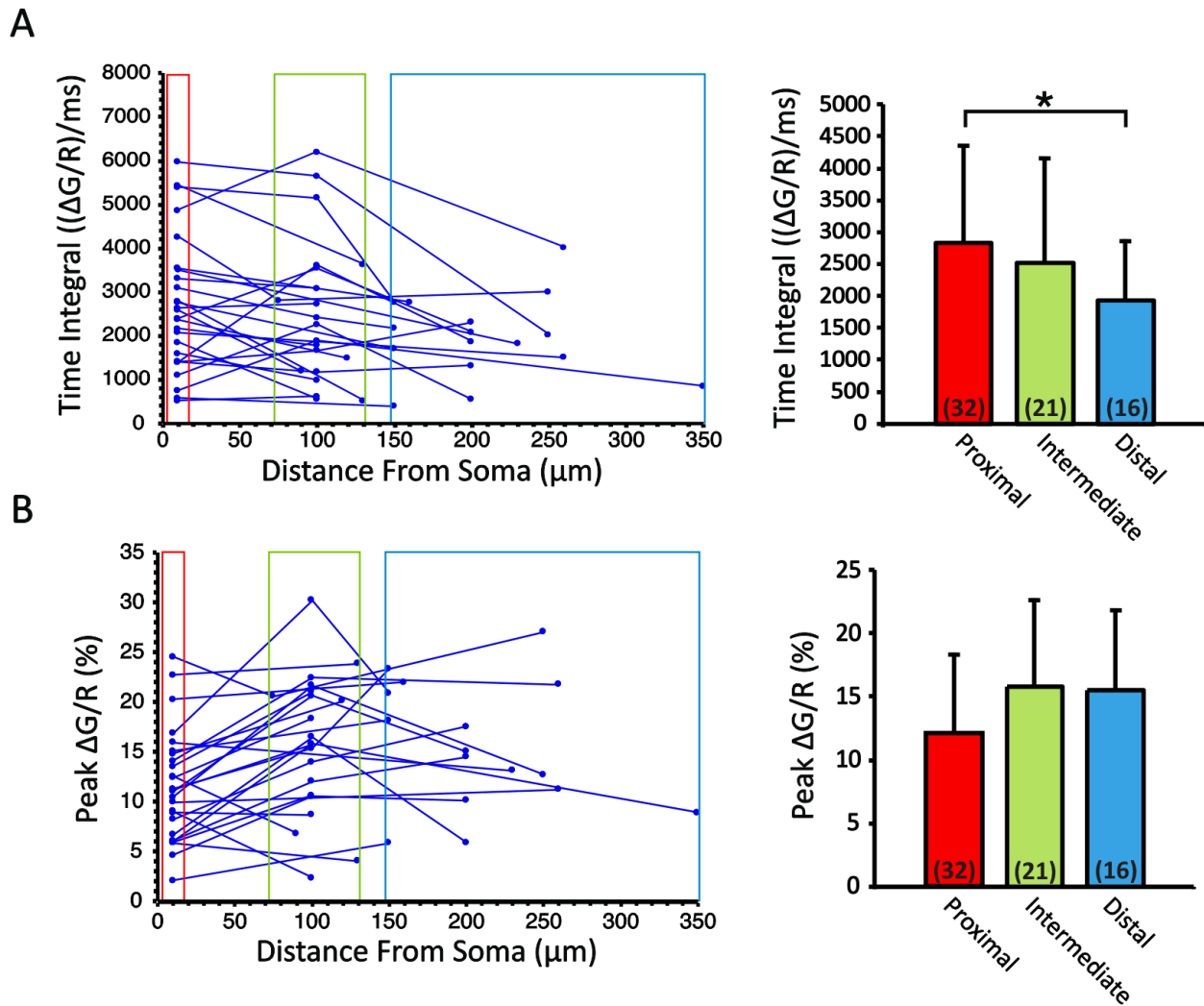


Figure 3.1: Dendritic calcium activity in higher frequency bursting TRN neurons. Dendritic calcium responses were measured following a somatic current injection eliciting an LTS. Experiments were conducted in TTX, and appropriate current to elicit a maximal depolarization was determined directly prior to recordings. (A) Integral (($\Delta G/R$)/ms) measurements of calcium activity within individual neurons bursting at > 100 Hz (left). Red, green, and blue boxes designate values included in proximal, intermediate, and distal locations, respectively. Histogram summarizing the data (right). (B) Peak $\Delta G/R$ measurements of calcium activity within

Figure 3.1 (cont'd)

individual bursting neurons (left) and a histogram summarizing the data (right). * Indicates $P < 0.05$ ANOVA, *Tukey post hoc*.

Dendritic burst mode-evoked calcium activity is reduced in lower frequency bursting neurons

Analysis of lower frequency bursting TRN neurons revealed that dendritic calcium signals were also evoked at all regions in response to a somatic evoked LTS. Integral measurements of the calcium signal along the dendrite showed a trend of larger responses at proximal sites (Figure 3.2 A; proximal: 1613 ± 1801 ($\Delta G/R$)/ms, $n = 25D, 25C$; intermediate: 688 ± 772 ($\Delta G/R$)/ms, $n = 13D, 13C$; distal: 603 ± 675 ($\Delta G/R$)/ms, $n = 13D, 13C$); however, similar to higher frequency bursting neurons, there was no statistical difference in the calcium signal along the dendritic extent ($F_{2,48} = 3.178$, $P = 0.051$, ANOVA). Like the higher frequency bursting neurons, there was a trend of stronger signal at the proximal locations of lower frequency bursting neurons that decreased throughout the length of the dendrite. Direct comparison of the integral measurements of calcium activity at each dendritic region between high and low frequency bursting neurons revealed that higher frequency bursting neurons had significantly more activated calcium along their dendrites (Figure 3.3 A, $P = 0.033$, ANOVA; proximal $P = 0.019$, intermediate $P = 0.005$, distal $P = 0.267$, post hoc *Tukey comparison*).

Measurements of peak calcium activity also revealed a consistent magnitude of activation along the dendrite (Figure 3.2 B; proximal: 7.3 ± 6.7 ($\Delta G/R$), $n = 25D, 25C$; intermediate: 6.6 ± 6.3 ($\Delta G/R$), $n = 13D, 13C$; distal: 6.4 ± 4.8 ($\Delta G/R$), $n = 13D, 13C$; $F_{2,48} = 0.102$, $P = 0.904$ ANOVA). Like the integral measurements, when peak calcium signals at each dendritic location between higher and lower frequency bursting neurons, there was greater activation within the higher frequency

bursting neurons (Figure 3.3 B; $P < 0.001$, ANOVA; proximal $P = 0.055$, intermediate $P = 0.001$, distal $P = 0.002$, *post hoc Tukey Comparison*).

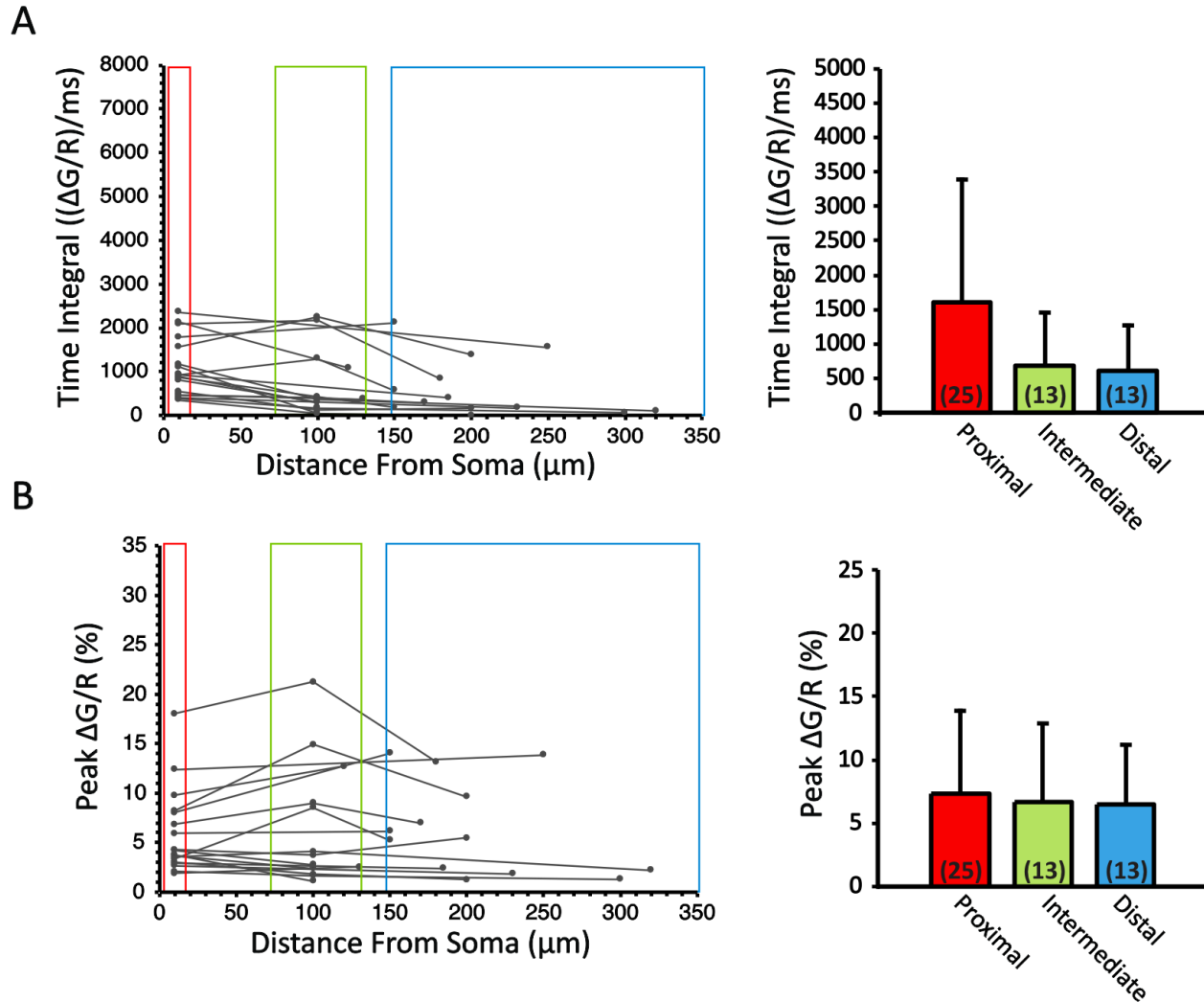


Figure 3.2: Dendritic calcium activity is reduced in lower frequency bursting TRN neurons.

(A) Integral (($\Delta G/R$)/ms) measurements of calcium activity in response to a maximally evoked LTS within individual neurons with initial burst frequencies ≤ 100 Hz (left). Red, green, and blue boxes designate values included in proximal, intermediate, and distal locations, respectively. Histogram summarizing the data (right). (B) Depicts the same measurements as in A, except peak

Figure 3.2 (cont'd)

values ($\Delta G/R$) are represented in the graphs for individual neuron responses (left) and the histogram summary (right). * Indicates $P < 0.05$.

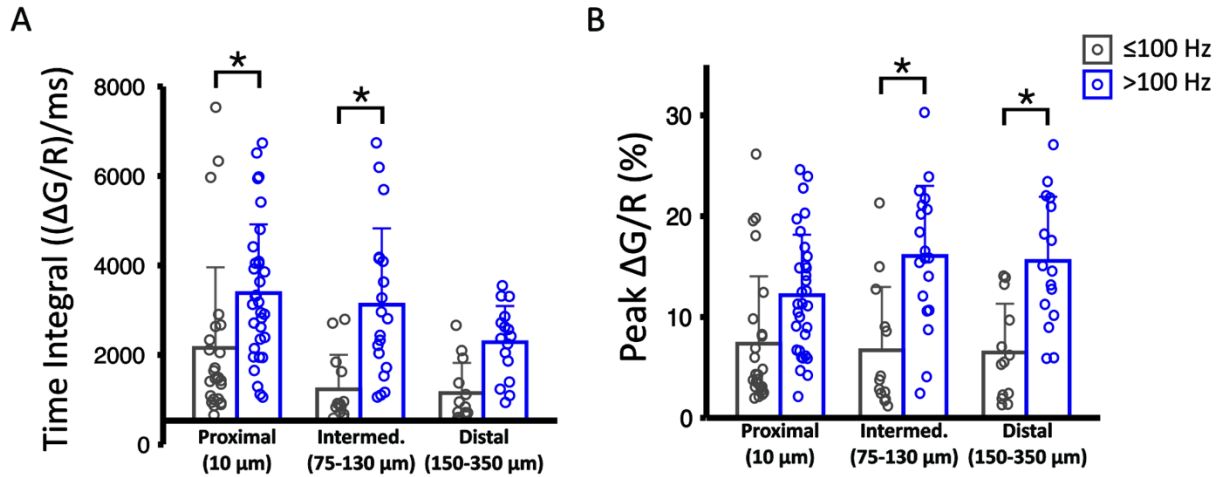


Figure 3.3: Comparison of dendritic calcium activity in higher and lower frequency bursting neurons. (A) Comparison of the time-integral of the calcium signal in response to an evoked burst between lower and higher frequency bursting neurons. Individual data points are represented as open circles. (B) Comparison of peak calcium signals in response to an evoked burst between lower (gray) and higher (blue) frequency bursting neurons. * indicates $P < 0.05$, *Two-way ANOVA*.

Activation of SK channels reduces the duration of the dendritic calcium responses

Our previous study (Chapter 2) revealed that application of the SK channel blocker apamin increased the burst duration, burst frequency, and number of action potentials per burst in both higher and lower frequency bursting neurons. It was next investigated whether SK channels could differentially affect the calcium signals at different dendritic locations. Two-photon laser

scanning microscopy was again used to image calcium activity at various dendritic distances before and after the addition of apamin (100 nM). Findings revealed that both higher and lower frequency bursting neurons responded to apamin with increased dendritic calcium influx in response to a somatic burst, however the dendritic region experiencing the largest increase in calcium influx differed between lower and higher frequency bursting neurons. Integral measurements revealed that in higher frequency bursting neurons (> 100 Hz), apamin significantly increased calcium responses at proximal (Figure 3.4 A-B: control: 3166 ± 1625 ($\Delta G/R$)/ms, apamin: 4378 ± 2324 ($\Delta G/R$)/ms, $n = 16D, 15C$; $P = 0.039$, *paired t-test*) and intermediate regions (control: 3097 ± 1603 ($\Delta G/R$)/ms, apamin: 4946 ± 2999 ($\Delta G/R$)/ms, $n = 14D, 11C$; $P = 0.038$, *paired t-test*). The distal calcium signal was not altered following the application of apamin (control: 2008 ± 865 ($\Delta G/R$)/ms, apamin: 2300 ± 1694 ($\Delta G/R$)/ms, $n = 10D, 10C$; $P = 0.633$, *paired t-test*). In contrast, lower frequency bursting neurons only experienced a strong increase in the proximal signal by apamin (Figure 3.4 D; control: 1030 ± 767 ($\Delta G/R$)/ms, apamin: 1800 ± 1420 ($\Delta G/R$)/ms, $n = 15 D, 14C$; $P = 0.005$, *paired t-test*). The calcium signal integrals observed in the intermediate (control: 841 ± 943 ($\Delta G/R$)/ms, apamin= 1392 ± 1822 ($\Delta G/R$)/ms, $n = 10D, 10C$; $P = 0.271$, *paired t-test*) and distal regions (control: 714 ± 736 ($\Delta G/R$)/ms, apamin= 2246 ± 3218 ($\Delta G/R$)/ms, $n = 10D, 10C$; $P = 0.120$, *paired t-test*) were unaffected by apamin (Figure 3.4 D).

Examination of the effect of apamin on peak calcium influx revealed a similar pattern of significant proximal and intermediate enhancement in higher frequency bursting neurons (Figure 3.4 C: Proximal, control: 12.3 ± 3.6 $\Delta G/R$, apamin: 16.9 ± 6.7 $\Delta G/R$, $n = 16D, 15C$, $P < 0.001$, *paired t-test*; Intermediate, control: 18.0 ± 7.0 $\Delta G/R$, apamin: 20.9 ± 7.9 $\Delta G/R$, $n = 14D, 11C$, $P = 0.015$,

paired t-test; Distal, control: $15.3 \pm 5.1 \Delta G/R$, apamin = $14.9 \pm 6.9 \Delta G/R$, n = 10D, 10C; P = 0.857, *paired t-test*). Lower frequency bursting neurons exhibited significant distal enhancement in addition to proximal when observing peak amplitudes of the signal (Figure 3.4 E: Proximal; control: $5.8 \pm 4.6 \Delta G/R$, apamin: $10.4 \pm 5.8 \Delta G/R$, n = 16; p < 0.001, *paired t-test*; Intermediate; control: $7 \pm 6.8 \Delta G/R$, apamin: $14.2 \pm 7.8 \Delta G/R$, n = 10; P = 0.070, *paired t-test*; Distal; control: $7.3 \pm 5.1 \Delta G/R$, apamin: $11.4 \pm 4.8 \Delta G/R$, n = 10; P = 0.035, *paired t-test*). While SK channel activation may not account for the differences between higher and lower frequency bursting neurons, these results indicate that dendritic region-specific SK channel modulation of burst output plays a role in diverse TRN burst output.

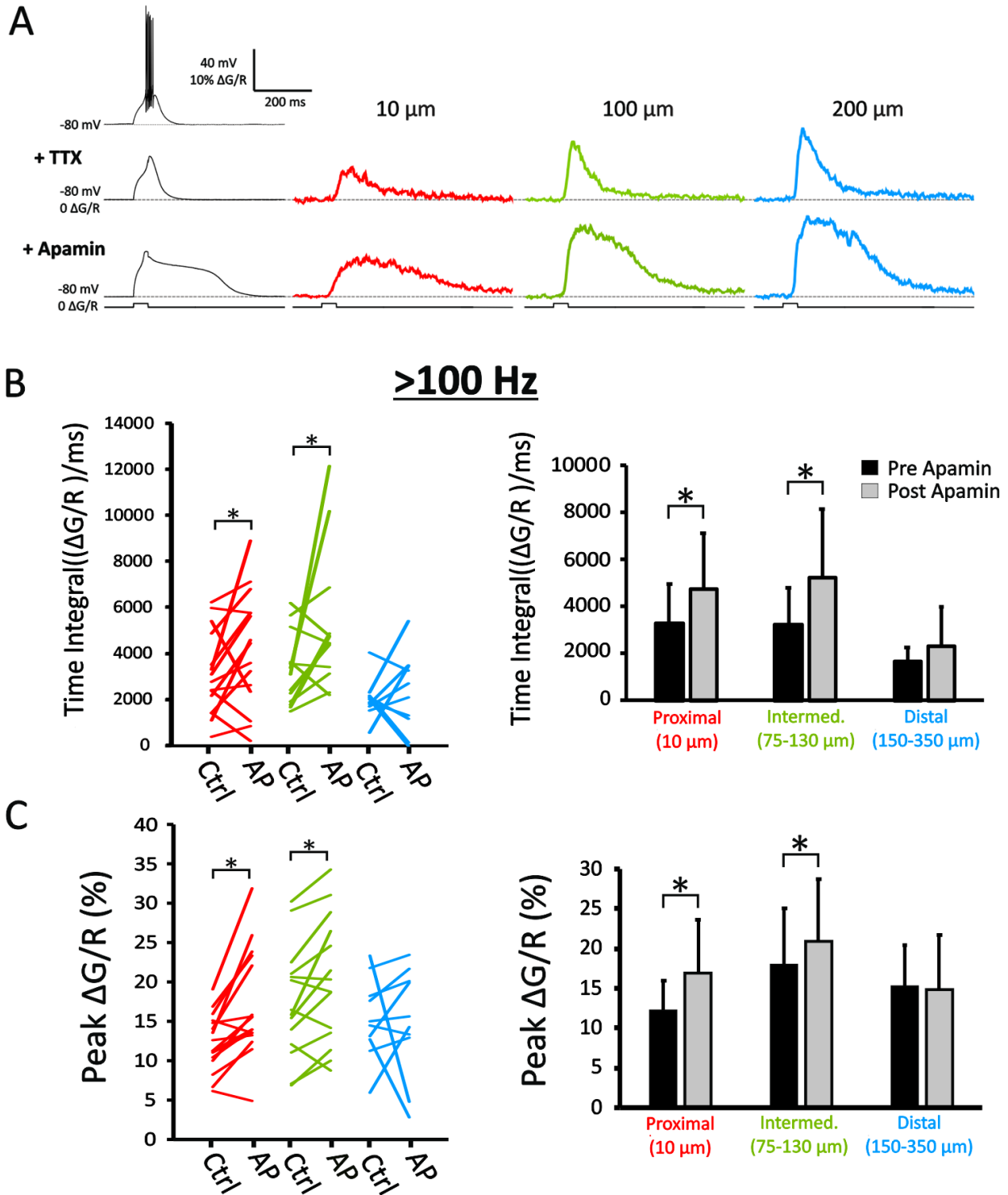
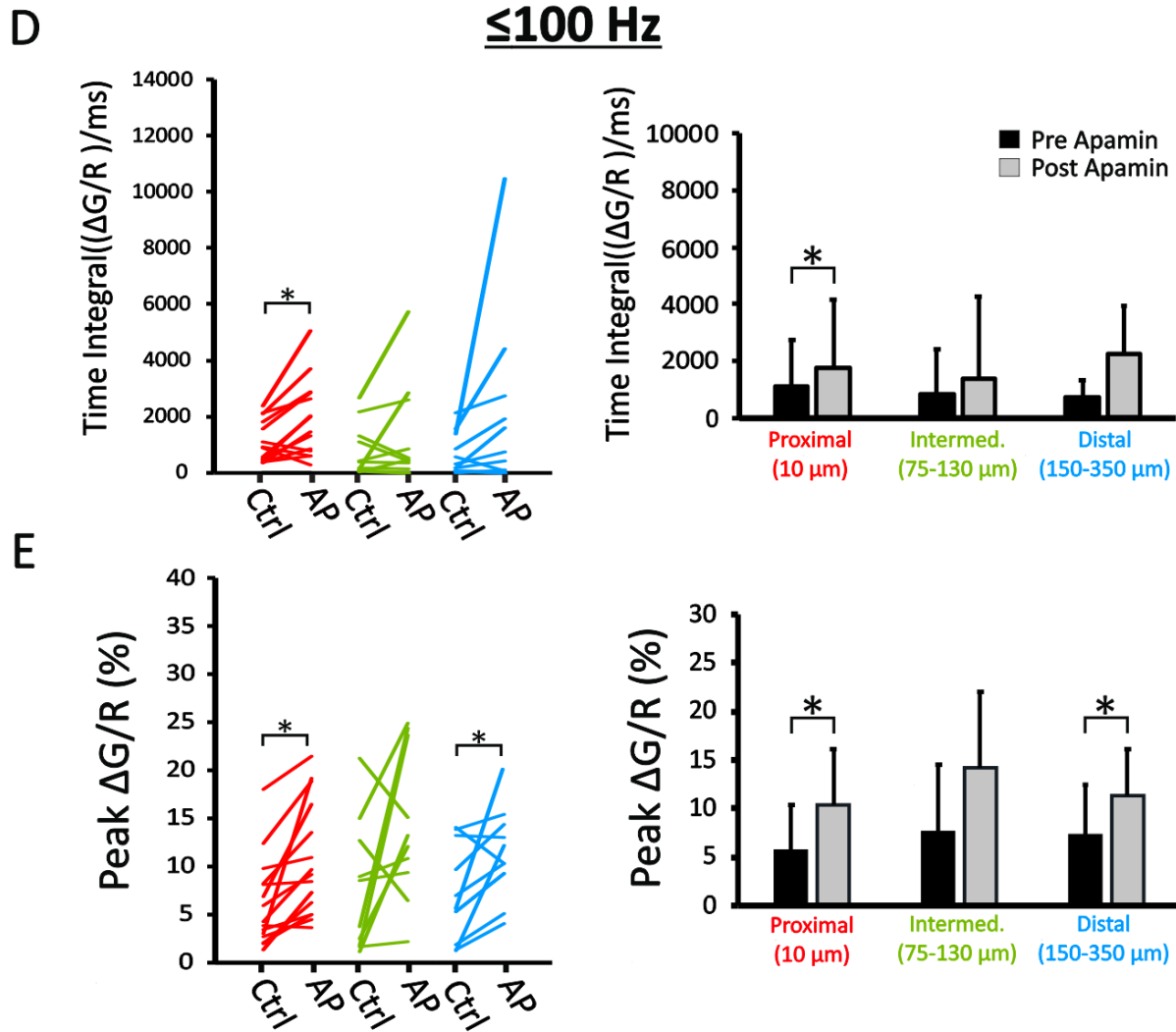


Figure 3.4: Apamin increases the duration of the calcium transient in both higher and lower frequency bursting neurons at different locations.

Figure 3.4 (cont'd)

(A) A 50 ms, 120 pA current step was somatically injected to produce a robust burst (236 Hz). Traces in the presence of TTX are shown in the middle row, and with the addition of apamin in the lower row. (B) Integrals of the calcium signal recorded from higher frequency bursting neurons at proximal (red), intermediate (green) and distal (blue) locations before and after the addition of apamin. Significant increases in duration are noted at proximal and intermediate dendritic locations with the addition of apamin. Ctrl: indicates TTX only. AP: addition of apamin (100 nM) in the presence of TTX. (C) Similar to B, C reports peak calcium signals recorded from higher frequency bursting neurons before and after the addition of apamin. Significant increases in duration are similarly noted at proximal and intermediate dendritic locations with the addition of apamin. (D-E) Reflect the same experimental parameters as B and C, except in lower burst frequency neurons. Signals at proximal locations significantly increased following apamin with either measurement, however only with measurement of the peak fluorescence were distal dendritic calcium signals additionally amplified. * Indicates $P < 0.05$, *paired t-test*.

Figure 3.4 (cont'd)



Discussion

These studies compared burst-evoked calcium activity at different dendritic regions in TRN neurons with burst frequencies ranging from 3-291 Hz. To analyze a possible relationship between dendritic calcium and burst frequency, this large neuronal population was split into two categories: those which fire action potentials at > 100 Hz in burst mode, and those which fire action potentials at ≤ 100 Hz. A current-evoked somatic burst activates dendritic calcium currents

throughout the proximal to distal extent of TRN dendrites, regardless of whether the current injection evokes a robust LTS in the recorded electrophysiology. Analysis of evoked calcium currents using time-based integrals revealed that lower frequency bursting neurons activate significantly less calcium current at proximal and intermediate dendritic regions compared to higher frequency bursting neurons. This disparity in the calcium was also apparent in the analysis of peak calcium influx, however this difference was significant at intermediate and distal regions, rather than proximal.

This study identified significant differences in calcium activity interpretation between the two general approaches to calcium signal analysis: a time-based integral of the calcium response, or a measurement of the peak calcium fluorescence. The time-integral of calcium influx in higher frequency bursting neurons suggests that the calcium activity, and likely channel density, is significantly increased proximal to the soma and diminishes throughout the dendritic arbor. Peak calcium influx curiously revealed the opposite trend; that calcium appeared highest at intermediate and distal sites, with the smallest peak at 10 μm from the soma. TRN neurons have long (up to 350 μm in this study) dendrites which become very thin (0.5-1 μm diameter) at distal locations. The concentration of Fluo5-ff at distal dendrites is expected to be less than at proximal dendrites, possibly underestimating calcium activity at distal dendrites.

When comparing calcium responses using time-integral analysis, higher frequency bursting neurons elicited the largest calcium response at proximal locations. In these neurons, the responses at proximal and intermediate regions were not significantly different, however activity at distal regions was decreased from proximal. In the lower frequency bursting neurons,

there was no significant difference in the calcium response throughout the length of the dendrite, however the largest responses were typically proximal.

Comparative analysis of peak calcium responses revealed that both neuron subsets had a statistically uniform distribution of calcium signals along their dendrites. Findings from Chapter 2 indicated that the smaller LTS potentials generated in burst mode by low frequency bursting neurons are also T-channel mediated as these signals were sensitive to low-concentrations of NiCl_2 application. These results further confirm that the LTS mediated by lower frequency bursting neurons are largely due to calcium activation along the length of the somatodendritic axis. One interpretation of the comparison of peak and integral measurements is that more distal sites may have larger peak calcium measurements with a faster reuptake leading to a smaller time integral. If considering this not to be a consequence of dye buffering, it could reveal that distal locations have faster reuptake, possibly via sarcoplasmic reticulum ATPases (SERCAs) and SK channels (Coulon et al., 2009; Errington et al., 2010). Further study into the relative density of SERCAs and SK channels along the dendrites may provide more insight into possible dendritic location-dependent modulation of signal integration.

A previous study of dendritic calcium activity in the TRN found that peak calcium signals were significantly larger in distal versus proximal dendrites (Connelly et al., 2015; Crandall et al., 2010). While our comparative analysis of peak calcium activity revealed a trend towards distal amplification, our data did not show significant differences between either of our three dendritic. There are several main differences between these two studies. First, these studies utilized a mouse model, while Crandall et. al. (2010) studies were conducted in rats. Second, Crandall et. al. conducted their recordings at room temperature (23°C), whereas these studies were

conducted at 32°C. Third, calcium indicator differences could also contribute to these findings, as Crandall et. al. utilized Fluo-4, whereas these studies use Fluo5-ff. Finally, our findings come from animals aged > PND 30 (average 42 ± 13) whereas Crandall et. al. studied animals PND 11-23. It is possible that younger animals have a denser distal distribution of T-channels that are then paired down developmentally. Further comparison of calcium signals in young mice would assist in determining whether this is a developmental difference.

Lower frequency bursting neurons appear to have less evoked T-channel activation in their dendritic arbors. An additional possibility is that instead of having fewer calcium channels, an antagonistic co-activating ion channel, SK, may more strongly counter the effect of I_T in some neurons, resulting in a shorter and potentially weaker activation. Our previous study revealed that blocking I_{SK} leads to an increase in burst duration, increasing the frequency, and increasing the number of action potentials per burst in all TRN neurons. This study similarly found that apamin increases the amplitude and duration of dendritic burst-evoked calcium influx in all neurons, however the sites of significant enhancement of the calcium signal varied between higher and lower frequency bursting neurons. In contrast to the higher frequency bursting neurons, which had the strongest apamin-induced increase in calcium at proximal and intermediate locations with either peak or time-integral measurements, lower frequency bursting neurons had the most significant increase at proximal locations via either measurement. With analysis of peak calcium, but not time-integral responses, a significant distal increase in calcium activity was also observed in lower frequency bursting neurons. One caveat to this experiment is the possibility that given the long length of TRN dendrites, a somatic burst may not fully activate I_{SK} at distal locations. While this is a variable, these studies observed consistent

calcium signals and a clear enhancement in the signal at distal locations, and this measure of proportional enhancement provides insight into the effect of I_{SK} at distal locations.

It is clear that I_{SK} plays a role in modulating the burst discharge in all TRN neurons, and it may have a greater role at proximal rather than distal locations, however it must be noted that blocking I_{SK} did not increase the calcium response in all neurons however, or at all locations within the same neuron. To better determine the effect of I_{SK} at distal dendrites it would be useful to repeat these measurements with synaptically activated bursts. Given that loss of I_{SK} activity interrupts TRN burst rhythms (Cueni et al., 2008b), further investigation is warranted to understand regarding the role of I_{SK} among the diverse neuron types within the TRN.

Throughout this study, it is possible that in addition to activating dendritic T-channels, as has been proposed to account for the vast majority of calcium currents on TRN neuron dendrites (Cueni et al., 2008a), other channels (L-type, N-type, R-type, see Chapter 1) could also contribute to the measured calcium responses. When apamin was applied to block I_{SK} , the calcium response lengthened to longer than would be expected for an isolated T-channel mediated response, sometimes surpassing 500 ms. Further pharmacological studies blocking these higher-voltage activated channels will be necessary to confirm that T-channels still produce the majority of the response under apamin conditions.

In developing the protocol used to elicit dendritic calcium within these studies, bursts were evoked using two different methods: depolarization from a hyperpolarized membrane potential, and rebound activation following a long hyperpolarizing current step back to a depolarized membrane potential. The rebound burst was elicited by holding the soma at -100 mV and then rapidly switching the membrane voltage to a more depolarized membrane potential

(-60 mV) to elicit a large rebound LTS. Releasing the cells from a similar hyperpolarized potential (e.g., -100 mV) is one way to standardize the strength of the burst activation given differences in input resistances and intrinsic burst responses. With the rebound burst protocol, but not short current step activation protocol, a large, long duration (> 8 s) calcium activation was observed that largely eclipsed the I_T (Supplemental Figure 3.5). Although the exact nature of this tail current was not further investigated in these studies, based on these activation characteristics it is likely a high voltage activated Ca^{2+} current. This tail-current was only apparent in the calcium analysis and not within the electrophysiology. The duration of the current was notably largest closer to the soma and decreased with distal progression. It is consideration that when TRN neurons are in an awake, tonic state, GABAergic input to TRN, such as from the basal forebrain (Asanuma and Porter, 1990; Bickford et al., 1994), globus pallidus (Asanuma, 1994; Gandia et al., 1993; Hazrati and Parent, 1991), substantia nigra pars reticulata (Paré et al., 1990), or internuclear connections (Sohal and Huguenard, 2003), could lead to rebound bursts that would lead to a different, stronger and longer lasting thalamocortical inhibition than a direct burst activation.

It was previously found that TRN neurons discharge voltage-dependent bursts of action potentials at a broad spectrum of frequencies, however the physiologic function of these heterogeneous bursts and their impact on downstream thalamocortical inhibition had yet to be clarified. In order to engage downstream $GABA_B$ receptors, eliciting a longer lasting inhibitory drive, neurons must fire fast trains (> 100 Hz) of many action potentials (Kim et al., 1997), and thus lower frequency bursting neurons may be physiologically designed to only engage thalamocortical $GABA_A$ receptors. In this present study, maximal somatic burst activation in lower

frequency bursting neurons elicited less dendritic calcium throughout the dendritic arbors compared to higher frequency bursting neurons. While TRN neurons bursting at either end of the frequency spectrum may have profoundly different impacts on thalamocortical inhibition of their downstream targets, these neurons do not appear to exist as separate groups, but as two ends of a complexly modulated spectrum of burst frequencies. In the TRN, bursting neurons are often studied as a homogenous cell type, however these studies have shown that bursts elicited from TRN neurons are highly variable and may act as uniquely designed processors for their specific synaptic inputs and thalamocortical target cells.

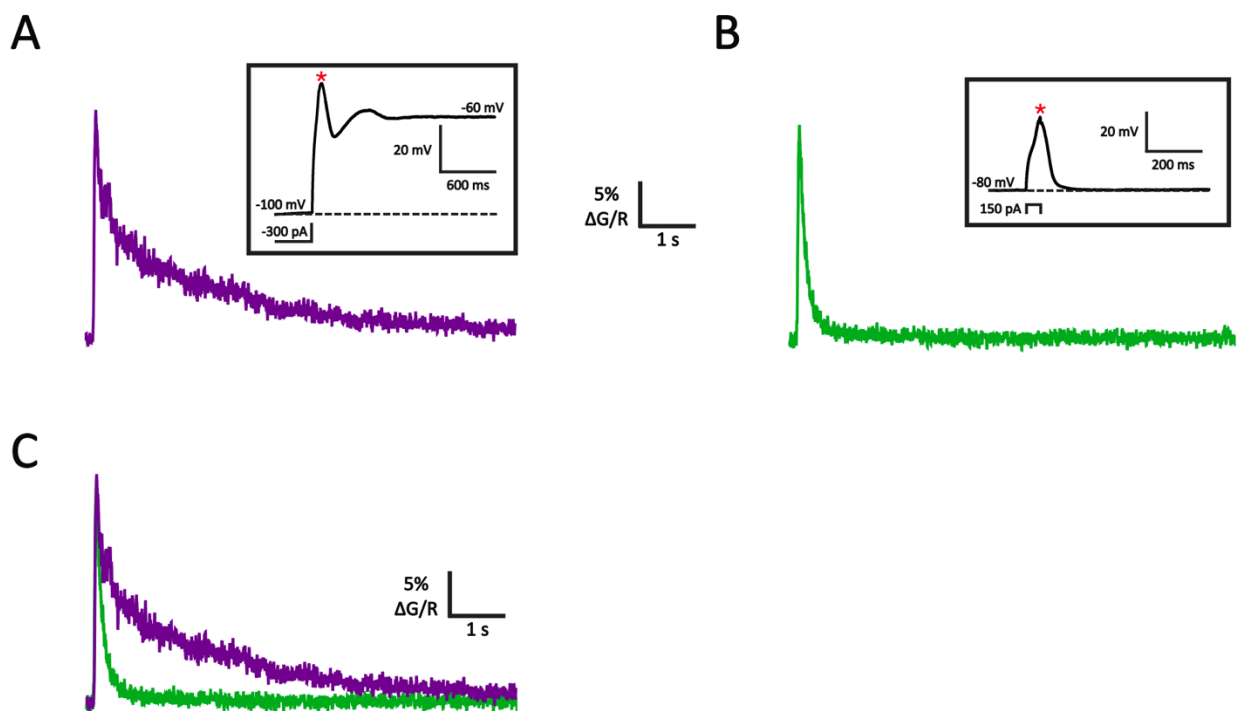


Figure 3.5: (Supplemental) Rebound bursts activate an additional longer lasting calcium transient. (A) Example trace of a dendritic calcium transient elicited from a hyperpolarizing

Figure 3.5 (cont'd)

rebound burst protocol in TTX ($1 \mu\text{M}$) recorded $100 \mu\text{m}$ from the soma. The inset box shows the voltage response and current protocol with a red asterisk indicating the peak low-threshold spike. Note the long ($> 8 \text{ sec}$) transient invading the T-current-mediated calcium response. (B) Example trace of a calcium transient elicited from a 50 ms depolarizing current pulse in TTX ($1 \mu\text{M}$). Inset box shows the voltage response and current protocol with a red asterisk indicating the peak low-threshold spike. Note the sharper decay and return to baseline levels within one sec. (C) Trace overlay of the hyperpolarizing protocol-evoked and short depolarizing protocol-evoked calcium transients.

REFERENCES

REFERENCES

- Asanuma, C., 1994. GABAergic and pallidal terminals in the thalamic reticular nucleus of squirrel monkeys. *Exp. Brain Res.* 101. <https://doi.org/10.1007/BF00227337>
- Asanuma, C., Porter, L.L., 1990. Light and electron microscopic evidence for a GABAergic projection from the caudal basal forebrain to the thalamic reticular nucleus in rats. *J. Comp. Neurol.* 302, 159–172. <https://doi.org/10.1002/cne.903020112>
- Bickford, M.E., Günlük, A.E., Horn, S.C. van, Sherman, S.M., 1994. GABAergic projection from the basal forebrain to the visual sector of the thalamic reticular nucleus in the cat. *J. Comp. Neurol.* 348, 481–510. <https://doi.org/10.1002/cne.903480402>
- Chausson, P., Leresche, N., Lambert, R.C., 2013. Dynamics of Intrinsic Dendritic Calcium Signaling during Tonic Firing of Thalamic Reticular Neurons. *PLOS ONE* 8, e72275. <https://doi.org/10.1371/journal.pone.0072275>
- Contreras, D., Curro Dossi, R., Steriade, M., 1992. Bursting and tonic discharges in two classes of reticular thalamic neurons. *J. Neurophysiol.* 68, 973–977. <https://doi.org/10.1152/jn.1992.68.3.973>
- Coulon, P., Herr, D., Kanyshkova, T., Meuth, P., Budde, T., Pape, H.-C., 2009. Burst discharges in neurons of the thalamic reticular nucleus are shaped by calcium-induced calcium release. *Cell Calcium* 46, 333–346. <https://doi.org/10.1016/j.ceca.2009.09.005>
- Connelly, W.M., Crunelli, V., Errington, A.C., 2015. The Global Spike: Conserved Dendritic Properties Enable Unique Ca²⁺ Spike Generation in Low-Threshold Spiking Neurons. *J. Neurosci.* 35, 15505–15522. <https://doi.org/10.1523/JNEUROSCI.2740-15.2015>
- Cox, C.L., Huguenard, J.R., Prince, D.A., 1997. Nucleus reticularis neurons mediate diverse inhibitory effects in thalamus. *PNAS* 94, 8854–8859. <https://doi.org/10.1073/pnas.94.16.8854>
- Crandall, S.R., Govindaiah, G., Cox, C.L., 2010. Low-threshold Ca²⁺ current (IT) amplifies distal dendritic signaling in thalamic reticular neurons. *J. Neurosci. Off. J. Soc. Neurosci.* 30, 15419–15429. <https://doi.org/10.1523/JNEUROSCI.3636-10.2010>
- Cueni, L., Canepari, M., Adelman, J.P., Lüthi, A., 2008a. Ca²⁺ signaling by T-type Ca²⁺ channels in neurons. *Pflüg. Arch. - Eur. J. Physiol.* 457, 1161. <https://doi.org/10.1007/s00424-008-0582-6>
- Cueni, L., Canepari, M., Luján, R., Emmenegger, Y., Watanabe, M., Bond, C.T., Franken, P., Adelman, J.P., Lüthi, A., 2008b. T-type Ca²⁺ channels, SK2 channels and SERCAs gate

- sleep-related oscillations in thalamic dendrites. *Nat. Neurosci.* 11, 683–692.
<https://doi.org/10.1038/nn.2124>
- Destexhe, A., Contreras, D., Steriade, M., Sejnowski, T.J., Huguenard, J.R., 1996. In vivo, in vitro, and computational analysis of dendritic calcium currents in thalamic reticular neurons. *J. Neurosci.* 16, 169–185.
- Errington, A.C., Renger, J.J., Uebele, V.N., Crunelli, V., 2010. State-Dependent Firing Determines Intrinsic Dendritic Ca²⁺ Signaling in Thalamocortical Neurons. *J. Neurosci.* 30, 14843–14853. <https://doi.org/10.1523/JNEUROSCI.2968-10.2010>
- Gandia, J., De Las Heras, S., García, M., Giménez-Amaya, J.M., 1993. Afferent projections to the reticular thalamic nucleus from the globus pallidus and the substantia nigra in the rat. *Brain Res. Bull.* 32, 351–358. [https://doi.org/10.1016/0361-9230\(93\)90199-L](https://doi.org/10.1016/0361-9230(93)90199-L)
- Guillery, R.W., Harting, J.K., 2003. Structure and connections of the thalamic reticular nucleus: Advancing views over half a century. *Journal of Comparative Neurology* 463, 360–371. <https://doi.org/10.1002/cne.10738>
- Hallworth, N.E., Wilson, C.J., Bevan, M.D., 2003. Apamin-Sensitive Small Conductance Calcium-Activated Potassium Channels, through their Selective Coupling to Voltage-Gated Calcium Channels, Are Critical Determinants of the Precision, Pace, and Pattern of Action Potential Generation in Rat Subthalamic Nucleus Neurons In Vitro. *J. Neurosci.* 23, 7525–7542. <https://doi.org/10.1523/JNEUROSCI.23-20-07525.2003>
- Hartings, J.A., Temereanca, S., Simons, D.J., 2003. State-Dependent Processing of Sensory Stimuli by Thalamic Reticular Neurons. *J. Neurosci.* 23, 5264–5271. <https://doi.org/10.1523/JNEUROSCI.23-12-05264.2003>
- Hazrati, L.-N., Parent, A., 1991. Projection from the external pallidum to the reticular thalamic nucleus in the squirrel monkey. *Brain Res.* 550, 142–146. [https://doi.org/10.1016/0006-8993\(91\)90418-U](https://doi.org/10.1016/0006-8993(91)90418-U)
- Helmchen, F., Imoto, K., Sakmann, B., 1996. Ca²⁺ buffering and action potential-evoked Ca²⁺ signaling in dendrites of pyramidal neurons. *Biophys. J.* 70, 1069–1081. [https://doi.org/10.1016/S0006-3495\(96\)79653-4](https://doi.org/10.1016/S0006-3495(96)79653-4)
- Kim, U., McCormick, D.A., 1998. The Functional Influence of Burst and Tonic Firing Mode on Synaptic Interactions in the Thalamus. *J. Neurosci.* 18, 9500–9516. <https://doi.org/10.1523/JNEUROSCI.18-22-09500.1998>
- Kim, U., Sanchez-Vives, M.V., McCormick, D.A., 1997. Functional Dynamics of GABAergic Inhibition in the Thalamus. *Science* 278, 130–134. <https://doi.org/10.1126/science.278.5335.130>

- Lee, S.-H., Govindaiah, G., Cox, C.L., 2007. Heterogeneity of firing properties among rat thalamic reticular nucleus neurons. *J. Physiol.* 582, 195–208.
<https://doi.org/10.1113/jphysiol.2007.134254>
- Liegeois, J., Mercier, F., Graulich, A., Graulich-Lorge, F., Scuvee-Moreau, J., Seutin, V., 2003. Modulation of Small Conductance Calcium-Activated Potassium (SK) Channels: A New Challenge in Medicinal Chemistry. *Curr. Med. Chem. Schiph.* 10, 625–47.
<http://dx.doi.org/10.2174/0929867033457908>
- Pare', D., Hazrati, L.-N., Parent, A., Steriade, M., 1990. Substantia nigra pars reticulata projects to the reticular thalamic nucleus of the cat: a morphological and electrophysiological study. *Brain Res.* 535, 139–146. [https://doi.org/10.1016/0006-8993\(90\)91832-2](https://doi.org/10.1016/0006-8993(90)91832-2)
- Sohal, V.S., Huguenard, J.R., 2003. Inhibitory Interconnections Control Burst Pattern and Emergent Network Synchrony in Reticular Thalamus. *J. Neurosci.* 23, 8978–8988.
<https://doi.org/10.1523/JNEUROSCI.23-26-08978.2003>

CHAPTER 4: ALTERED PROPERTIES OF TRN NEURONS IN FRAGILE X SYNDROME

Abstract

Fragile X syndrome (FXS) is the leading monogenetic cause of autism spectrum disorder (ASD), yet to date, research identifying neural pathological mechanisms have focused on cortical structures, leaving subcortical alterations poorly understood. Individuals with FXS experience an array of symptoms including intellectual disability, altered sensory perception, sleep disturbances, and epilepsy. To date, pharmacologic therapies for FXS have been largely ineffective, indicating a critical need for investigation of additional mechanisms and treatments. We proposed that abnormal functioning in the thalamic reticular nucleus (TRN), a critical subcortical region for sensory processing, contributes to the altered sensory processing in FXS.

The TRN is a layer of inhibitory neurons that receives synaptic input from major sensory processing circuits between the thalamus and neocortex. TRN neurons project only to the dorsal thalamus where they influence the outflow of sensory information in response to corticothalamic and thalamocortical afferents. The objectives of this study were to 1) determine whether there are sensory circuitry dysfunctions of the TRN in the *Fmr1*-KO mouse and, 2) to better define how TRN plasticity may influence regulation of sensory information processing. We hypothesized that in FXS, dysfunctional signal integration at synapses onto TRN neurons disrupts the modulatory role of TRN in sensory processing.

In this study, we assessed differences in intrinsic electrophysiological properties in wild-type (WT) and *Fmr1*-KO mice. Additionally, electrical and optogenetic stimulation techniques, as well as application of group 1 mGluR-agonist DHPG, were utilized to study evoked synaptic plasticity changes at afferent TRN synapses. No intrinsic differences were found between WT and

Fmr1-KO mice. Additionally, while the TRN may exhibit long or short-term potentiation in response to burst-paired stimulus and DHPG-induced plasticity protocols, there is no apparent difference in plasticity between the WT and *Fmr1*-KO mice. While this study did not find any *Fmr1*-deficiency related alterations in plasticity of TRN neurons, it is possible that with the discovery of a more robust plasticity-evoking protocol, changes could become apparent.

Introduction

Fragile X Syndrome (FXS) is a leading cause of both Autism Spectrum Disorder (ASD) and intellectual disability (Abbeduto et al., 2014; Budimirovic and Kaufmann, 2011). FXS usually results from an increase in the number of CGG nucleotide repeats in the 5' untranslated region of the *Fmr1* gene. This increased CGG copy number leads to hypermethylation and silencing of the gene and a decrease of the protein product, fragile X mental retardation protein (FMRP). FMRP functions to repress translation at postsynaptic dendrites, and decreased expression leads to dysregulated synaptic mRNA translation neural transmission (Bear et al., 2004). In addition to ASD and intellectual disability, FXS individuals have very high co-morbidities with sensory processing disorders (CDC, 2016; Miller et al., 1999; Sinclair et al., 2017; Watling et al., 2001). Other features common to FXS are increased rate of epilepsy (20%), and abnormal EEG patterns independent of seizure activity (Berry-Kravis, 2002; Hunter et al., 2014; Riley et al., 2017; Sinclair et al., 2017), and sleep difficulties (e.g., initiating and maintaining sleep) (Kidd et al., 2014; Riley et al., 2017).

The TRN is a thin layer of inhibitory neurons located between the dorsal thalamic nuclei and neocortex that functions to modulate sensory information and facilitate appropriate behavioral responses. TRN neurons are innervated by axon collaterals of corticothalamic and thalamocortical neurons and send outputs only to the thalamic nuclei (Guillery and Harting, 2003; Jones, 1975; Pinault, 2004; Zikopoulos and Barbas, 2007). In addition to modulating sensory information flow, the TRN facilitates sleep rhythmogenesis and selective attention (Fernandez et al., 2018; Gent et al., 2018; McAlonan et al., 2006). TRN dysfunction is also strongly associated with absence seizures (Bovenkamp-Janssen et al., 2004; Chen et al., 2014; Steriade, 2005). Patients with FXS have a high incidence of comorbidities associated with these functions (sensory processing disorder, altered sleep patterns, and epilepsy (Hagerman and Hagerman, 2002)), bringing forth speculation as to a possible role of TRN pathology in the FXS phenotype.

Evidence that TRN may have a causal role in neurodevelopmental disorders is additionally contributed by studies in the *PTCHD1* deletion autism mouse model. In this study, a calcium-dependent potassium ion channel (*SK*) deficit in the TRN of the *PTCHD1* deletion autism mouse model was linked to behavioral deficits, exemplifying the potential of TRN pathology to affect behavioral outcomes (Wells et al., 2016). Furthermore, FMRP is found distributed in relatively high amounts throughout the thalamus, including in the TRN, further increasing suspicion of TRN pathology in FXS (Zorio et al., 2017).

FXS results from the significant decrease of Fragile X Mental Retardation Protein (FMRP), a translational regulator of mRNA in neurons. The *Fmr1*-KO mouse model of FXS displays a variety of pathological phenotypes and is frequently used as a genetic model of ASD. Several abnormalities among ion channels have also been reported, resulting from changes in channel

number, location, or function. Some of these dysfunctional channels include: $K_v3.1$, $K_v4.2$, Slack, and N- and L-type calcium channels among others (Brager and Johnston, 2014; Brown et al., 2010; Contractor et al., 2015; Ferron, 2016; Gross et al., 2011; Meredith et al., 2007; Zhang et al., 2012). Due to some of these deficiencies, neurons within the *Fmr1*-KO mouse may exhibit increased excitability (Contractor et al., 2015; Gibson et al., 2008) and reduced inhibition (Centonze et al., 2008; D'Hulst et al., 2006; Olmos-Serrano et al., 2010; Paluszkiewicz et al., 2011). The TRN lies at an interface of several highly influential sensory circuits where it is largely responsible for appropriate circuit modulation. The consequence of any one of these *Fmr1*-KO-related deficiencies could lead to disordered thalamic sensory processing.

Neuroplasticity describes the brain's ability to adapt and potentially re-wire in response to synaptic input. FMRP associates with mRNAs that function in synapse development, dendritic spine development, and synaptic vesicle transport (Brown et al., 2001; Darnell et al., 2011, 2001). Several studies have identified alterations in synaptic plasticity in *Fmr1*-KO mice; however, a major unresolved issue is why these changes occur, and why the alterations greatly differ by region. For example, in the hippocampus, there is an enhancement of long-term depression (LTD), while long-term potentiation (LTP) is unaltered (Huber et al., 2002). In contrast, in the neocortex and amygdala, LTP is greatly attenuated (Larson et al., 2005; Li et al., 2002; Suvrathan et al., 2010; Wilson and Cox, 2007). There is a clear regional difference in outcomes in the absence of FMRP, yet little is known of the impact of FMRP loss in regions of the thalamus, such as the TRN, which exerts carefully balanced regulatory control over the information flow between cortical and thalamic brain regions. The metabotropic glutamate receptor (mGluR) theory of FXS, which originated from initial findings in the hippocampus, predicts that FMRP functions as a

postsynaptic translational modulator of a subset of mRNAs at excitatory group I mGluR (mGluR1/5) synapses (Bear et al., 2004). When FMRP is suppressed, the synapse lacks translational repression, which leads to enhanced receptor activity. Selective mGluR5 antagonists have been proposed as a possible treatment for FXS (Dölen et al., 2007), however clinical trials have not completely recovered phenotypes, indicating a need for more thorough mechanistic studies of FXS pathology (Youssef et al., 2018).

FMRP associates with over 800 mRNAs, many of which are directly involved in synaptic transmission (Brown et al., 2001; Darnell et al., 2011, 2001). The functions of these transcripts include long-term potentiation/depression, GABA_A regulation, and calcium signaling, indicating that FMRP activity extends beyond group 1 mGluR receptors. Decreased dendritic calcium transient currents have been reported in the *Fmr1*-KO cortex, as have abnormalities in several potassium channels and increased input resistance (Brager and Johnston, 2014; Brown et al., 2010; Gibson et al., 2008; Meredith et al., 2007; Zhang et al., 2012). The mGluR theory accounts for one component of FXS; however, numerous studies suggest several other roles for FMRP in the brain that have yet to be understood. Investigating these other roles is critical to understanding the disorder and may divulge new avenues for treatment development.

Activity-dependent synaptic plasticity onto TRN neurons has only recently been identified in wild-type (WT) animals (Fernandez et al., 2017; Sevetson et al., 2017; Sun et al., 2016). While the mechanisms are not fully characterized, studies show involvement of mGluRs, N-Methyl-D-aspartate receptors (NMDARs), and calcium-dependence. However, loss of FMRP impairs several potentially involved ion channels, such as mGluRs, and L-type and N-type calcium channels

(Brager and Johnston, 2014; Comery et al., 1997; Darnell et al., 2011; Irwin et al., 2001; Meredith et al., 2007).

Previous findings suggest that corticothalamic plasticity in TRN is dependent upon mGluR or NMDA activation (Fernandez et al., 2017), and to date there is little evidence of mGluR receptors or plasticity in general at thalamocortical synapses (Govindaiah et al., 2012). FMRP-regulated mGluRs may have abnormal function in FXS, and if only corticothalamic synapses contain these receptors, FMRP loss may affect corticothalamic afferents to a greater degree than thalamocortical. This study investigates whether synaptic plasticity of excitatory afferents onto TRN neurons is altered in the *Fmr1*-KO mouse. Such pathology could significantly alter the inhibitory drive from TRN onto thalamocortical neurons, and ultimately dysregulate normal sensory information processing. Further investigation into the role of plasticity in the TRN, and the effects of TRN pathology on these processes may better reveal etiologies behind the neural deficits in FXS and potentially other ASD-related disorders.

The following studies utilize an *Fmr1*-KO mouse model to investigate the role of *Fmr1* in the TRN. It is clear that in the brain, *Fmr1* plays a diverse yet significant role in ion channel expression and trafficking, synaptic plasticity, and calcium signaling. Loss of *Fmr1* expression manifests in Fragile X Syndrome, and is associated with conditions such as epilepsy, abnormal sensory processing, intellectual disability. The TRN plays a critical role in regulating sensory processing circuits, and pathology is tied to epilepsy. TRN also utilizes many implicated ion channels and group 1 mGluRs, suggesting possible undiscovered pathology in the *Fmr1*-KO mouse.

Materials and Methods

Slice Preparation

Wild-type (WT) female and male C57BL/6J or Ntsr1-Cre/Ai32 (Ai32(RCL-ChR2(H134R))/EYFP; Jackson Laboratories # 024109) x Tg(Ntsr1-cre)GN220Gsat/Mmucd; MMUCD # 017266-UCD) mice were compared with *Fmr1*-KO mice (C57BL/6J/*Fmr1*^{-/-}), at a range of ages older than postnatal day (PND) 14 (average PND 40 ± 14, range 14-111). Animals were deeply anesthetized (3% isoflurane) and perfused with cold, oxygenated (95% O₂, 5% CO₂) slicing solution containing (in mM): 2.5 KCl, 1.25 NaH₂PO₄, 10.0 MgSO₄, 0.5 CaCl₂, 26.0 NaHCO₃, 10.0 glucose, and 234.0 sucrose. Horizontal brain slices (300 μm thickness) were sectioned and transferred to a warmed holding chamber (35°C) containing oxygenated (95%O₂, 5%CO₂) artificial cerebrospinal fluid (ACSF) solution containing (in mM): 126.0 NaCl, 2.5 KCl, 1.25 NaH₂PO₄, 2.0 MgCl₂, 2.0 CaCl₂, 26.0 NaHCO₃, and 10.0 glucose. After 30 minutes, chamber temperature was gradually returned to room temp and slices incubated for a minimum of 60 minutes prior to recording.

Electrophysiology

Borosilicate glass micropipettes (4-6 MΩ resistance) were used to perform whole-cell TRN neuron recordings. Micropipettes were filled with a solution of (in mM): 117 K-gluconate, 13 KCl, 1.0 MgCl₂, 0.07 CaCl₂, 0.1 EGTA, 10 HEPES, 2.0 ATP, and 0.4 GTP. Only cells with an input resistance greater than 100 MΩ, a resting membrane potential more negative than -50 mV, a stable resting membrane potential (fluctuation < 10 mV), a lack of spontaneous action potential firing, and evoked action potential peak > +20 mV. Data were obtained using a MultiClamp 700b amplifier and sampled at a rate of 20 kHz. Data were filtered at 10 kHz using a Digidata 1440a

digitizer. PClamp software was used for data acquisition and analysis. Voltages are corrected for an 8 mV liquid junction potential. For procedures involving electrical stimulation, a bipolar stimulation electrode was placed in the internal capsule, and current was passed 50-400 μ A (100 μ s duration) until a peak stimulus without a Na^+ action potential was observed. Mid-amplitude excitatory postsynaptic potential/current (EPSP/C) were observed. Experiments utilized the stimulus that produced a peak EPSP/C that was half of the maximum magnitude.

Optogenetic Targeting

Two methods were utilized to selectively activate corticothalamic afferents in TRN. In four plasticity recordings (two burst-paired induction, two DHPG induction), an adeno-associated virus expressing channelrhodopsin 2 membrane channel (rAAV2/camKII-hChR2 (H134R)EYFP-WPREPA; University of North Carolina Vector Core) was injected into layer VI of the visual cortex in vivo. Stereotactic techniques were used to inject virus (0.5 μ l, 3.5×10^{12} viral particles/mL) into anesthetized mice (3% isoflurane, 97% O_2) at postnatal day 14-16. A small craniotomy was made over the target site (coordinates from the bregma were: 3.5 mm posterior, 2.3 mm lateral, and 0.8 mm ventral), and a thin borosilicate glass pipette attached to a Picospritzer micro pressure injector system was lowered to the ventral location the tissue. Virus was slowly injected (20-30 minutes), and the pipette was left in place for an additional 15-20 minutes post injection to ensure tissue absorption of the virus. Animals recovered in their home cage for at least 14 days to ensure sufficient expression of channelrhodopsin prior to recording. All stimulus protocols directed the center of the optical stimulation over internal capsule rather than the TRN to maximize more physiologic stimulation. In the remainder of the recordings, the Ntsr1-Cre/Ai32

mouse model, which labels neurons within layer VI of the cortex, was used to optically drive corticothalamic synapses in a similar manner.

Plasticity Induction

WT and *Fmr1*-KO mice (injected with a channelrhodopsin-expressing AAV as previously described) or *Ntsr1*-Cre/*Ai32* mice, were used in these experiments where corticothalamic terminals were selectively activated. Voltage or current clamp recordings using whole-cell configuration were obtained from TRN neurons at a -60 mV membrane voltage. Prior to plasticity induction, synaptic responses were optically evoked (1 ms, 0.1 Hz) with a stimulus intensity that evoked a half-maximum postsynaptic current to allow for subsequent facilitation or depression of the response. After obtaining a stable baseline for at least 5 minutes, either an optical stimulation-paired burst protocols (Astori and Lüthi, 2013), or bath application of group I mGluR agonist *a* (S)-3,5- Dihydroxyphenylglycine (DHPG; 50 μ M, 5 min; Sun et al., 2016), were used for induction. Following induction, measurements of synaptic responses at -60 mV membrane voltage were resumed until either the synaptic response returned to baseline, or at least 30 minutes had passed post- induction (if any change in synaptic strength had been observed).

Analysis

Analysis of electrophysiological recordings was completed using Clampfit software (Molecular Devices). All reported comparisons between WT and *Fmr1*-KO mice were conducted via Mann-Whitney U-tests in Mathematica unless otherwise stated. Values are reported as average \pm standard deviation. Resting membrane potential was calculated from the averaged potential 200 ms before the current injections. Input resistance was measured from the average slope of the current-voltage relationship during the last 200 ms of the current injection (Δ 10-20

pA, averaged from 1-4 points above and below 0 pA). Action potential half-width and threshold were both measured from a depolarizing current injection ($\Delta 20$ pA) while holding the cell held at -60 mV (traces not shown). Action potential half-width was measured from the width (in ms) of the action potential at half maximum voltage for the first elicited action potential. Threshold was similarly measured from the point at which the first action potential rise slope surpassed 10 mV/ms. Baseline and post protocol recordings of plasticity were analyzed using excitatory postsynaptic potentials (EPSP) in current clamp or excitatory postsynaptic currents (EPSC) in voltage clamp at a -60 mV hold. EPSP/Cs were measured every 10 s, and upon analysis the peak current or voltage values were averaged over 50 seconds to represent each graphical data point. Significant change in synaptic plasticity was determined by the box car average values surpassing 2 standard deviations of the baseline mean in the positive direction (potentiation) or negative direction (depression). Because the responses were so varied, for the purpose of reporting long-term (> 30 m) or short term (< 30 m) plasticity were not distinguished.

Results

Intrinsic properties of TRN neurons in WT and Fmr1-KO mice

Whole-cell recordings were performed to measure resting membrane potential, input resistance, action potential firing threshold, and action potential half-width (Table 4.0). No intrinsic properties were found to be statistically different between the WT and *Fmr1*-KO mice. Both WT and *Fmr1*-KO mice had very similar membrane potentials (WT: -75.7 ± 11.7 mV, $n = 198$; *Fmr1*-KO: -76.1 ± 7.3 mV, $n = 134$; $p = 0.882$), and action potential thresholds (WT: -41.5 ± 10.7 mV, $n = 71$; *Fmr1*-KO: -41.4 ± 6.3 mV, $n = 52$; $p = 0.467$). While input resistance and action

potential half-width appeared slightly more variable in the *Fmr1*-KO neurons, there was no statistical difference in distributions (WT input resistance: $241.8 \pm 180.5 \text{ M}\Omega$, $n = 170$; *Fmr1*-KO input resistance: $265.6 \pm 268.1 \text{ M}\Omega$, $n = 115$; $p = 0.803$. WT action potential half-width: $-0.256 \pm 0.052 \text{ ms}$, $n = 71$; *Fmr1*-KO action potential half-width: $0.276 \pm 0.085 \text{ ms}$, $n = 52$; $p = 0.363$). While the lack of apparent differences between the TRN neuron intrinsic properties between WT and *Fmr1*-KO mice is reassuring that the cellular properties that underlie firing properties, such as ion channel distribution and function, are not altered by the lack of FMRP, there remains the possibility that synaptic properties could affect cellular function.

	WT		KO		P-Value (Mann-Whitney U-Test)
	Average \pm Standard Deviation	N	Average \pm Standard Deviation	N	
Resting Membrane Potential (mV)	-75.7 ± 11.7	198	-76.1 ± 7.3	134	0.882
Input Resistance (M Ω)	241.8 ± 180.5	170	265.6 ± 268.1	115	0.803
AP Half-Width (ms)	0.256 ± 0.052	71	0.276 ± 0.085	52	0.363
AP Threshold (mV)	-41.5 ± 10.7	71	-41.4 ± 6.3	52	0.467

Table 4.0: Comparison of TRN neuron intrinsic properties within WT and *Fmr1*-KO mice.

Burst evoked synaptic plasticity of electrically stimulated TRN afferent and efferent fibers in WT and Fmr1-KO mice

To induce synaptic plasticity utilizing a burst-paired induction protocol, a burst was paired with an electrical stimulus timed so that the stimulus occurred at the peak of the burst (Figure 4.0 A-B). The electrical stimulus produced during the induction protocol was identical to that introduced every 10 seconds during baseline measurements and consisted of a current intensity

tuned to elicit a half-maximal intensity (see methods). Because both corticothalamic and thalamocortical axons travel within the internal capsule, this protocol was expected to stimulate both corticothalamic and thalamocortical synapses: orthodromic propagation through corticothalamic axons, and antidromic propagation through thalamocortical axons. Of the 12 WT neurons tested, one neuron exhibited potentiation, and two exhibited depression (Figure 4.0 C). In the *Fmr1*-KO, three of 14 neurons experience increased synaptic strength of activation, while two of the 14 experienced depression. (Figure 4.0 C).

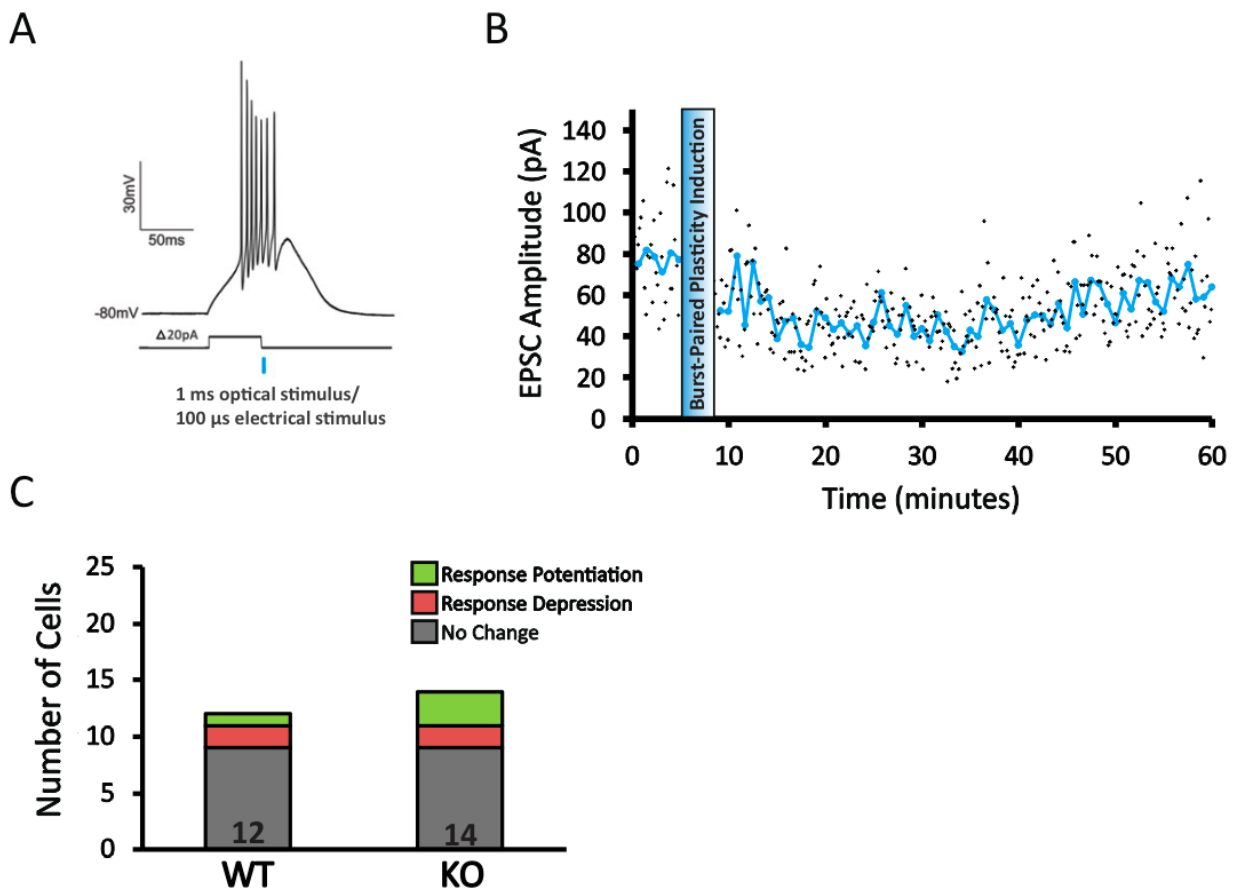


Figure 4.0: Electrical stimulation of afferent and efferent fibers can induce potentiation or depression of synapses onto TRN neurons. (A) Example burst-paired induction protocol. (B) A

Figure 4.0 (cont'd)

WT neuron exhibits depression in response to a burst-paired induction protocol utilizing electrical stimulation. Black data points indicate individual peak EPSC measurements, taken every 10 seconds. The thick blue line indicates a box-car average of 5 consecutive data points. (C) Stacked column histogram showing the incidence of potentiating (green, top) and depressing (red, middle) responses within each genotype following the induction protocol.

DHPG induced synaptic plasticity of TRN synapses in WT and Fmr1-KO mice

A second method of plasticity induction reported in the literature is elicited by mGluR activation via DHPG (Bear et al., 2004; Huber et al., 2002; Sun et al., 2016). mGluR activation is known to increase long-term depression in hippocampal *Fmr1*-KO neurons (Huber et al., 2002), however in WT TRN, it has been shown to activate cholinergic long-term potentiation (Sun et al., 2016). The next experiment investigated how mGluR1 agonist DHPG would affect TRN synapses measured with electrical stimulation. DHPG induced potentiation at a small subset of TRN neurons in both WT and *Fmr1*-KO animals via electrical stimulation (WT: 3 of 21; *Fmr1*-KO: 3 of 16), however there was no depression and no observable difference between WT and *Fmr1*-KO mice (Figure 4.1 A-B).

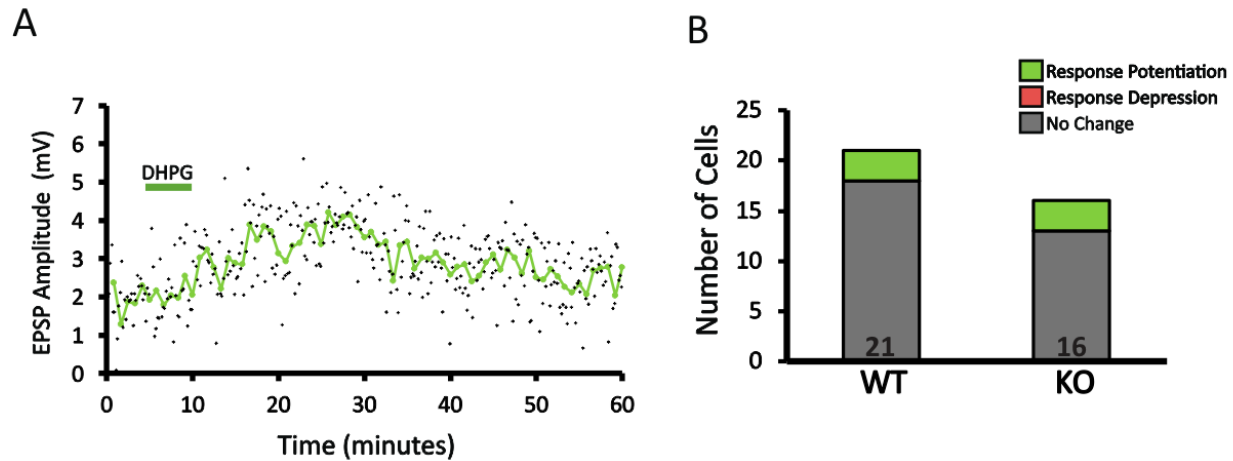


Figure 4.1: Effect of DHPG on synaptic strength within the TRN. (A) A WT neuron exhibits DHPG-induced potentiation of electrically stimulated synapses. Black data points indicate individual peak amplitude measurements, and the thick green line indicates a box-car average of 5 consecutive data points. (B) A stacked histogram shows the proportion of potentiating (green) or depressing (red) electrically stimulated synapses in the TRN in response DHPG induction in WT and *Fmr1*-KO neurons.

Burst-evoked synaptic plasticity of corticothalamic TRN synapses in WT and *Fmr1*-KO mice

Simultaneously activating TRN synaptic contacts while eliciting a calcium-mediated burst discharge induced a mix of synaptic potentiation and depression (Figure 4.0). Given this mixed response, the next objective was to determine whether selective corticothalamic or thalamocortical synapse activation would reveal whether either synapse type was more likely to result in either type of plasticity. The same burst induction procedure was utilized and paired with selective optical stimulation of corticothalamic axons (see methods). In the majority of WT TRN neurons (17 of 18), a change in synaptic strength was not induced by this protocol. However, one

WT neuron did experience a depression of the synaptic response which slowly recovered approximately 45 minutes (Figure 4.2 A). A limited number of *Fmr1*-KO neurons were also tested from three different animals, and no changes in synaptic response were elicited (0 of 4; Figure 4.2 B).

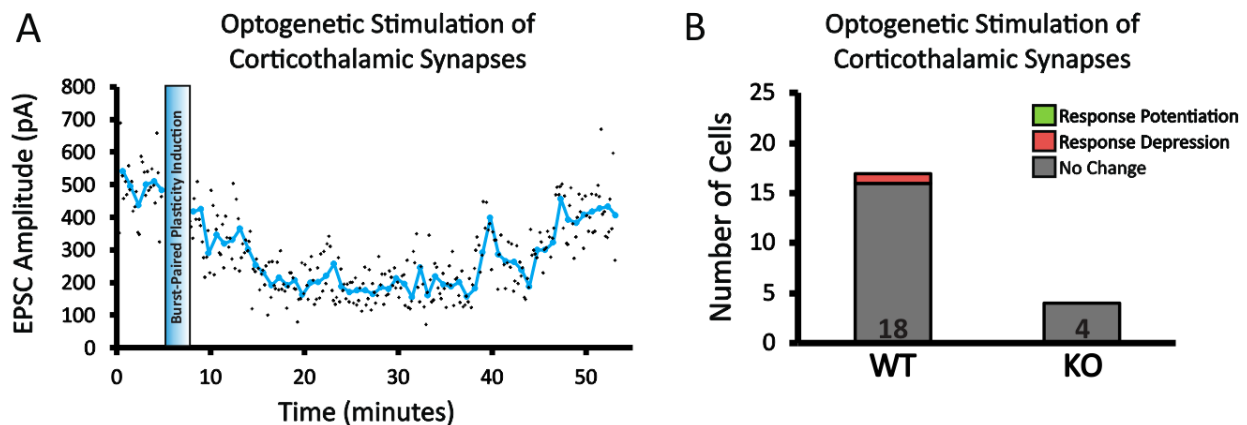


Figure 4.2: Synaptic plasticity induction via burst-paired optical stimulation of corticothalamic synapses. (A) A WT (*Ntsr1*-Cre) neuron exhibits synaptic depression following plasticity induction via burst-paired optical stimulation of corticothalamic synapses. Black data points indicate individual peak amplitude measurements, and the thick blue line indicates a box-car average of 5 consecutive data point (B) Stacked column histogram shows the number of depressing (red, 1 of 18 WT neurons) or potentiating (green, none) cells per genotype. The number at the base of each column represents the total number of recorded cells.

DHPG induced synaptic plasticity of corticothalamic TRN synapses in WT and *Fmr1*-KO mice

Non-selectively stimulating internal capsule fibers and evoking plasticity with a burst-paired induction protocol produces in a mix of synaptic potentiation and depression in both WT

and *Fmr1*-KO mice. Under the same experimental conditions with selective corticothalamic fiber stimulation instead, synaptic depression was elicited in one instance in a WT animal. Plasticity induction via activation of group 1 mGluR receptors via DHPG with selective activation of corticothalamic fibers resulted in exclusively potentiation in both WT and *Fmr1*-KO animals. The next objective was to determine whether selective corticothalamic synapse activation paired with DHPG-induced plasticity would similarly result in exclusively potentiation. DHPD-induced plasticity was measured in 13 neurons from eight WT animals while selectively measuring corticothalamic synapse strength. In contrast to electrical stimulation, no potentiation of the synaptic response was observed, however one incidence of depression occurred (Figure 4.3).

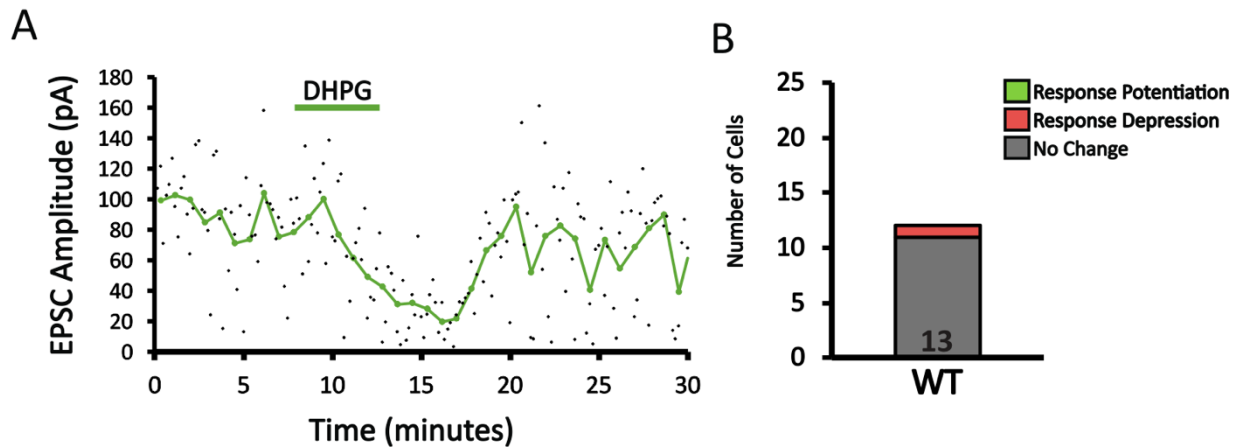


Figure 4.3: Effect of DHPG on corticothalamic synaptic strength in the TRN. (A) A WT(*Ntsr1*-Cre) neuron exhibits relatively short-lasting DHPG-induced depression of electrically stimulated synapses. Black data points indicate individual peak amplitude measurements, and the thick green line indicates a box-car average of 5 consecutive data points. (B) A stacked histogram shows the proportion of potentiating (green, none) or depressing (red, 1 of 13) electrically stimulated synapses in the TRN in response DHPG induction in 13 WT neurons.

Discussion

The TRN is a unique brain region that facilitates appropriate sensory processing, slow-wave sleep rhythms, and attentional gating. The involvement of TRN in these processes, as well as several disease state implications (Bovenkamp-Janssen et al., 2004; Krol et al., 2018; Steullet et al., 2017; Wells et al., 2016), establishes suspicion that TRN pathology may manifest in a number of functional deficits. In this study of the TRN within the *Fmr1*-KO mouse model of Fragile X Syndrome, however, no indication appeared that the TRN is affected by the loss of the *Fmr1* protein product, FMRP. The *Fmr1*-KO mouse exhibits a variety of ion channel and receptor pathologies affecting intrinsic properties in several brain regions. Neuron hyperexcitability has been reported within both the neocortex (Gibson et al., 2008; Zhang et al., 2014, 2012) and hippocampus (Brager and Johnston, 2014). Abnormal plasticity and GABAergic signaling is seen in the hippocampus (Curia et al., 2009; Huber et al., 2002), and a variety of additional plasticity abnormalities are noted in the neocortex (Larson et al., 2005; Li et al., 2002; Wilson and Cox, 2007) and amygdala (Suvrathan et al., 2010). In this investigation of the intrinsic properties of the TRN, no changes in resting membrane potential, input resistance, action potential half-width, or threshold were measured. Implications of these findings are that the *Fmr1*-KO mouse lacks major alterations in ion channel expression or function that would affect the intrinsic excitability of TRN neurons in the *Fmr1*-KO mouse.

Mechanisms of activity-dependent plasticity have been reported within the TRN (Astori and Lüthi, 2013; Fernandez et al., 2017; Sun et al., 2016), however the extent to which TRN plasticity plays a role in TRN function is not clear. With the utilization of burst-paired stimulation and DHPG application as plasticity induction protocols, the rate of successful plasticity induction

was quite low in TRN (Supplemental Figure 4.4). The highest rate of induction success was via electrical stimulation of internal capsule fibers (WT: 25%, KO 36 %). In both the WT and *Fmr1*-KO animals, both potentiation and depression of the synaptic responses were observed during electrical burst-paired induction, with no apparent differences between the genotypes. During non-selective electrical stimulation with DHPG induction of plasticity, only potentiation of synaptic strength was observed. In contrast, when corticothalamic fibers alone were stimulated during either burst-paired or DHPG induction protocols, only depressive responses were observed (Supplemental Figure 4.4). One possible interpretation of this could be that stimulating corticothalamic afferents leads to depression, whereas thalamocortical afferents in the TRN must also be stimulated to elicit potentiation.

Although not reported in this study due to low labeling success, a small set of four cells (2 WT, 2 *Fmr1*-KO) were recorded with burst-paired induction protocols where the thalamocortical fibers were selectively activated via optical activation of fibers originating from the dLGN. Of these cells, one WT and one *Fmr1*-KO neuron experienced synaptic potentiation in response to the burst-paired induction, leading to a success rate of 50% plasticity induction, with a caveat being the small sample size. Discovery of a more robust mechanism of plasticity induction with selective optogenetic activation of thalamocortical neurons in particular may clarify whether these receptors are responsible for the synaptic potentiation seen within the electrical activation studies. While limited in our cases of evoked plasticity, it appears that corticothalamic and thalamocortical fibers may differently respond to mechanisms of plasticity induction. Additional studies addressing the relative contributions of corticothalamic and

thalamocortical inputs to overall plasticity outcomes in the TRN will be of interest, given that synaptic potentiation was only observed with non-selective fiber activation.

Synapses within the TRN contain mechanisms for experience-dependent plasticity that can alter the relative influence of afferent signals to TRN neurons. While no apparent changes in intrinsic properties or plasticity in the *Fmr1*-KO mouse were uncovered during this study, further investigation into more robust mechanisms of plasticity induction will be helpful in evaluating the functional effects.

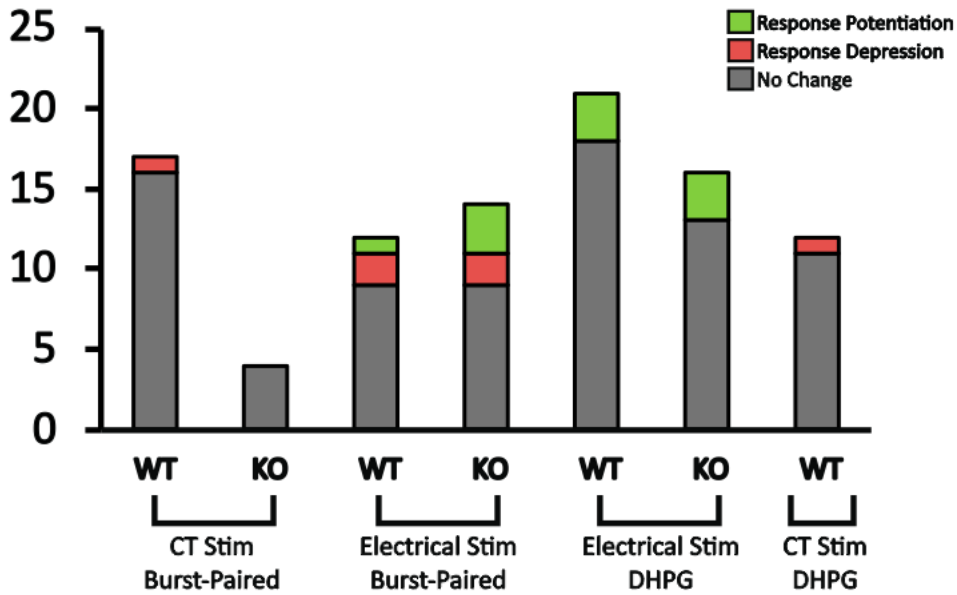


Figure 4.4. Summary of plasticity changes seen via DHPG or burst-paired induction in WT and *Fmr1*-KO mice.

REFERENCES

REFERENCES

- Abbeduto, L., McDuffie, A., Thurman, A.J., 2014. The fragile X syndrome–autism comorbidity: what do we really know? *Front. Genet.* 5. <https://doi.org/10.3389/fgene.2014.00355>
- Astori, S., Lüthi, A., 2013. Synaptic Plasticity at Intrathalamic Connections via CaV3.3 T-type Ca²⁺ Channels and GluN2B-Containing NMDA Receptors. *J. Neurosci.* 33, 624–630. <https://doi.org/10.1523/JNEUROSCI.3185-12.2013>
- Bear, M.F., Huber, K.M., Warren, S.T., 2004. The mGluR theory of fragile X mental retardation. *Trends Neurosci.* 27, 370–377. <https://doi.org/10.1016/j.tins.2004.04.009>
- Berry-Kravis, E., 2002. Epilepsy in fragile X syndrome. *Dev. Med. Child Neurol.* 44, 724–728. <https://doi.org/10.1111/j.1469-8749.2002.tb00277.x>
- Bovenkamp-Janssen, M.C. van de, Scheenen, W.J.J.M., Kuijpers-Kwant, F.J., Kozicz, T., Veening, J.G., Luijtelaar, E.L.J.M. van, McEnery, M.W., Roubos, E.W., 2004. Differential expression of high voltage-activated Ca²⁺ channel types in the rostral reticular thalamic nucleus of the absence epileptic WAG/Rij rat. *J. Neurobiol.* 58, 467–478. <https://doi.org/10.1002/neu.10291>
- Brager, D.H., Johnston, D., 2014. Channelopathies and Dendritic Dysfunction in Fragile X syndrome. *Brain Res. Bull.* 103, 11–17. <https://doi.org/10.1016/j.brainresbull.2014.01.002>
- Brown, M.R., Kronengold, J., Gazula, V.-R., Chen, Y., Strumbos, J.G., Sigworth, F.J., Navaratnam, D., Kaczmarek, L.K., 2010. Fragile X mental retardation protein controls gating of the sodium-activated potassium channel Slack. *Nat. Neurosci.* 13, 819–821. <https://doi.org/10.1038/nn.2563>
- Brown, V., Jin, P., Ceman, S., Darnell, J.C., O'Donnell, W.T., Tenenbaum, S.A., Jin, X., Feng, Y., Wilkinson, K.D., Keene, J.D., Darnell, R.B., Warren, S.T., 2001. Microarray Identification of FMRP-Associated Brain mRNAs and Altered mRNA Translational Profiles in Fragile X Syndrome. *Cell* 107, 477–487. [https://doi.org/10.1016/S0092-8674\(01\)00568-2](https://doi.org/10.1016/S0092-8674(01)00568-2)
- Budimirovic, D.B., Kaufmann, W.E., 2011. What Can We Learn about Autism from Studying Fragile X Syndrome? *Dev. Neurosci.* 33, 379–394. <https://doi.org/10.1159/000330213>
- CDC, 2016. Diagnostic Criteria | Autism Spectrum Disorder (ASD) | NCBDDD | CDC [WWW Document]. *Cent. Dis. Control Prev.* URL <https://www.cdc.gov/ncbddd/autism/hcp-dsm.html> (accessed 2.26.18).
- Centonze, D., Rossi, S., Mercaldo, V., Napoli, I., Ciotti, M.T., De Chiara, V., Musella, A., Prosperetti, C., Calabresi, P., Bernardi, G., Bagni, C., 2008. Abnormal Striatal GABA

- Transmission in the Mouse Model for the Fragile X Syndrome. *Biol. Psychiatry, Genes, Brain Development, and Disorders of Childhood Onset* 63, 963–973.
<https://doi.org/10.1016/j.biopsych.2007.09.008>
- Chen, Y., Parker, W.D., Wang, K., 2014. The Role of T-Type Calcium Channel Genes in Absence Seizures. *Front. Neurol.* 5. <https://doi.org/10.3389/fneur.2014.00045>
- Comery, T.A., Harris, J.B., Willems, P.J., Oostra, B.A., Irwin, S.A., Weiler, I.J., Greenough, W.T., 1997. Abnormal dendritic spines in fragile X knockout mice: Maturation and pruning deficits. *Proc. Natl. Acad. Sci.* 94, 5401–5404.
- Contractor, A., Klyachko, V.A., Portera-Cailliau, C., 2015. Altered Neuronal and Circuit Excitability in Fragile X Syndrome. *Neuron* 87, 699–715.
<https://doi.org/10.1016/j.neuron.2015.06.017>
- Curia, G., Papouin, T., Séguéla, P., Avoli, M., 2009. Downregulation of Tonic GABAergic Inhibition in a Mouse Model of Fragile X Syndrome. *Cereb. Cortex* 19, 1515–1520.
<https://doi.org/10.1093/cercor/bhn159>
- Darnell, J.C., Jensen, K.B., Jin, P., Brown, V., Warren, S.T., Darnell, R.B., 2001. Fragile X Mental Retardation Protein Targets G Quartet mRNAs Important for Neuronal Function. *Cell* 107, 489–499. [https://doi.org/10.1016/S0092-8674\(01\)00566-9](https://doi.org/10.1016/S0092-8674(01)00566-9)
- Darnell, J.C., Van Driesche, S.J., Zhang, C., Hung, K.Y.S., Mele, A., Fraser, C.E., Stone, E.F., Chen, C., Fak, J.J., Chi, S.W., Licatalosi, D.D., Richter, J.D., Darnell, R.B., 2011. FMRP Stalls Ribosomal Translocation on mRNAs Linked to Synaptic Function and Autism. *Cell* 146, 247–261. <https://doi.org/10.1016/j.cell.2011.06.013>
- D’Hulst, C., De Geest, N., Reeve, S.P., Van Dam, D., De Deyn, P.P., Hassan, B.A., Kooy, R.F., 2006. Decreased expression of the GABAA receptor in fragile X syndrome. *Brain Res.* 1121, 238–245. <https://doi.org/10.1016/j.brainres.2006.08.115>
- Dölen, G., Osterweil, E., Shankaranarayana Rao, B.S., Smith, G.B., Auerbach, B.D., Chattarji, S., Bear, M.F., 2007. Correction of fragile X syndrome in mice. *Neuron* 56, 955–962.
<https://doi.org/10.1016/j.neuron.2007.12.001>
- Fernandez, L.M., Vantomme, G., Osorio-Forero, A., Cardis, R., Béard, E., Lüthi, A., 2018. Thalamic reticular control of local sleep in mouse sensory cortex. *eLife* 7, e39111.
<https://doi.org/10.7554/eLife.39111>
- Fernandez, L.M.J., Pellegrini, C., Vantomme, G., Béard, E., Lüthi, A., Astori, S., 2017. Cortical afferents onto the nucleus Reticularis thalami promote plasticity of low-threshold excitability through GluN2C-NMDARs. *Sci. Rep.* 7, 12271.
<https://doi.org/10.1038/s41598-017-12552-8>

- Ferron, L., 2016. Fragile X mental retardation protein controls ion channel expression and activity. *J. Physiol.* 594, 5861–5867. <https://doi.org/10.1113/JP270675>
- Gent, T.C., Bandarabadi, M., Herrera, C.G., Adamantidis, A.R., 2018. Thalamic dual control of sleep and wakefulness. *Nat. Neurosci.* 21, 974. <https://doi.org/10.1038/s41593-018-0164-7>
- Gibson, J.R., Bartley, A.F., Hays, S.A., Huber, K.M., 2008. Imbalance of Neocortical Excitation and Inhibition and Altered UP States Reflect Network Hyperexcitability in the Mouse Model of Fragile X Syndrome. *J. Neurophysiol.* 100, 2615–2626. <https://doi.org/10.1152/jn.90752.2008>
- Govindaiah, G., Wang, T., Gillette, M.U., Cox, C.L., 2012. Activity-Dependent Regulation of Retinogeniculate Signaling by Metabotropic Glutamate Receptors. *J. Neurosci.* 32, 12820–12831. <https://doi.org/10.1523/JNEUROSCI.0687-12.2012>
- Gross, C., Yao, X., Pong, D.L., Jeromin, A., Bassell, G.J., 2011. Fragile X Mental Retardation Protein Regulates Protein Expression and mRNA Translation of the Potassium Channel Kv4.2. *J. Neurosci.* 31, 5693–5698. <https://doi.org/10.1523/JNEUROSCI.6661-10.2011>
- Guillery, R.W., Harting, J.K., 2003. Structure and connections of the thalamic reticular nucleus: Advancing views over half a century. *J. Comp. Neurol.* 463, 360–371. <https://doi.org/10.1002/cne.10738>
- Hagerman, R.J., Hagerman, P.J., 2002. *Fragile X Syndrome: Diagnosis, Treatment, and Research.* Taylor & Francis US.
- Huber, K.M., Gallagher, S.M., Warren, S.T., Bear, M.F., 2002. Altered synaptic plasticity in a mouse model of fragile X mental retardation. *Proc. Natl. Acad. Sci.* 99, 7746–7750. <https://doi.org/10.1073/pnas.122205699>
- Hunter, J., Rivero-Arias, O., Angelov, A., Kim, E., Fotheringham, I., Leal, J., 2014. Epidemiology of fragile X syndrome: A systematic review and meta-analysis. *Am. J. Med. Genet. A.* 164, 1648–1658. <https://doi.org/10.1002/ajmg.a.36511>
- Irwin, S.A., Patel, B., Idupulapati, M., Harris, J.B., Crisostomo, R.A., Larsen, B.P., Kooy, F., Willems, P.J., Cras, P., Kozlowski, P.B., Swain, R.A., Weiler, I.J., Greenough, W.T., 2001. Abnormal dendritic spine characteristics in the temporal and visual cortices of patients with fragile-X syndrome: A quantitative examination. *Am. J. Med. Genet.* 98, 161–167. [https://doi.org/10.1002/1096-8628\(20010115\)98:2<161::AID-AJMG1025>3.0.CO;2-B](https://doi.org/10.1002/1096-8628(20010115)98:2<161::AID-AJMG1025>3.0.CO;2-B)
- Jones, E.G., 1975. Some aspects of the organization of the thalamic reticular complex. *J. Comp. Neurol.* 162, 285–308. <https://doi.org/10.1002/cne.901620302>

- Kidd, S.A., Lachiewicz, A., Barbouth, D., Blitz, R.K., Delahunty, C., McBrien, D., Visootsak, J., Berry-Kravis, E., 2014. Fragile X Syndrome: A Review of Associated Medical Problems. *Pediatrics* 134, 995–1005. <https://doi.org/10.1542/peds.2013-4301>
- Krol, A., Wimmer, R.D., Halassa, M.M., Feng, G., 2018. Thalamic Reticular Dysfunction as a Circuit Endophenotype in Neurodevelopmental Disorders. *Neuron* 98, 282–295. <https://doi.org/10.1016/j.neuron.2018.03.021>
- Larson, J., Jessen, R.E., Kim, D., Fine, A.-K.S., Hoffmann, J. du, 2005. Age-Dependent and Selective Impairment of Long-Term Potentiation in the Anterior Piriform Cortex of Mice Lacking the Fragile X Mental Retardation Protein. *J. Neurosci.* 25, 9460–9469. <https://doi.org/10.1523/JNEUROSCI.2638-05.2005>
- Li, J., Pelletier, M.R., Perez Velazquez, J.-L., Carlen, P.L., 2002. Reduced Cortical Synaptic Plasticity and GluR1 Expression Associated with Fragile X Mental Retardation Protein Deficiency. *Mol. Cell. Neurosci.* 19, 138–151. <https://doi.org/10.1006/mcne.2001.1085>
- McAlonan, K., Brown, V.J., Bowman, E.M., 2006. Thalamic Reticular Nucleus Activation Reflects Attentional Gating during Classical Conditioning 5.
- Meredith, R.M., Holmgren, C.D., Weidum, M., Burnashev, N., Mansvelder, H.D., 2007. Increased Threshold for Spike-Timing-Dependent Plasticity Is Caused by Unreliable Calcium Signaling in Mice Lacking Fragile X Gene *Fmr1*. *Neuron* 54, 627–638. <https://doi.org/10.1016/j.neuron.2007.04.028>
- Miller, L.J., McIntosh, D.N., McGrath, J., Shyu, V., Lampe, M., Taylor, A.K., Tassone, F., Neitzel, K., Stackhouse, T., Hagerman, R.J., 1999. Electrodermal responses to sensory stimuli in individuals with fragile X syndrome: A preliminary report. *Am. J. Med. Genet.* 83, 268–279. [https://doi.org/10.1002/\(SICI\)1096-8628\(19990402\)83:4<268::AID-AJMG7>3.0.CO;2-K](https://doi.org/10.1002/(SICI)1096-8628(19990402)83:4<268::AID-AJMG7>3.0.CO;2-K)
- Olmos-Serrano, J.L., Paluszkiwicz, S.M., Martin, B.S., Kaufmann, W.E., Corbin, J.G., Huntsman, M.M., 2010. Defective GABAergic Neurotransmission and Pharmacological Rescue of Neuronal Hyperexcitability in the Amygdala in a Mouse Model of Fragile X Syndrome. *J. Neurosci.* 30, 9929–9938. <https://doi.org/10.1523/JNEUROSCI.1714-10.2010>
- Paluszkiwicz, S.M., Martin, B.S., Huntsman, M.M., 2011. Fragile X Syndrome: The GABAergic System and Circuit Dysfunction. *Dev. Neurosci.* 33, 349–364. <https://doi.org/10.1159/000329420>
- Pinault, D., 2004. The thalamic reticular nucleus: structure, function and concept. *Brain Res. Rev.* 46, 1–31. <https://doi.org/10.1016/j.brainresrev.2004.04.008>
- Riley, C., Mailick, M., Berry-Kravis, E., Bolen, J., 2017. The Future of Fragile X Syndrome: CDC Stakeholder Meeting Summary. *Pediatrics* 139, S147–S152. <https://doi.org/10.1542/peds.2016-1159B>

- Sevetson, J., Fittro, S., Heckman, E., Haas, J.S., 2017. A calcium-dependent pathway underlies activity-dependent plasticity of electrical synapses in the thalamic reticular nucleus. *J. Physiol.* 595, 4417–4430. <https://doi.org/10.1113/JP274049>
- Sinclair, D., Oranje, B., Razak, K.A., Siegel, S.J., Schmid, S., 2017. Sensory processing in autism spectrum disorders and Fragile X syndrome—From the clinic to animal models. *Neurosci. Biobehav. Rev.* 76, 235–253. <https://doi.org/10.1016/j.neubiorev.2016.05.029>
- Steriade, M., 2005. Sleep, epilepsy and thalamic reticular inhibitory neurons. *Trends Neurosci., INMED/TINS special issue: Multiple facets of GABAergic synapses* 28, 317–324. <https://doi.org/10.1016/j.tins.2005.03.007>
- Steullet, P., Cabungcal, J.-H., Bukhari, S.A., Ardelt, M.I., Pantazopoulos, H., Hamati, F., Salt, T.E., Cuenod, M., Do, K.Q., Berretta, S., 2017. The thalamic reticular nucleus in schizophrenia and bipolar disorder: role of parvalbumin-expressing neuron networks and oxidative stress. *Mol. Psychiatry.* <https://doi.org/10.1038/mp.2017.230>
- Sun, Y.-G., Rupprecht, V., Zhou, L., Dasgupta, R., Seibt, F., Beierlein, M., 2016. mGluR1 and mGluR5 Synergistically Control Cholinergic Synaptic Transmission in the Thalamic Reticular Nucleus. *J. Neurosci.* 36, 7886–7896. <https://doi.org/10.1523/JNEUROSCI.0409-16.2016>
- Suvrathan, A., Hoeffler, C.A., Wong, H., Klann, E., Chattarji, S., 2010. Characterization and reversal of synaptic defects in the amygdala in a mouse model of fragile X syndrome. *Proc. Natl. Acad. Sci.* 107, 11591–11596. <https://doi.org/10.1073/pnas.1002262107>
- Watling, R.L., Deitz, J., White, O., 2001. Comparison of Sensory Profile Scores of Young Children With and Without Autism Spectrum Disorders. *Am. J. Occup. Ther.* 55, 416–423. <https://doi.org/10.5014/ajot.55.4.416>
- Wells, M.F., Wimmer, R.D., Schmitt, L.I., Feng, G., Halassa, M.M., 2016. Thalamic reticular impairment underlies attention deficit in *Ptchd1* Y/– mice. *Nature* 532, 58–63. <https://doi.org/10.1038/nature17427>
- Wilson, B.M., Cox, C.L., 2007. Absence of metabotropic glutamate receptor-mediated plasticity in the neocortex of fragile X mice. *Proc. Natl. Acad. Sci.* 104, 2454–2459. <https://doi.org/10.1073/pnas.0610875104>
- Youssef, E.A., Berry-Kravis, E., Czech, C., Hagerman, R.J., Hessler, D., Wong, C.Y., Rabbia, M., Deptula, D., John, A., Kinch, R., Drewitt, P., Lindemann, L., Marcinowski, M., Langeland, R., Horn, C., Fontoura, P., Santarelli, L., Quiroz, J.A., Group, F.S., 2018. Effect of the mGluR5-NAM Basimglurant on Behavior in Adolescents and Adults with Fragile X Syndrome in a Randomized, Double-Blind, Placebo-Controlled Trial: FragXis Phase 2 Results. *Neuropsychopharmacology* 43, 503–512. <https://doi.org/10.1038/npp.2017.177>

- Zhang, Y., Bonnan, A., Bony, G., Ferezou, I., Pietropaolo, S., Ginger, M., Sans, N., Rossier, J., Oostra, B., LeMasson, G., Frick, A., 2014. Dendritic channelopathies contribute to neocortical and sensory hyperexcitability in *Fmr1* $-/y$ mice. *Nat. Neurosci.* 17, 1701–1709. <https://doi.org/10.1038/nn.3864>
- Zhang, Y., Brown, M.R., Hyland, C., Chen, Y., Kronengold, J., Fleming, M.R., Kohn, A.B., Moroz, L.L., Kaczmarek, L.K., 2012. Regulation of neuronal excitability by interaction of Fragile X Mental Retardation Protein with Slack potassium channels. *J. Neurosci. Off. J. Soc. Neurosci.* 32, 15318–15327. <https://doi.org/10.1523/JNEUROSCI.2162-12.2012>
- Zikopoulos, B., Barbas, H., 2007. Circuits for multisensory integration and attentional modulation through the prefrontal cortex and the thalamic reticular nucleus in primates. *Rev. Neurosci.* 18, 417–438.
- Zorio, D.A.R., Jackson, C.M., Liu, Y., Rubel, E.W., Wang, Y., 2017. Cellular distribution of the fragile X mental retardation protein in the mouse brain. *J. Comp. Neurol.* 525, 818–849. <https://doi.org/10.1002/cne.24100>

CHAPTER 5: CONCLUSION

Summary and Future Directions

The TRN is a relatively understudied region of the brain that is anatomically and physiologically central to highly influential sensorimotor circuits. When I began to conduct whole cell electrophysiological recordings within the mouse TRN, I observed a neuron population that contained highly diverse electrophysiological characteristics. The literature describes TRN population composition as predominantly bursting neurons with a small sub-population of non-bursting neurons, and thus it was surprising to see the consistent heterogeneity of the action potential firing properties. With further investigation into TRN burst classification, I encountered many discrepancies as to how burst discharge is defined. Heterogeneity among TRN neurons could have important implications for studies where variable neuronal populations could respond differently to treatments yet be analyzed as a population. The goal of these studies was to provide a more detailed analysis of the TRN neuron population and provide functional context to the heterogeneity of the neurons.

I have reported several findings that provide insight into the functional properties of the TRN. In Chapter 2, I describe how TRN neurons in the adult mouse are a heterogeneous population that lack any clear subtype demarcation based upon burst frequency. The action potential discharge of both higher and lower frequency bursting TRN neurons is similarly mediated by I_T , and the magnitude of I_T directly correlates with the frequency of the burst. Blocking small-conductance calcium-activated potassium current (I_{SK}) enhances burst characteristics in both higher and lower frequency bursting neurons. In Chapter 3, I report that all TRN neurons have low-threshold calcium currents along their somatodendritic axis, however

lower frequency bursting TRN neurons have a smaller, more uniform distribution of calcium current along their dendrites. Blocking I_{SK} typically enhances the amplitude and duration of the calcium currents in both higher and lower frequency bursting neurons. In Chapter 4, I report that in the *Fmr1*-KO mouse model of Fragile X Syndrome, intrinsic neuron properties do not appear to be affected by FMRP loss as they are in some other brain regions. While synaptic plasticity could be evoked in a few instances, there is no evidence of synaptic alteration in the *Fmr1*-KO mouse.

Several studies have reported variation in burst characteristics and frequencies within the TRN both *in vitro* (Brunton and Charpak, 1992.; Contreras et al., 1992; Lee et al., 2007; Martinez-Garcia et al., 2020) and *in vivo* (Huh and Cho, 2016; Marlinski and Beloozerova, 2014). The extent to which these variable characteristics are found among adult TRN neurons, and the mechanisms underlying the variance had not yet been reported. I have reported that the TRN does not consist of distinct populations of bursting and non-bursting neurons. Instead, the population is evenly distributed by action potential firing frequency in burst mode. Neurons on the higher frequency bursting end of the spectrum discharge many action potentials in discrete clusters with quiescent recovery intervals, as previously described by the literature (Guido and Weyand, 1995), while the neurons discharging action potentials on the slowest end of the spectrum fire in a tonic pattern. Neuron populations analyzed by higher (> 100 Hz) and lower (≤ 100 Hz) frequencies contain distinct electrophysiological characteristics with functional consequences. Higher frequency bursting neurons evoke a significantly larger calcium response throughout their somatodendritic axis which likely represents a larger number of T-type calcium channels. Higher frequency bursting neurons are also likely to engage both short-acting ionotropic GABA_A and longer-lasting

metabotropic GABA_B receptors on downstream thalamic relay neurons, while lower frequency firing neurons will activate mainly GABA_A (Kim and McCormick, 1998).

Between the high frequency bursting and tonically firing populations of neurons remains the curiosity of the “slowly bursting” neurons. These neurons often discharge action potentials with a mix of burst and tonic firing patterns and are underrepresented in literature. Like the classic higher frequency bursting neurons, I found that the burst mode discharge of all lower frequency bursting TRN neurons was of the same nature: voltage-dependent and I_T-driven. These neurons may be expected to activate GABA_A and perhaps more weakly activate additional GABA_B on a sliding spectrum related to the number and frequency of the action potentials in the burst-mode discharge. This difference in downstream effect further implies that these neurons produce dramatically different responses to similar afferent signals: phasic large magnitude responses for higher frequency bursting neurons, or smaller longer lasting responses for lower frequency bursting neurons. Lower frequency bursting may exemplify the intricacy with which the TRN is able to mediate thalamic inhibition, modulating specific network afferents with what could be precise magnitude and temporal patterns.

Recent genetic analysis of single TRN neurons revealed that there is large variation in their gene expression (Li et al., 2020). In the study, there appeared to be two key identified sets of genes which vary inversely with each other: i.e., as one set is expressed more, the other is expressed less in a somewhat mutually exclusive manner. Testing the expression of these gene sets within cells at several points along my identified spectrum of burst frequencies would be useful in determining whether the burst frequency is correlated with the expression of these gene sets.

Studies building upon these findings should further examine the anatomical characteristics of the individual neurons within the nucleus with respect to their firing properties. If neurons located within certain sectors of the nucleus tend to have similar firing properties, this could have important implications on how the TRN may modulate the gain of different sensory modality networks. TRN neurons also display distinct patterns of axonal arborizations that may span one or multiple thalamic nuclei (Cox et al., 1996). It will be of interest to determine whether lower frequency bursting neurons project to specific thalamic nuclei, have similar patterns of arborization, or whether they span multiple nuclei, perhaps acting as cross-modal integrators. Additionally, the various receptor populations at axon terminals of TRN neurons have been studied as a homogeneous characteristic and it is unknown whether characteristics of the terminals may vary based on different TRN cell types. Further studies into the pre- and postsynaptic receptor populations, such as GABA_A and GABA_B receptors, at thalamic relay neuron synapses will add further context to the functionality of this heterogeneous population of neurons.

During typical somatic recordings of burst discharge, the membrane potential of the dendrites, and therefore the dendritic burst mode, is unknown. This presents a challenge in measuring burst discharge due to voltage-dependent I_T because it is unknown whether the T-channels are fully activated along the dendrite. A study of somatic burst discharge while manipulating the dendritic membrane voltage with membrane potential-altering agents would add insight into whether dendritic membrane state changes affect burst discharge. TRN neurons contain very long (> 350 μm) and thin (< 1 μm) dendrites which can sometimes span previously described TRN sectors (Crabtree, 1996; Guillery and Harting, 2003). TRN dendrites contain low

threshold calcium channels along their entire length that may act as voltage-state-dependent amplifiers of afferent synaptic inputs. A consequence of this voltage dependence is that a whole-cell holding potential of -80 mV will not reach the distal dendritic regions. It is then possible that for any recorded neuron, and lower frequency bursting neurons in particular, more distal dendritic membranes could remain more depolarized than the activation threshold (\sim -65 mV) of T channels. An interesting feature of TRN neurons with relation to this issue, is that they receive modulatory inputs that both hyperpolarize (Acetylcholine: ACh) (McCormick and Prince, 1986) and depolarize (Cholecystokinin: CCK) (Cox et al., 1995) the cell membrane. These endogenous neuromodulators would be useful in manipulating the dendritic membrane within this proposed study. This change in voltage state is significant because it could activate or deactivate local T-channels, essentially tuning up or down the amplification and integration of the inputs independent of somatic membrane potential. Implications of this could mean that afferent fibers releasing ACh or CCK could enhance or decrease the local glutamatergic input, adding an additional level of afferent modulation.

I have shown that I_{SK} significantly modifies the characteristics of the burst on both higher and lower frequency bursting neurons. Initial efforts to find an endogenous neuromodulator of SK channels were not successful, however the existence of such a molecule would have implications for the ability of TRN to dynamically and rapidly modulate burst discharge in response to network activity. Future studies may investigate the ability of endogenous molecules to modify I_{SK} within the TRN, and attention of cholinergic molecules may be of interest given their propensity to excite TRN neurons and distal dendritic contacts (Hallanger and Wainer, 1988; Liegeois et al., 2003; Stocker, 2004). I identified a difference in the distribution of I_{SK} on TRN

dendrites. Higher frequency bursting neurons experience the greatest enhancement of calcium activity at proximal and intermediate sites, while lower frequency bursting neurons instead experienced augmented signal at proximal and distal calcium locations. The distribution of both I_T and I_{SK} along the dendrite has additional implications when considering that anatomical studies have found that corticothalamic synapses may be located more distally and thalamocortical more proximally along the dendrite. An intriguing future study would utilize selective optogenetic activation of either thalamocortical or corticothalamic synapses along the dendrite to further determine where these synapses have the largest influence in both a tonic state, to inactivate I_T , and a burst state where I_T is fully activated. The addition of an I_{SK} antagonist would further reveal whether there is differential modulation of these two synapse types by I_{SK} .

In the final chapter of this study, I investigated the function of the TRN in the *Fmr1*-KO mouse. Plasticity evoked via burst-paired stimulation or DHPG-mediated group 1 mGluR activation (Astori and Lüthi, 2013; Fernandez et al., 2017; Sun et al., 2016), was observed within the TRN. I found that the rate at which plasticity was evoked varied largely in either genotype (0-36% success), leaving the question of whether a more robust induction method exists if TRN plasticity is a prominent physiologic process in the TRN. Future studies of TRN chemical synapse plasticity with a more robust method of induction could reveal any changes in the *Fmr1*-KO animal not uncovered by this study.

I also found that when the excitation of corticothalamic synapses alone was measured, only depression of the synapse was induced. With electrical stimulation of the internal capsule, which additionally engages antidromic thalamocortical activation, potentiation was observed with both burst-paired and DHPG induction. Given that thalamocortical fibers likely lack mGluRs

activated by DHPG, the mechanism could be mediated by presynaptic cholinergic activation of the synapses (Sun et al., 2016). Further investigation in which thalamocortical synapses may be optogenetically targeted and tested under DHPG and burst-paired induction paradigms would add considerable understanding to the functions of the thalamocortical circuit.

The experiments within this dissertation have demonstrated that contrary to a long-held assumption, the TRN is a very heterogeneous population of neurons that likely have distinct functional dynamics. Burst output of lower frequency bursting neurons is driven by a smaller T-type calcium current, and likely provides more muted thalamic inhibition. I predict that future studies looking into the specific synaptic inputs onto these neurons, likely arising from certain thalamic nuclei, may reveal that these neurons are designed to provide this muted inhibition in response specific afferent network connections. These afferent synapses onto TRN dendrites may be postsynaptically amplified in a voltage-dependent manner by the presence of local T-channels. Location-specific densities of SK channels could additionally broaden and shorten calcium currents resulting from region-specific synapses. The burst discharge, which determines the magnitude of downstream thalamic inhibition, is related to both dendritic T-channel and SK-channel densities, both of which influence the synaptic integration of afferent inputs. These findings foreshadow that TRN neurons with different burst properties may be uniquely integrated into the networks involved in sensory processing, sleep, attention, or epilepsy. Future studies investigating these potentially unique roles will broaden our understanding of how the TRN facilitates these functions.

REFERENCES

REFERENCES

- Astori, S., Lüthi, A., 2013. Synaptic Plasticity at Intrathalamic Connections via CaV3.3 T-type Ca²⁺ Channels and GluN2B-Containing NMDA Receptors. *J. Neurosci.* 33, 624–630. <https://doi.org/10.1523/JNEUROSCI.3185-12.2013>
- Brunton, J., Charpak, S., 1992. HETEROGENEITY OF CELL FIRING PROPERTIES AND OPIOID SENSITIVITY IN THE THALAMIC RETICULAR NUCLEUS 5.
- Contreras, D., Curro Dossi, R., Steriade, M., 1992. Bursting and tonic discharges in two classes of reticular thalamic neurons. *J. Neurophysiol.* 68, 973–977. <https://doi.org/10.1152/jn.1992.68.3.973>
- Cox, C.L., Huguenard, J.R., Prince, D.A., 1996. Heterogeneous axonal arborizations of rat thalamic reticular neurons in the ventrobasal nucleus. *J. Comp. Neurol.* 366, 416–430. [https://doi.org/10.1002/\(SICI\)1096-9861\(19960311\)366:3<416::AID-CNE4>3.0.CO;2-7](https://doi.org/10.1002/(SICI)1096-9861(19960311)366:3<416::AID-CNE4>3.0.CO;2-7)
- Cox, C.L., Huguenard, J.R., Prince, D.A., 1995. Cholecystokinin depolarizes rat thalamic reticular neurons by suppressing a K⁺ conductance. *J. Neurophysiol.* 74, 990–1000. <https://doi.org/10.1152/jn.1995.74.3.990>
- Crabtree, J.W., 1996. Organization in the somatosensory sector of the cat's thalamic reticular nucleus. *J. Comp. Neurol.* 366, 207–222. [https://doi.org/10.1002/\(SICI\)1096-9861\(19960304\)366:2<207::AID-CNE2>3.0.CO;2-9](https://doi.org/10.1002/(SICI)1096-9861(19960304)366:2<207::AID-CNE2>3.0.CO;2-9)
- Fernandez, L.M.J., Pellegrini, C., Vantomme, G., Béard, E., Lüthi, A., Astori, S., 2017. Cortical afferents onto the nucleus Reticularis thalami promote plasticity of low-threshold excitability through GluN2C-NMDARs. *Sci. Rep.* 7, 12271. <https://doi.org/10.1038/s41598-017-12552-8>
- Guido, W., Weyand, T., 1995. Burst responses in thalamic relay cells of the awake behaving cat. *J. Neurophysiol.* 74, 1782–1786. <https://doi.org/10.1152/jn.1995.74.4.1782>
- Guillery, R.W., Harting, J.K., 2003. Structure and connections of the thalamic reticular nucleus: Advancing views over half a century. *J. Comp. Neurol.* 463, 360–371. <https://doi.org/10.1002/cne.10738>
- Hallanger, A.E., Wainer, B.H., 1988. Ultrastructure of ChAT-immunoreactive synaptic terminals in the thalamic reticular nucleus of the rat. *J. Comp. Neurol.* 278, 486–497. <https://doi.org/10.1002/cne.902780403>
- Huh, Y., Cho, J., 2016. Differential Responses of Thalamic Reticular Neurons to Nociception in Freely Behaving Mice. *Front. Behav. Neurosci.* 10. <https://doi.org/10.3389/fnbeh.2016.00223>

- Kim, U., McCormick, D.A., 1998. The Functional Influence of Burst and Tonic Firing Mode on Synaptic Interactions in the Thalamus. *J. Neurosci.* 18, 9500–9516.
<https://doi.org/10.1523/JNEUROSCI.18-22-09500.1998>
- Lee, S.-H., Govindaiah, G., Cox, C.L., 2007. Heterogeneity of firing properties among rat thalamic reticular nucleus neurons. *J. Physiol.* 582, 195–208.
<https://doi.org/10.1113/jphysiol.2007.134254>
- Li, Y., Lopez-Huerta, V.G., Adiconis, X., Levandowski, K., Choi, S., Simmons, S.K., Arias-Garcia, M.A., Guo, B., Yao, A.Y., Blosser, T.R., Wimmer, R.D., Aida, T., Atamian, A., Naik, T., Sun, X., Bi, D., Malhotra, D., Hession, C.C., Shema, R., Gomes, M., Li, T., Hwang, E., Krol, A., Kowalczyk, M., Peça, J., Pan, G., Halassa, M.M., Levin, J.Z., Fu, Z., Feng, G., 2020. Distinct subnetworks of the thalamic reticular nucleus. *Nature* 583, 819–824.
<https://doi.org/10.1038/s41586-020-2504-5>
- Liegeois, J., Mercier, F., Graulich, A., Graulich-Lorge, F., Scuvee-Moreau, J., Seutin, V., 2003. Modulation of Small Conductance Calcium-Activated Potassium (SK) Channels: A New Challenge in Medicinal Chemistry. *Curr. Med. Chem. Schiph.* 10, 625–47.
<http://dx.doi.org/10.2174/0929867033457908>
- Marlinski, V., Beloozerova, I.N., 2014. Burst firing of neurons in the thalamic reticular nucleus during locomotion. *J. Neurophysiol.* 112, 181–192.
<https://doi.org/10.1152/jn.00366.2013>
- Martinez-Garcia, R.I., Voelcker, B., Zaltsman, J.B., Patrick, S.L., Stevens, T.R., Connors, B.W., Cruikshank, S.J., 2020. Two dynamically distinct circuits drive inhibition in the sensory thalamus. *Nature* 583, 813–818. <https://doi.org/10.1038/s41586-020-2512-5>
- McCormick, D.A., Prince, D.A., 1986. Acetylcholine induces burst firing in thalamic reticular neurones by activating a potassium conductance. *Nature* 319, 402–405.
<https://doi.org/10.1038/319402a0>
- Stocker, M., 2004. Ca²⁺-activated K⁺ channels: molecular determinants and function of the SK family. *Nat. Rev. Neurosci.* 5, 758–770. <https://doi.org/10.1038/nrn1516>
- Sun, Y.-G., Rupprecht, V., Zhou, L., Dasgupta, R., Seibt, F., Beierlein, M., 2016. mGluR1 and mGluR5 Synergistically Control Cholinergic Synaptic Transmission in the Thalamic Reticular Nucleus. *J. Neurosci.* 36, 7886–7896.
<https://doi.org/10.1523/JNEUROSCI.0409-16.2016>